Propagation of nonclassical light in structured media

Dissertation

Zur Erlangung des akademischen Grades
Doctor rerum naturalium (Dr. rer. nat.)

Vorgelegt der
Mathematisch-Naturwissenschaftlichen Fakultät
der Universität Rostock

Von Dmytro Vasylyev
geboren am 04.02.1982 in Winnitsa (Ukraine)

URN: urn:nbn:de:gbv:28-diss2009-0213-8

Gutachter: Prof. Dr. Werner Vogel, Institut für Physik, Universität Rostock

Prof. Dr. Klaus Henneberger, Institut für Physik, Universität Rostock

Prof. Dr. Andreas Knorr, Institut für Theoretische Physik, Technische Universität Berlin

Rostock, den 17. Juni 2009

Thanks

I want to thank Prof. Dr. Werner Vogel very much for the opportunity to work with him. The very nice and fruitful discussions with him helped me to get a deeper insight into many current problem in the field of quantum optics. I am very thankful to Prof. Dr. Klaus Henneberger and Dr. Andrey Semenov for the scientific collaboration and profitable discussions. I am also very grateful to all my colleagues and collaborators of the Quantum Optics groups in Rostock and in Jena and to my colleagues from Bogolubov Institute of Theoretical Physics in Kiev, in particular Prof. Dr. Dirk-Gunnar Welsch and Prof. Dr. Bohdan Lev for effective collaboration and scientific consulting. I am also very grateful to Dr. Günter Manzke, Felix Richter, Dr. Tim Schmielau, and Dr. Evgeny Shchukin for discussing physical and other problems and for the agreeable time spent together in Rostock. Last but not least I also want to thank my wife and daughter who have greatly supported me many times.

Contents

Introduction

The fundamental objects of study of the contemporary theoretical physics are quantum fields and their interactions. The gauge field theory within the standard model of particle interactions establishes the relationship between the electromagnetic, weak and strong interactions. The great challenge for the theoretical physics of our days is to extend the standard model in order to include gravitation as well.

The electromagnetic interactions are a source of forces in a vast number of physical systems, and accordingly deserve to be singled out. The quantum theory of these interactions, called *quantum electrodynamics*, underlies the foundations of most modern areas of physics. Optics and electrodynamics, atomic and molecular physics, the solid-state physics and physics of fluids, gases, and plasmas are all special applications of quantum electrodynamics. In all these areas of physics the first and foremost important object of study is the electromagnetic field and its interaction with particles or other fields.

Quantum optics originates from the low energy sector of quantum electrodynamics and deals merely with the phenomena in the energy range of optical waves and microwaves, i.e., in an energy range where the relativistic effects can be neglected. Moreover, due to the coherent properties of a large number of these phenomena, the classical theory of the electromagnetic field can be successfully applied for their description in a good approximation degree.

The main research area of quantum optics is the study of light-matter interaction, at a microscopic level of understanding. The characterization of light-matter coupling requires the use of quantum theory, which can be used to describe the electromagnetic field, and also the matter itself. But there exist some less sophisticated approaches for the description of light interaction with matter that can give a better insight into the physics of processes that supplement this interaction. For some particular systems the semiclassical approach (the field treated classically and the matter – quantum mechanically) to the problem is more favorable than the fully quantum one. For example, R. Glauber [1] has shown in early 60's that the interaction of matter with the coherent light from the perfectly stabilized laser can be described semiclassically by representing the field amplitude by the so-called *coherent states*. A coherent state is defined as a specific kind of quantum state of the quantum harmonic oscillator that describes a maximal kind of coherence and a classical kind of behavior. Another example of electromagnetic field whose dynamics can be treated classically is the thermal radiation. This radiation was modeled in the early days of quantum theory by an ensemble of classical, radiating harmonic oscillators in order to describe the black body radiation [2].

Since quantum optics is a closest descendant of quantum electrodynamics it inherited

also the whole mathematical apparatus of the latter. Among the various mathematical tools the formalism of *Green's functions* (i.e., correlation functions of radiation and matter fields) play an outstanding role. Indeed, in quantum optics, the usually considered physical quantities are the electromagnetic fields; in addition to their macroscopic averages, their correlations and their fluctuations due to the underlying quantum character of the states are of great relevance. On the other hand, for the description of the dynamics of these correlations and fluctuations of interacting electromagnetic fields the knowledge of the medium correlation functions is usually required. Therefore, Green's functions (GFs) are perfectly suited for purposes of quantum optics. The formalism of Green's functions has been applied successfully in atomic quantum optics [3], in nonlinear quantum optics [4], quantum optics of dielectrics and semiconductors [5], to name just a few.

Another area of quantum optics involves *nonclassical light*, such as squeezed states of light, having unusual quantum noise properties. By nonclassical light is meant a light whose observed properties cannot be described with customary visualization by considering a light beam as a set of waves. In other terms, the nonclassical light produces effects that have no classical analogies. Usually, the nonclassicality manifests itself in specific properties of quantum statistics, which sometimes cannot be described in the framework of the probability theory [6]. Usually the nonclassical light is generated in the nonlinear optical processes and in contrast to the classical fields the interaction of such a field with matter should be performed fully quantum mechanically.

Recent years have witnessed a flowering of theoretical and experimental interest in the nonclassical properties of the radiation field. New technical possibilities led to the direct experimental realization of large variety of nonclassical quantum states of the electromagnetic field. Starting from the first realization of squeezed radiation in four-wave mixing experiments by the group of R. E. Slusher [7], in the last 20 years dozens of new quantum states have been produced. Among them are the famous Schrödinger cat states [8], single photon states [9], multi-quantum Fock states [10], to name just a few (see for review also Ref. [11]).

After the first observation of the Bose-Einstein condensate (BEC) [12] it has been soon realized that the matter waves, produced by condensates, have similar coherence properties to that of electromagnetic waves [13]. Hence it was natural to expect that introducing the nonlinearity in BEC systems one can also produce some nonclassical states by condensate. After the experimental realization in BECs of spin-squeezed states [14] and BECs-entanglement states [15] the notion of nonclassicality has propagated as well to atomic systems. These experiments show that the concept of nonclassicality is not only characteristic for electromagnetic field but it is merely the peculiar feature of the whole quantum world.

The nonclassical properties play also a crucial role in understanding the fundamentals of quantum theory. This concept is the main theoretical background for many applications, such as quantum information processing [16], including teleportation [17], dense coding [18] and quantum cryptography [19]. Historically, the phenomenon of nonclassicality was first considered in the famous work by Einstein, Podolsky and Rosen [20] for the demonstration of contradictions between quantum mechanics and the concept of "local realism". As shown by Bell [21], the latter leads to some inequalities violated for usual quantum mechanics. Experiments of Aspect and collaborators [22] confirmed that this fact as well as the assumption that quantum phenomena are characterized by a specific feature, nonlocality, which cannot be explained in terms of classical physics. The evidence of the violation of Bell's inequalities has made a significant contribution to the interpretation of the foundations of quantum physics [23]. Nowadays we know some other criteria for testing the presence of this kind of nonclassicality (entanglement) [24–27].

The main problem for testing the nonclassicality for realistic systems are different *dissipative processes* (*losses*) [28, 29]. Uncontrolled interaction of the system with an environment leads to substantial effects on nonclassical properties. Depending on the system, the environment may have various physical properties. A well-known example of such a system is an electromagnetic field being brought in contact with a thermodynamic heat bath. Quantum fluctuations of the field are then modified by the interaction with the thermal field.

The experiments for generation and detection of nonclassical light involve a variety of optical instruments put together in some definite manner. Usually the instruments in optical setups are spatially separated so that light propagates in *structured media* before being detected. This dissertation deals with the influence of various loss mechanisms presented in the optical instruments on the nonclassical properties of optical radiation fields.

Semitransparent plates, mirrors, wave guides, active media for laser resonators, optical fibers, spectral filters, etc. are standard parts of any optical setup, which is typically built up by dielectric or semiconductor materials. The optical properties of the light beam propagating in these devices are modified by the temperature, dispersion, and absorption in the media. The statistical properties of light are influenced also by reflection on the boundaries of an optical device. Finally, when the instrument has nonzero temperature, the quantum statistical features of the transmitted beam are distorted by the addition of, or interference with, spontaneously emitted radiation.

As an example of structured optical device we shall consider optical cavities. From the early days of quantum optics cavity quantum electrodynamics (cavity QED) has been a powerful tool in a lot of investigations dealing with fundamentals of quantum physics and

applications such as quantum information processing, for a review see, e.g., Refs. [30, 31]. It has offered a number of proposals for quantum-state generation, manipulation, and transfer between remote nodes in quantum networks in recent years. The cavity is a resonator-like device with one or more fractionally transparent mirrors characterized by small transmission coefficients such that large quality values Q can be realized. Hence one may regard the mode spectrum of the intracavity field as consisting of narrow lines. As a rule, excited atoms inside the cavity serve as source of radiation, and the fractionally transparent mirrors are used to release radiation for further applications and to feed radiation in the cavity in order to modify the intracavity field and thereby the outgoing field either.

The problem of the influence of the environment on quantum systems is of great importance in cavity QED. On the one hand, an optical cavity enhances the interaction between matter placed in it (e.g. atoms) and light. This can lead to reducing the decoherence rate and to retaining the quantum coherence properties of matter-light coupled systems for relatively long times. On the other hand, the number of external modes plays the role of the environment, which interacts with the system through the semitransparent mirror. This unwanted noise can spoil the nonclassical properties of the intracavity field [32, 33]. The same effect comes from another example of unwanted noise, associated with absorption and scattering of the electromagnetic field by cavity mirrors, while the intercavity mode is extracted for further use [35].

Unwanted noise in high-Q cavities usually plays a crucial role in experiments in cavity QED. Even small values of the corresponding absorption/scattering coefficients may lead to dramatic changes of the quantum properties of the radiation. For typical high-Q cavities the unwanted losses can be of the same order of magnitude as the wanted ones, the radiative losses due to the input-output coupling [36]. In such a case the process of quantum-state extraction from a high Q-cavity is characterized by an efficiency of about 50% [35]. This feature gives a serious restriction for the implementation of many proposals in cavity QED. Particularly, nowadays a lot of schemes for quantum-state engineering of the intracavity field are known. For example, in Ref. [37] a scheme for the generation of an arbitrary quantum state of the field was proposed. Also schemes for the generation of entangled states are known [38]. Unfortunately, due to the small efficiency of the quantum-state extraction, the states of the field may lose essential nonclassical properties after escaping from the cavity. Therefore, it is quite desirable to describe the quantum radiation extracted from the cavity by including all noise sources.

In the last years, with the advent of engineered semiconductor nanostructures, quantum optics become important for the field of semiconductor physics. In specially designed nanostructures one has succeeded to realize and observe such purely quantum optical ef-

fects like gain without inversion [39], antibunching of emission spectra [40], sub-Poissonian statistics [41], enhancement and inhibition of spontaneous emission rates [42], quantum beats [43], to name just a few. Since semiconductors are the standard materials for many of today's technologies, they have also been studied for the generation of nonclassical radiation fields [44]. For early examples we refer to experiments with semiconductor lasers [45], for more details see [46]. On the other hand, the further developments of nano-structured systems opens new possibilities of generation and application of nonclassical radiation fields in integrated systems. For example, the correlated emission of single photons could be demonstrated by using quantum dots [47,48] and bound excitons in semiconductors [49]. First experiments with quantum wells [50, 51] and quantum dots [52–54] also show the potential of semiconductor systems for the generation of entangled photons, which are of interest for quantum information processing. Similar to the optical cavities, the nonclassical properties of radiation generated or propagating in semiconductor lasers, light-emitting diodes or slabs are affected by different loss mechanisms due to absorption, dispersion, dephasing [55, 56]. Since the application and usefulness of nonclassical light generated in semiconductors is limited to low-loss systems, the consistent description of losses in realistic semiconductor devices is of great importance.

In the present dissertation I consider some aspects of the influence of various kinds of losses on the nonclassical properties of radiation propagating in structured material systems. Most of the results presented here have been published in Refs. [I-VI]. These articles are collected at the end of my dissertation. The results obtained by the author of the present work are numbered in text by roman numbers, other papers are numbered by arabic ones.

In Chap. 1 an overview of Green's function methods is given, as far as it is needed in the following. With the help of the functional integration technique the particle and photon Green's functions are obtained both for (thermal) equilibrium and nonequilibrium situations. In the second part of this chapter I discuss the simple statistical properties of optical radiation and their detection techniques. Then the characterization of nonclassicality based on field-field correlation functions is considered. In particular these correlation functions are expressed with the help of corresponding quasi-probability functions and generation functionals (characteristic functions). Finally, I discuss the simple examples of generation of nonclassical state by using nonlinear medium. The next two chapters are devoted to the characterization of nonclassical light propagating in structured media with an account of possible loss mechanisms. In Chap. 2 the characterization of nonclassicality of quantum state of radiation is outlined and the modification of nonclassicality criteria due to thermal losses is presented [I]. The application of the modified criterion is presented for some quantum optical systems, where the influence of thermal fluctuations is significant.

Also in this chapter I analyze in detail absorption and scattering losses in high Q-cavities operating in the optical domain [II, III]. In particular, I introduce a beam-splitter-based replacement scheme which is suitable for modelling the unwanted noise of a one-sided cavity. The effect of noise-induced mode coupling between intracavity and input modes is considered and unbalanced and cascaded homodyning schemes for the measurement of an intracavity mode are presented. In Chap. 3, some problems of semiconductor quantum optics are presented [IV, V, VI]. I firstly discuss the propagation problem of nonclassical light in a dispersive, absorbing or/and amplifying semiconductor medium. This problem is treated by methods of both microscopic and macroscopic quantum electrodynamics. I also investigate the semiconductor carrier kinetics by taking into account the quantum fluctuation effects that stem from the interaction of the semiconductor with nonclassical light. Finally, as an application of the theory, the propagation of nonclassical squeezed light in a semiconductor slab is studied.

Chapter 1

Light-Matter Interaction and Nonclassical Light

In this chapter we shall discuss the problem of treating the light interaction with matter from the point of view of quantum field theory. The quantum field theory exists in three different versions for nonrelativistic many-particle systems: the ground-state theory at zero temperature, the Matsubara formalism for systems in thermal equilibrium, and the Keldysh formalism for nonequilibrium systems. For the description of the elementary processes of the light-matter interaction (e.g. polarization of a medium, renormalization of charges and masses, etc.), we shall extensively use the formalism of functional integrals. This approach uses the convenient integral representation for partition functions, Green's functions, and so on. The remarkable advantage of this technique in comparisson to the standard operator methods is that the functional integrals yield compact equations which replace the complex conventional perturbative expansion schemes. The natural formulation of the quasi-classical approximation within this method is another advantage. Therefore the functional integrals turn out to be ideally suited for examining macroscopic optical effects. We shall use this fact extensively in the following chapters.

Despite the Green's functions contain a vast amount of useful information about the quantum dynamics of charged particles and photons, the Green's functions are not directly observable quantities. In usual optical experiments one measures the photon correlation functions with some definite ordering prescription. The calculation of such correlation functions relies generally on the perturbative treatment. The resulting series of the Feynman diagrams are usually divergent and the proper regularization and cut-off procedures are used in order to obtain meaningful result.

On the other side, for some applications it is much easier to use the generating functional for ordered photon correlation functions from the very beginning. As one should

expect, the knowledge of this generating functional enables one to investigate the coherence properties of the radiation field of interest. Since the coherence properties of light sometimes cannot be described by classical probability theory, we introduce the concept of nonclassical light that has such peculiar quantum statistical properties.

The present chapter is organized as follows: In Sec. 1.1 the general model of light-matter interaction is studied by using the apparatus of nonequilibrium Green functionsand and the methods of functional integration. The influence of the light-matter and Coulomb interaction effects on the dynamics of particles and the electromagnetic field is also studied. The relation of self-energies and polarization functions to the measured quantities is outlined. In Sec. 1.2 we show how the quantum statistical properties of radiation can be described in terms of the normally-ordered correlation functions. We also briefly introduce the characteristic functions for moments of photon operators with definite operator orderings and the corresponding quasi-probability functions, which are used to describe noise in quantum optical systems. Then we discuss the generation of nonclassical sqeezed light in a nonlinear optical parametric process.

1.1 Green's functions and sources

In this section we shall introduce the basic methods of the non-equilibrium quantum field theory (QFT) for dealing the light-matter interactions by using preferably the formalism of the functional integration. In the following we shall use the Coulomb gauge, which implies that the electromagnetic vector potential, $\hat{\boldsymbol{A}}$, is purely transverse. We start with the general model of light coupled with the charged particles. The Hamiltonian of the system, written in the second-quantization representation, reads as

$$\begin{aligned}\hat{H} =&\hat{H}^0_{\rm ph} + \sum_s \frac{1}{2m_s}\int d^3\boldsymbol{r}\hat{\psi}^\dagger_s(\boldsymbol{r})\Big[\frac{\hbar}{i}\frac{\partial}{\partial\boldsymbol{r}} - eZ_s\hat{\boldsymbol{A}}(\boldsymbol{r})\Big]^2\hat{\psi}_s(\boldsymbol{r})\\ &+\frac{1}{2}\sum_{ss'} eZ_s eZ_{s'}\int d^3\boldsymbol{r}d^3\boldsymbol{r}' :\hat{\rho}_s(\boldsymbol{r})v(\boldsymbol{r}-\boldsymbol{r}')\hat{\rho}_{s'}(\boldsymbol{r}'):.\end{aligned} \tag{1.1}$$

The eZ_s and m_s are charge and mass of particle s, respectively, $\hat{\psi}_s$ and $\hat{\psi}^\dagger_s$ are the annihilation and creation fermion field operators[1], respectively. The notation :: represents the operation of normal ordering, i.e., with all the creation operators being placed to the left of the annihilation operators.

The last term in Eq. (1.1) represents the (dressed) interaction between the charges by the two-particle potential $v(\boldsymbol{r})$, where $\hat{\rho}_s = \hat{\psi}_s{}^\dagger\hat{\psi}_s$ is the density operator for a fermion

[1]We restrict our attention to particles obeying Fermi statistics since we intend in the following to apply the model Hamiltonian (1.1) to degenerate electrons in solids and particularly to electrons and holes in semiconductors.

of species s. For the noninteracting systems $\hat{\rho}_s$ simplifies to $\delta(\boldsymbol{r}-\hat{\boldsymbol{r}}_s)$ with $\hat{\boldsymbol{r}}_s$ being the position operator of particle s. The first two terms on the right hand side of Eq. (1.1) can be rewritten as

$$\begin{aligned}\hat{H}^0_{\rm ph}+\hat{H}^{(1)}_{\rm ph}+\hat{H}^{(2)}_{\rm ph}+\hat{H}^0_{\rm ch}=&\frac{1}{2}\int d^3\boldsymbol{r}\left[\varepsilon_0\hat{\boldsymbol{E}}^{\perp 2}(\boldsymbol{r})+\frac{1}{\mu_0}\hat{\boldsymbol{B}}^2(\boldsymbol{r})\right]\\&-\int d^3\boldsymbol{r}\hat{\boldsymbol{J}}^{\rm par}(\boldsymbol{r})\cdot\hat{\boldsymbol{A}}(\boldsymbol{r})-\frac{1}{2}\int d^3\boldsymbol{r}\hat{\boldsymbol{J}}^{\rm dia}(\boldsymbol{r})\cdot\hat{\boldsymbol{A}}(\boldsymbol{r})-\sum_s\frac{\hbar^2}{2m_s}\hat{\psi}^\dagger_s(\boldsymbol{r})\Delta_{\boldsymbol{r}}\hat{\psi}_s(\boldsymbol{r}),\end{aligned}\tag{1.2}$$

where the electric and magnetic fields are defined as $\hat{\boldsymbol{E}}^\perp=-\partial\hat{\boldsymbol{A}}/\partial t$ and $\hat{\boldsymbol{B}}=\nabla\times\hat{\boldsymbol{A}}$, respectively. In the following we will omit the superscript $\perp$ in the notation of the transverse component of the electromagnetc field whenever there is no danger of confusion. Here, we have also defined the paramagnetic and diamagnetic components of the current density as

$$\hat{\boldsymbol{J}}^{\rm par}(\boldsymbol{r})=\frac{eZ}{2m}\{\hat{\boldsymbol{p}},\hat{\rho}(\boldsymbol{r})\}=\sum_s\frac{eZ_s}{2m_s}[\delta(\boldsymbol{r}-\hat{\boldsymbol{r}}_s)\hat{\boldsymbol{p}}_s+\hat{\boldsymbol{p}}_s\delta(\boldsymbol{r}-\hat{\boldsymbol{r}}_s)],\tag{1.3}$$

$$\hat{\boldsymbol{J}}^{\rm dia}(\boldsymbol{r})=-\frac{(eZ)^2}{2m}\{\hat{\boldsymbol{A}}(\boldsymbol{r}),\hat{\rho}(\boldsymbol{r})\}=-\sum_s\frac{(eZ_s)^2}{m_s}\hat{\rho}_s(\boldsymbol{r})\hat{\boldsymbol{A}}(\boldsymbol{r}),\tag{1.4}$$

where $\{...,...\}$ denotes anti-commutator and $\hat{\boldsymbol{p}}_s$ is the momentum operator of particle s. The Hamiltonian $\hat{H}^0_{\rm ph}$ describes the free radiation field, $\hat{H}^{(1)}_{\rm ph}$ and $\hat{H}^{(2)}_{\rm ph}$ are the first and second-order contributions with regard to the vector potential into the field-charges interaction Hamiltonian, respectively. The Hamiltonian $\hat{H}^{(1)}_{\rm ph}$ contains the photon annihilation and creation operators, contributing to the one-photon absorption and emission of light. The Hamiltonian $\hat{H}^{(2)}_{\rm ph}=\sum_s\frac{(eZ_s)^2}{2m_s}\hat{\boldsymbol{A}}^2$, which is quadratic in $\hat{a}_{\boldsymbol{k}_\nu}$ and $\hat{a}^\dagger_{\boldsymbol{k}_\nu}$, contributes to two-photon processes such as light scattering. However in many quantum-optical problems such two-photon processes occur with small probability and we can omit this part of the total Hamiltonian in the so called "dipole" approximation. Finally, $\hat{H}^0_{\rm ch}$ represents the free evolution of the charged particles.

The fundamental commutation relation between the electromagnetic field and the vector potential can be obtained by quantization of the Maxwellian field, namely

$$\left[\hat{A}_\mu(\boldsymbol{r},t),\hat{E}^\perp_\nu(\boldsymbol{r}',t)\right]=-\frac{i\hbar}{\varepsilon_0}\delta^\perp_{\mu\nu}(\boldsymbol{r}-\boldsymbol{r}'),\tag{1.5}$$

where the transverse delta function is defined as[1]

$$\delta^\perp_{\mu\nu}(\boldsymbol{r})=\frac{1}{\mathfrak{v}}\sum_{\boldsymbol{k}}e^{i\boldsymbol{k}\cdot\boldsymbol{r}}\delta^\perp_{\mu\nu}(\boldsymbol{k})=\frac{1}{\mathfrak{v}}\sum_{\boldsymbol{k}}e^{i\boldsymbol{k}\cdot\boldsymbol{r}}\left(\delta_{\mu\nu}-\frac{k_\mu k_\nu}{\boldsymbol{k}^2}\right),\tag{1.6}$$

[1]We use here for convenience the summation over the discrete wave vectors instead of integration. In the thermodynamic limit, $\mathfrak{v}\to\infty$, the summation is replaced by the integration via $\frac{1}{\mathfrak{v}}\sum_{\boldsymbol{k}}\to\int\frac{d^3\boldsymbol{k}}{(2\pi)^3}$.

where υ is the quantization volume. The photon field in the Schrödinger picture is specified by

$$\hat{\boldsymbol{A}}(\boldsymbol{r}) = \sum_{n,\boldsymbol{k}_n} \sqrt{\frac{\hbar}{2\varepsilon_0 \omega_n \upsilon}} \sum_{p=1,2} \boldsymbol{e}_p \, \hat{a}_{p,\boldsymbol{k}_n} e^{i\boldsymbol{k}_n \cdot \boldsymbol{r}} + \text{H.c.} \tag{1.7}$$

where in the transverse gauge the two perpendicular unit polarization vectors, $\boldsymbol{e}_p$, are also perpendicular to the wave vector $\boldsymbol{k}_n$ of the photon of n-th mode with the absolute value $|\boldsymbol{k}_n| = \omega_n/c$. The annihilation $\hat{a}_{p,\boldsymbol{k}_n}$ and creation $\hat{a}^\dagger_{p,\boldsymbol{k}_n}$ operators of the n-th field mode satisfy the following commutation relations

$$\left[\hat{a}_{p,\boldsymbol{k}_n}, \hat{a}^\dagger_{p',\boldsymbol{k}'_m}\right] = \delta_{pp'}\delta_{\boldsymbol{k}_n,\boldsymbol{k}'_m}, \quad \left[\hat{a}_{p,\boldsymbol{k}_n}, \hat{a}_{p',\boldsymbol{k}'_m}\right] = \left[\hat{a}^\dagger_{p,\boldsymbol{k}_n}, \hat{a}^\dagger_{p',\boldsymbol{k}'_m}\right] = 0 \tag{1.8}$$

which follow from Eq. (1.5). Using the mode-expansion formula, we rewrite the Hamiltonian $\hat{H}_{\text{ph}}$=$\hat{H}^0_{\text{ph}}$+$\hat{H}^{(1)}_{\text{ph}}$+$\hat{H}^{(2)}_{\text{ph}}$ of Eq. (1.2) as

$$\hat{H}_{\text{ph}} = \sum_{p,n,\boldsymbol{k}_n} \left[\hbar\omega_n \hat{a}^\dagger_{p,\boldsymbol{k}_n}\hat{a}_{p,\boldsymbol{k}_n} - \sqrt{\frac{\hbar}{2\varepsilon_0\omega_n}}\left(\hat{J}_{p,\boldsymbol{k}_n}\hat{a}^\dagger_{p,\boldsymbol{k}_n} + \hat{a}_{p,\boldsymbol{k}_n}\hat{J}^\dagger_{p,\boldsymbol{k}_n}\right)\right], \tag{1.9}$$

$$\hat{J}_{p,\boldsymbol{k}_n} = \frac{1}{\sqrt{\upsilon}}\int d^3\boldsymbol{r} e^{-i\boldsymbol{k}_n\cdot\boldsymbol{r}}\boldsymbol{e}_p \cdot \left[\hat{\boldsymbol{J}}^{\text{par}}(\boldsymbol{r}) + \frac{1}{2}\hat{\boldsymbol{J}}^{\text{dia}}(\boldsymbol{r})\right], \quad \hat{J}^\dagger_{p,\boldsymbol{k}_n} = \hat{J}_{p,-\boldsymbol{k}_n}. \tag{1.10}$$

In this expression we have dropped within the rotating-wave approximation (RWA) the off-resonant coupling terms $\hat{J}^\dagger\hat{a}^\dagger$ and $\hat{J}\hat{a}$ [57]. In the following, for the convenience of notations, we will drop the summation over the polarization and mode indices p, n and suppress these indices. The Hamiltonian in (1.9) reads than as

$$\hat{H}_{\text{ph}} = \sum_{\boldsymbol{k}}\left[\hbar\omega_{\boldsymbol{k}}\hat{a}^\dagger_{\boldsymbol{k}}\hat{a}_{\boldsymbol{k}} - \sqrt{\frac{\hbar}{2\varepsilon_0\omega_{\boldsymbol{k}}}}\left(\hat{J}_{\boldsymbol{k}}\hat{a}^\dagger_{\boldsymbol{k}} + \hat{a}_{\boldsymbol{k}}\hat{J}^\dagger_{\boldsymbol{k}}\right)\right] \tag{1.11}$$

where $\omega_{\boldsymbol{k}} = c|\boldsymbol{k}|$. In Eqs (1.9) and (1.11) we have omitted the "zero point" energy $\sum_{\boldsymbol{k}}\hbar\omega_{\boldsymbol{k}}/2$, which can be eliminated by the renormalization procedure [58].

1.1.1 Nonequilibrium Green's functions

During the process of light-matter interaction the system under study sometimes is in a nonequilibrium. The so-called time-path approach that has been developed in the early works of Schwinger, Keldysh and others [59–63] is an appropriate way to describe the many-particle systems out of equilibrium. It is based on the concept of a closed time contour in the complex plane running parallel to the real-time axis and back (see Fig. 1.1). It involves the use of the time-ordered Green's functions (GFs) both on the lower and upper branches of the contour and gives rise to a doubling of the degrees of freedom. The

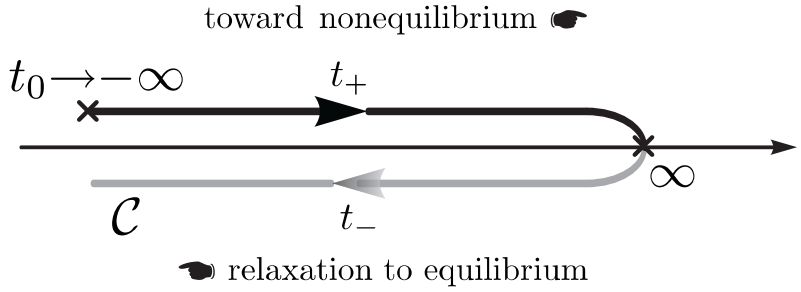

Figure 1.1: Time contour for time ordering in nonequilibrium.

doubling of degrees of freedom leads to a 2×2 matrix structure of propagators and self-energies. Physically, this is due to the fact that one has to calculate both the spectrum and the population of the interacting particle states.

The formalism of Green's functions can be constructed in the most convenient way using the method of *functional integration* [64–66]. The functional integration, originated from the Feynman path integral paradigm [67], is an alternative approach to the operator methods of ordinary quantum mechanics and quantum field theory (see Appendix A). It describes efficiently the entire set of the Feynman diagrams describing Green's functions or scattering amplitudes, the quantities containing the information about the system under consideration. This is the reason why the functional integrals became very popular tool among the field-theorists in last decades.

In Appendix B the basic methods of equilibrium QFT for the description of light-matter interaction are summarized. The equilibrium GFs merely describe only the intrinsic microscopic properties of the system. Electromagnetic fields, as well as charge densities there are considered as internal quantities. However in order to drive the considered system out of equilibrium an additional time dependent external perturbation is needed. To obtain a coupling of the system to the outside world, we have to introduce an external current density $\boldsymbol{J}^{\text{ext}}$ and an external charge density ρ_s^{ext}, which give rise to additional, explicitly time-dependent contributions to the interaction Hamiltonian (1.1),

$$\hat{V}^{\text{ext}}(t) = \int d^3\boldsymbol{r}\big[eZ_s\rho_s^{\text{ext}}(\boldsymbol{r},t)\hat{\phi}_s(\boldsymbol{r}) - \boldsymbol{J}^{\text{ext}}(\boldsymbol{r},t)\cdot\hat{\boldsymbol{A}}(\boldsymbol{r}) + \frac{(eZ_s)^2}{2m_s}\rho_s^{\text{ext}}(\boldsymbol{r},t)\hat{A}^2(\boldsymbol{r})\big]. \quad (1.12)$$

Here we have introduce the operator $\hat{\phi}_s$ that is dual to the density operator $\hat{\rho}_s$. The term $eZ_s\rho_s^{\text{ext}}\hat{\phi}_s$ in (1.12) describes then the coupling of externaly induced charges $eZ\rho^{\text{ext}}$ to the static electromagnetic potential $\langle\hat{\phi}\rangle$ of the medium. We assume that the reaction of the system back onto the external sources can be neglected so that we represent the effect of these fields by the c-number current and charge densities.

The Green functions for a non-equilibrium system are defined as

$$G_s(1,1') = \tfrac{1}{i\hbar}\langle \mathcal{T}_c \hat{\psi}_s(1)\hat{\psi}_s^\dagger(1')\rangle, \tag{1.13a}$$

$$D_{\mu\nu}(1,1') = \tfrac{1}{i\hbar\mu_0}\langle \mathcal{T}_c \hat{A}_\mu(1);\hat{A}_\nu(1')\rangle, \tag{1.13b}$$

$$D_{00}(1,1') = \tfrac{1}{i\hbar}\tfrac{1}{e^2 Z_s Z_{s'}}\langle \mathcal{T}_c \hat{\phi}_s(1);\hat{\phi}_{s'}(1')\rangle \tag{1.13c}$$

for electrons, transversal photons and longitudinal photons, respectively. Here the operator $\mathcal{T}_c$ orders the time argument along a contour, known as *the Keldysh contour* (see Fig. 1.1), connecting the two points t_1 and t_2 in the complex time plane. The operator $\mathcal{T}_c$ orders the time argument along a contour connecting the two points t_1 and t_2 in the complex time plane.

The photon GFs are defined in such a way that they describe the incoherent parts of the fluctuations of the transverse and longitudinal electromagnetic fields, such that

$$\langle \mathcal{T}_c \hat{\mathscr{A}}_\mu(1);\hat{\mathscr{A}}_\nu(1')\rangle = \langle \mathcal{T}_c \hat{\mathscr{A}}_\mu(1)\hat{\mathscr{A}}_\nu(1')\rangle - \langle \hat{\mathscr{A}}_\mu(1)\rangle\langle \hat{\mathscr{A}}_\nu(1')\rangle, \qquad \hat{\mathscr{A}} = \{\hat{\phi}_s, \hat{\boldsymbol{A}}\}. \tag{1.14}$$

In perturbation theory it should be possible to express the Green functions of the interacting system in terms of the equilibrium GFs. To that end we assume that in the remote past, prior to time t_i, the system has been brought to the equilibrium state characterized by temperature T. At this instant the interaction is switched on and the system evolves to time t. Then there exists a unitary time-evolution operator (the S-matrix)

$$\hat{\mathcal{S}}_c(t_2,t_1) = \mathcal{T}_c \exp\Big[-\frac{i}{\hbar}\int_{t_1}^{t_2} dt' \hat{V}^{\rm ext}(t')\Big] \tag{1.15}$$

which transforms the initial fields $\hat{\psi}_s^0$, $\hat{\boldsymbol{A}}^0$, and $\hat{\phi}^0$ into the Heisenberg field of the nonequilibrium system at time t_2 according to

$$\hat{\psi}_s = \hat{\mathcal{S}}_c^\dagger(t_2,t_1)\hat{\psi}_s^0\hat{\mathcal{S}}_c(t_2,t_1), \quad \hat{\boldsymbol{A}} = \hat{\mathcal{S}}_c^\dagger(t_2,t_1)\hat{\boldsymbol{A}}^0\hat{\mathcal{S}}_c(t_2,t_1), \quad \hat{\phi} = \hat{\mathcal{S}}_c^\dagger(t_2,t_1)\hat{\phi}^0\hat{\mathcal{S}}_c(t_2,t_1). \tag{1.16}$$

In Eq. (1.15) the interaction Hamiltonian $\hat{V}^{\rm ext}$ is expressed in terms of interaction-picture fields.

Let us pick a time t_f as some latest time after which the interaction is switched off. The successive contours connecting t_i to t, t to t_f, and t_f to t_i, may be joined together to form the contour $\mathcal{C}$ running from t_i to t_f and then back to t_i; see Fig. 1.1. We can then rewrite the expression (1.16) in the compact form (Eventually we shall take the limit $t_i \to -\infty$ and $t_f \to \infty$)

$$\hat{\psi}_s = \mathcal{T}_c\big[\hat{\mathcal{S}}_c^\dagger(\infty,-\infty)\hat{\psi}_s^0\hat{\mathcal{S}}_c(\infty,-\infty)\big] = \mathcal{T}_c\big\{\hat{\psi}_s^0 \exp\big[-\frac{i}{\hbar}\int_{\mathcal{C}} d1 \hat{V}^{\rm ext}(1)\big]\big\} \tag{1.17}$$

and the analogous expressions for $\hat{A}$ and $\hat{\phi}$ fields. The generalization on $\mathcal{T}_c$-ordered products of Heisenberg fields leads to the following expression for the contour ordered S-matrix functional of the non-equilibrium Green's functions:

$$\begin{aligned}\mathcal{S}_{\rm c}[J,\rho,\boldsymbol{J}^{\rm ph}] &= \frac{1}{\mathcal{Z}_0}\Big\langle \mathcal{T}_c \exp\big[-\frac{i}{\hbar}\int_{\mathcal{C}} d1(\hat{V}^{\rm ext}+J^*\hat{\psi}_s+\hat{\psi}_s^\dagger J_s+eZ_s\rho_s\hat{\phi}_s+\hat{\boldsymbol{A}}\cdot\boldsymbol{J}^{\rm ph})\big]\Big\rangle \\ &= \frac{1}{\mathcal{Z}_0}\int \mathcal{D}[\psi]\mathcal{D}[\phi]\mathcal{D}[\boldsymbol{A}]\exp\Big(-\frac{i}{\hbar}\mathscr{S}_{\mathcal{C}}[\psi,\phi,\boldsymbol{A},J,\rho,\boldsymbol{J}^{\rm ph}]\Big),\end{aligned} \tag{1.18}$$

where the time variable in the action functional $\mathscr{S}_{\mathcal{C}}$ runs along the time contour $\mathcal{C}$. The angular brackets indicate averaging with respect to some initial ensemble. The integration must be performed by taking into account the periodicity condition for the fields, i.e., the system that was driven out of equilibrium in the remote past evolves along the time contour back to this equilibrium state. In Eq. (1.18) the functional integration measures

$$\begin{aligned}\mathcal{D}[\psi] &= \prod_s d\psi_s^* d\psi_s = -\prod_s d\psi_s d\psi_s^*, \\ \mathcal{D}[\phi] &= \prod_s \frac{d\phi_s^* d\phi_s}{2\pi i}, \qquad \mathcal{D}[\boldsymbol{A}] = \frac{d^3\boldsymbol{A}^* d^3\boldsymbol{A}}{(2\pi i)^3}\end{aligned} \tag{1.19}$$

are introduced for fermionic (ψ) and bosonic ($\phi, \boldsymbol{A}$) fields.

The nonequilibrium GFs are defined in a similar way as the equilibrium ones [cf. Eqs (B.19), (B.21), (B.25)] and for two times defined on different parts of the contour they read as

$$G_s(\underline{1},\underline{1}') = \frac{\overrightarrow{\partial}}{\partial J_s^*(\underline{1})}\ln\mathcal{S}_{\rm c}[J,\rho,\boldsymbol{J}^{\rm ph}]\frac{\overleftarrow{\partial}}{\partial J_s(\underline{1}')}\Big|_{\substack{J=0\\ \rho=0\\ \boldsymbol{J}^{\rm ph}=0}}, \tag{1.20a}$$

$$D_{00}(\underline{1},\underline{1}') = -\frac{\varepsilon_0}{eZ_{s'}}\frac{\delta\langle\hat{\phi}_s(\underline{1})\rangle}{\delta\rho_{s'}^{\rm ext}(\underline{1}')} = \frac{\partial^2}{\partial\rho_s(\underline{1})\partial\rho_{s'}(\underline{1}')}\ln\mathcal{S}_{\rm c}[J,\rho,\boldsymbol{J}^{\rm ph}]\Big|_{\substack{J=0\\ \rho=0\\ \boldsymbol{J}^{\rm ph}=0}}, \tag{1.20b}$$

$$D_{\mu\nu}(\underline{1},\underline{1}') = -\frac{1}{\mu_0}\frac{\delta\langle\hat{A}_\mu(\underline{1})\rangle}{\delta J_\nu^{\rm ext}(\underline{1}')} = \frac{\partial^2}{\partial J_\mu^{\rm ph}(\underline{1})\partial J_\nu^{\rm ph}(\underline{1}')}\ln\mathcal{S}_{\rm c}[J,\rho,\boldsymbol{J}^{\rm ph}]\Big|_{\substack{J=0\\ \rho=0\\ \boldsymbol{J}^{\rm ph}=0}}, \tag{1.20c}$$

where $\underline{1}=(\boldsymbol{r}_1,t_1,\eta_1)$ and η refers to the upper ($\eta=+$) and lower ($\eta=-$) parts of the contour $\mathcal{C}$ (see Fig. 1.1). In Eq. (1.20) we have also defined the longitudinal and transverse photon GFs as variational derivatives in order to stress the physical meaning of these Green's functions. For example, $D_{\mu\nu}(\underline{1},\underline{1}')$ describes the response of the μ-th vector component of the effective field, $\langle\hat{A}_\mu\rangle$, at the Keldysh time-space coordinate $\underline{1}$ on the infinitesimal variation of the external current $J_\nu^{\rm ext}$ at $\underline{1}'$. Besides the effective fields $\langle\hat{\phi}_s\rangle$ and $\langle\hat{\boldsymbol{A}}\rangle$, other observable quantities of interest are the ensemble averaged induced source densities $\langle\hat{\rho}_s\rangle$ and $\langle\hat{\boldsymbol{J}}\rangle$, which are connected with the effective fields by the averaged Maxwell's equations

$$\nabla^2\langle\hat{\phi}_s(\boldsymbol{r},t)\rangle = -\frac{eZ_s}{\varepsilon_0}\big[\langle\rho_s(\boldsymbol{r},t)\rangle+\rho_s^{\rm ext}(\boldsymbol{r},t)\big] \tag{1.21}$$

$$\Box\langle\hat{\boldsymbol{A}}(\boldsymbol{r},t)\rangle = -\mu_0\big[\langle\hat{\boldsymbol{J}}(\boldsymbol{r},t)\rangle + \boldsymbol{J}^{\rm ext}(\boldsymbol{r},t)\big] \tag{1.22}$$

We refer the averaged sources $\langle\hat{\boldsymbol{J}}\rangle$ and $\langle\hat{\rho}_s\rangle$ as the induced sources, because in equilibrium these averages are zero. Nonzero current and charge density are induced in the medium by the perturbing fields.

A very elegant alternative representation of Green's function (1.20) has been given by Keldysh. Any quantity defined on the contour can be interpreted as a matrix, the indices of which are η_1 and $\eta_{1'}$. Then we have, for example

$$A(\underline{1},\underline{1}') = \begin{pmatrix} A^{++}(1,1') & A^{+-}(1,1') \\ A^{-+}(1,1') & A^{--}(1,1') \end{pmatrix} = \begin{pmatrix} A^{\rm c}(1,1') & A^{<}(1,1') \\ A^{>}(1,1') & A^{\rm a}(1,1') \end{pmatrix} \tag{1.23}$$

where A stands for G_s, D_{00}, or $D_{\mu\nu}$. The matrix elements of the nonequilibrium Green's functions are called "causal" (subscript c), "anticausal" (subscript a) Green's functions as well as lesser ($<$) and greater ($>$) components of Green's functions. To complete the apparatus of Green's functions, we introduce retarded and advanced Green's functions

$$A^{\rm ret/adv}(1,1') = \pm\theta(\pm[t_1 - t_{1'}])\big[A^{>}(1,1') - A^{<}(1,1')\big], \tag{1.24}$$

such that

$$\begin{aligned} &A^{\rm ret} = A^{\rm c} - A^{<} = A^{>} - A^{\rm a}, \quad A^{\rm adv} = A^{\rm c} - A^{>} = A^{<} - A^{\rm a}, \\ &A^{\rm ret} - A^{\rm adv} = A^{>} - A^{<}, \qquad A^{\rm ret} + A^{\rm adv} = A^{\rm c} - A^{\rm a}. \end{aligned} \tag{1.25}$$

The usefulness of retarded and advanced GFs is connected with their peculiar analytical properties in the complex frequency plane. Using these properties one can obtain these GFs from the Matsubara GFs by analytic continuation.

We finish this section by listing the *Langreth rules* [68] . Let us consider the following integral

$$C(\underline{1},\underline{1}') = \int_{\mathcal{C}} dt_2 A(\underline{1},\underline{2})B(\underline{2},\underline{1}'). \tag{1.26}$$

Using the Langreth rules one obtains (in short-hand notations):

$$C^{\gtrless} = \int_t \big[A^{\rm ret}B^{\gtrless} + A^{\gtrless}B^{\rm adv}\big], \quad C^{\rm ret} = \int_t A^{\rm ret}B^{\rm ret}, \quad C^{\rm adv} = \int_t A^{\rm adv}B^{\rm adv}. \tag{1.27}$$

For further references we write down the Langreth relations for the product of three functions

$$\begin{aligned} &D^{\gtrless} = \int_t \big[A^{\rm ret}B^{\rm ret}C^{\gtrless} + A^{\rm ret}B^{\gtrless}C^{\rm adv} + A^{\gtrless}B^{\rm adv}C^{\rm adv}\big] \\ &D^{\rm ret} = \int_t A^{\rm ret}B^{\rm ret}C^{\rm ret}, \qquad D^{\rm adv} = \int_t A^{\rm adv}B^{\rm adv}C^{\rm adv}. \end{aligned} \tag{1.28}$$

One should note, hovewer, that by evaluating self energies one accounts usually with the expressions like

$$C(\underline{1},\underline{1}') = \int_{\mathcal{C}} dt_2 A(\underline{1},\underline{2})B(\underline{1}',\underline{2}),$$

that stem for example from the polarization bubbles or self-energy's "shell"-diagrams for electrons. It can be shown that the Langreth relations (1.27) for this case read as [68]

$$\begin{aligned} C^{\rm ret}(t,t') &= A^{<}(t,t')B^{\rm ret}(t,t') + A^{\rm ret}(t,t')B^{<}(t,t') + A^{\rm ret}(t,t')B^{\rm ret}(t,t'), \\ C^{\gtrless}(t,t') &= A^{\gtrless}(t,t')B^{\gtrless}(t,t'). \end{aligned} \tag{1.29}$$

Despite the Eqs (1.20) determine the full GFs, it is rarely possible to evaluate the exact expressions for them. On the other hand, as we have mentioned already, the full Green's functions for the interacting system are connected with the free GFs via the so-called Dyson equations. The Dyson equations represent the iterative equations that couple the full and free GFs (i.e., GFs of non-interacting system) by the proper self-energy insertions. The perturbative quantum field theory is based on the calculation of the full GFs by truncation of the iteration procedure on some stage. The self-energies are also calculated in the appropriate approximations. For the case of the longitudinal and transverse photon fields the self-energies are the measurable density-density and current-current correlation functions that contribute to the screening and polarization effects in many-particle system. As it is shown in the next section, the transverse correlation function is essential for the description of absorption and amplification effects of light propagating in many-particle system.

1.1.2 Dyson equations, self-energies and medium characteristics

In this section we will derive the so-called Dyson equations for the nonequilibrium Green functions. Here we follow the strategy applied to the equilibrium temperature GFs which is outlined in Appendix B. Starting from the contour-ordered S-matrix functional (1.18) one gets the following expressions:

$$G_s^{-1}(\underline{1},\underline{1}') = G_s^{(0)-1}(\underline{1},\underline{1}') - \Sigma_s(\underline{1},\underline{1}') = \frac{\overrightarrow{\partial}}{\partial\psi_s^*(\underline{1})} \ln \mathcal{S}_{\rm c}[0,0,0] \frac{\overleftarrow{\partial}}{\partial\psi_s(\underline{1}')}\Big|_{\substack{\psi=0\\ \phi=0\\ \boldsymbol{A}=0}}, \tag{1.30a}$$

$$D_{00}^{-1}(\underline{1},\underline{1}') = D_{00}^{(0)-1}(\underline{1},\underline{1}') - e^2 Z_s Z_{s'} \Pi_{\parallel}(\underline{1},\underline{1}') = \frac{\partial^2}{\partial\phi_s(\underline{1})\partial\phi_{s'}(\underline{1}')} \ln \mathcal{S}_{\rm c}[0,0,0]\Big|_{\substack{\psi=0\\ \phi=0\\ \boldsymbol{A}=0}}, \tag{1.30b}$$

$$D_{\mu\nu}^{-1}(\underline{1},\underline{1}') = D_{\mu\nu}^{(0)-1}(\underline{1},\underline{1}') - P_{\mu\nu}(\underline{1},\underline{1}') = \frac{\partial^2}{\partial\mathcal{A}_\mu(\underline{1})\partial\mathcal{A}_\nu(\underline{1}')} \ln \mathcal{S}_{\rm c}[0,0,0]\Big|_{\substack{\psi=0\\ \phi=0\\ \boldsymbol{A}=0}}. \tag{1.30c}$$

It is, however, instructive to derive these equations starting from the equations of motion for the Green functions. Since the polarization function of the transversal photons is of the

main interest for the characterization of the optical properties of medium, we will restrict our attention on the equation of motion for the photon Green function only. The equation for $D_{\mu\nu}$ follows directly from Eq. (1.22) after variation with respect to the infinitesimal excitation $\delta\boldsymbol{j}^{\rm ext}$,

$$\Box_{\underline{1}}\frac{\delta\langle\hat{A}_\mu(\underline{1})\rangle}{\delta j_\nu^{\rm ext}(\underline{1}')} = -\mu_0\Box_{\underline{1}}D_{\mu\nu}(\underline{1},\underline{1}') = -\mu_0\Big[\frac{\delta\langle\hat{J}_\mu(\underline{1})\rangle}{\delta j_\nu^{\rm ext}(\underline{1}')} + \delta^\perp_{\mu\nu}(\underline{1}-\underline{1}')\Big]. \tag{1.31}$$

Transformation of the first term on the right hand side of Eq. (1.31) by using the chain rule yields[1]

$$\Box_{\underline{1}}D_{\mu\nu}(\underline{1},\underline{1}') - \int d\underline{2}P_{\mu\rho}(\underline{1},\underline{2})D_{\rho\nu}(\underline{2},\underline{1}') = \delta^\perp_{\mu\nu}(\underline{1}-\underline{1}'), \tag{1.32}$$

where we defined the photon polarization function

$$P_{\mu\nu}(\underline{1},\underline{1}') = -\mu_0\frac{\delta\langle\hat{J}_\mu(\underline{1})\rangle}{\delta\langle\hat{A}_\nu(\underline{1}')\rangle}. \tag{1.33}$$

Thus, the polarization can be viewed as the response of the induced currents in the medium on the variation of the effective electromagnetic field.

Let us now write Eq. (1.32) for different Keldysh components. The equation of motion for the $\gtrless$ components of photon GF,

$$D^{>}_{\mu\nu}(\boldsymbol{r},\boldsymbol{r}',t,t') = D^{<}_{\nu\mu}(\boldsymbol{r}',\boldsymbol{r},t',t) = \frac{1}{i\hbar\mu_0}\langle\hat{A}_\mu(\boldsymbol{r},t);\hat{A}_\nu(\boldsymbol{r}',t')\rangle, \tag{1.34}$$

is obtained from (1.32) by using the Langreth result (1.27) and reads as

$$\begin{aligned}\Box_1 D^{\gtrless}_{\mu\nu}(1,1') - \int d2\Big[P^{\rm ret}_{\mu\rho}(1,2)D^{\gtrless}_{\rho\nu}(2,1') + P^{\gtrless}_{\mu\rho}(1,2)D^{\rm adv}_{\rho\nu}(2,1')\Big]\\ = \int d2\Big[D^{{\rm ret}-1}_{\mu\rho}(1,2)D^{\gtrless}_{\rho\nu}(2,1') - P^{\gtrless}_{\mu\rho}(1,2)D^{\rm adv}_{\rho\nu}(2,1')\Big] = 0.\end{aligned} \tag{1.35}$$

Multiplying this expression on the right by $D^{\rm ret}$, one finally obtains the so-called *Optical Theorem*

$$D^{\gtrless}_{\mu\nu}(1,2) = \int d3\int d4\, D^{\rm ret}_{\mu\rho}(1,3)P^{\gtrless}_{\rho\lambda}(3,4)\, D^{\rm adv}_{\lambda\nu}(4,2). \tag{1.36}$$

This equation is called sometimes the fluctuation-dissipation theorem, since it establishes the relation between the quantum fluctuations described by $D^{\gtrless}$ and dissipation processes characterized by means of the current correlation functions $P^{\gtrless}$.

[1]Namely we have $\frac{\delta\langle J_\mu(\underline{1})\rangle}{\delta j_\nu^{\rm ext}(\underline{1}')} = \int d\underline{2}\frac{\delta\langle\hat{J}_\mu(\underline{1})\rangle}{\delta\langle\hat{A}_\rho(\underline{2})\rangle}\frac{\delta\langle\hat{A}_\rho(\underline{2})\rangle}{\delta j_\nu^{\rm ext}(\underline{1}')}$, where as usually summation over ρ is implied. The appearance of the transversal delta function is clearly understood by noting that $J_\mu^{\rm ext}(\underline{1}) = \int d\underline{2}\delta^\perp_{\mu\nu}(\underline{1}-\underline{2})j_\nu^{\rm ext}(\underline{2})$.

Let us now consider the equation of motion for the retarded Green's functions. From Eqs (1.32) and (1.27) one obtains the following equation

$$\Box_1 D^{\rm ret}_{\mu\nu}(1,1') - \int d2 P^{\rm ret}_{\mu\rho}(1,2) D^{\rm ret}_{\rho\nu}(2,1') = \delta^{\perp}_{\mu\nu}(1-1'), \tag{1.37}$$

which for the special case of steadily excited, spatially homogeneous medium can be solved by performing the Fourier transform as

$$D^{\rm ret}_{\mu\nu}(\boldsymbol{k},\omega) = \frac{\delta^{\perp}_{\mu\nu}(\boldsymbol{k})}{(\omega+i0^+)^2/c^2 - \boldsymbol{k}^2 - P_{\perp}(\boldsymbol{k},\omega)}. \tag{1.38}$$

This solution is equal to the ones obtained in Eq. (B.34) within the framework of Matsubara Green's functions.

The Keldysh components for the polarization function can be obtained from the contour ordered functional $\Phi_{\rm c}[G,D]$ in similar manner as it was done in Eq. (B.36) within the Matsubara formalism. Using the RPA approximation one obtains by means of the Fourier transform the retarded component of the dsusceptibility function in the form

$$\begin{aligned}\chi^{\rm ret}_{\mu\nu}(\boldsymbol{k},\omega) &= -\frac{1}{\mathfrak{v}}\sum_{s,\boldsymbol{q}}(eZ_s)^2 v_{\boldsymbol{k}} \frac{f(\varepsilon^s_{\boldsymbol{k}+\boldsymbol{q}}) - f(\varepsilon^s_{\boldsymbol{q}})}{\varepsilon^s_{\boldsymbol{k}+\boldsymbol{q}} - \varepsilon^s_{\boldsymbol{q}} - \hbar(\omega+i0^+)}\delta_{\mu\nu}(\boldsymbol{k}) \\ &= i\frac{e^2}{\omega^2\mathfrak{v}}\sum_s \int \frac{d\omega'}{2\pi} Z_s^2 \frac{\widehat{P}_{\mu\nu}(\boldsymbol{k},\omega')}{\omega-\omega'+i0^+},\end{aligned} \tag{1.39}$$

where in the last line the spectral polarization function $\widehat{P}_{\mu\nu}{=}{-}2\,{\rm Im}\,P^{\rm ret}_{\mu\nu}{=}P^{>}_{\mu\nu}{-}P^{<}_{\mu\nu}$ in the RPA approximation has been used. In the equilibrium $f(\varepsilon^s_{\boldsymbol{k}})$ is found to be the Fermi-Dirac distribution function. For the general nonequilibrium problem one is forced to solve the quantum Boltzmann equation in order to determine $f(\omega)$. Another way to calculate the susceptibility function (1.39) is to obtain the spectral polarization function $\widehat{P}$ by solving the so called Kadanoff-Baym equations for $P^{\gtrless}$ [60, 69]. In Chapter 3, where we consider the two band model for semiconductor media, we will use the third method for the calculation of $\chi(\boldsymbol{k},\omega)$ based on the Bloch equations for the interband polarizations.

1.2 Quantum coherence and nonclassical states

The recent developments of experimental techniques render it possible to perform a complete characterization of rather elementary quantum states of light and matter by quantum-state tomography [70] or related methods, for a review see [71]. Such a characterization includes the knowledge of the correlation properties of the considered quantum system. For the example of quantized radiation fields methods have been proposed that even allow one to detect high-order correlation functions of the most general type by balanced homodyne correlation measurements [72].

The correlation properties of optical radiation fields are ultimatelly connected with the fundamental concept of coherence. This concept is observed in interferometric experiments. Two optical beams are called coherent if interference is observed when two beams overlap at the same temporal and spatial position. The classical Young's experiment shows the interference between two beams from two slits (see Fig. 1.2). The visibility of the interference fringe is determined by the first-order coherence of light, and is described by the first-order correlation function of the electric field at two spatial and temporal positions:

$$\Gamma_{12}^{(1)}(\boldsymbol{r}_1, \boldsymbol{r}_2, t_1, t_2) = \langle \hat{E}_1^{(-)}(\boldsymbol{r}_1, t_1) \hat{E}_2^{(+)}(\boldsymbol{r}_2, t_2) \rangle. \tag{1.40}$$

On the other hand, the information on the fluctuations of light is enclosed in the second-order correlation function. In the famous detection scheme proposed by Hanbury and Twiss [73] one can measure the intensity correlation function. In this experiment, an incoming field is split into two channels by using a semi-transparent plate (beam splitter), and split beams are detected by two photodetectors located at the different spatial regions $\boldsymbol{r}_1$ and $\boldsymbol{r}_2$. The joint photon counting rate at the two detectors is proportional to the (normally- and time-ordered) second-order correlation function

$$\Gamma^{(2)}(\boldsymbol{r}_1, \boldsymbol{r}_2; t_1, t_2) = \langle \hat{E}^{(-)}(\boldsymbol{r}_1, t_1) \hat{E}^{(-)}(\boldsymbol{r}_2, t_2) \hat{E}^{(+)}(\boldsymbol{r}_2, t_2) \hat{E}^{(+)}(\boldsymbol{r}_1, t_1) \rangle. \tag{1.41}$$

Here and in the following discussion the time ordering is chosen in such a way that $t_1 \leq t_2$. The dimensionless second-order crrelation function directly follows from (1.41):

$$g^{(2)}(\boldsymbol{r}_1, \boldsymbol{r}_2; t_1, t_2) = \frac{\langle \hat{a}^\dagger(\boldsymbol{r}_1, t_1) \hat{a}^\dagger(\boldsymbol{r}_2, t_2) \hat{a}(\boldsymbol{r}_2, t_2) \hat{a}(\boldsymbol{r}_1, t_1) \rangle}{\langle \hat{a}^\dagger(\boldsymbol{r}_1, t_1) \hat{a}(\boldsymbol{r}_1, t_1) \rangle \langle \hat{a}^\dagger(\boldsymbol{r}_2, t_2) \hat{a}(\boldsymbol{r}_2, t_2) \rangle}. \tag{1.42}$$

The classical analog of (1.41)

$$\Gamma_{\rm cl}^{(2)}(\boldsymbol{r}_1, \boldsymbol{r}_2; t_1, t_2) = \overline{\mathcal{E}^{(-)}(\boldsymbol{r}_1, t_1) \mathcal{E}^{(-)}(\boldsymbol{r}_2, t_2) \mathcal{E}^{(+)}(\boldsymbol{r}_2, t_2) \mathcal{E}^{(+)}(\boldsymbol{r}_1, t_1)} \tag{1.43}$$

can also be expressed as the correlation function $\overline{\mathcal{I}(t_2)\mathcal{I}(t_1)}$ of the light intensity $\mathcal{I}$. This is not the case for the quantum expression (1.41), where the normal and time order must be conserved.

Such a feature has an important consequence. Semi-classical results such as (1.43) are submitted to some mathematical restrictions which can be violated by quantum fields. For example one can show that any classical field contributes to a photoelectron "*bunching*". Based on the Schwarz-type inequality $\overline{\mathcal{I}(t_2)\mathcal{I}(t_1)}^2 \leq \overline{\mathcal{I}^2(t_2)}\ \overline{\mathcal{I}^2(t_1)}$ one can derive the following classical inequalities [74]:

$$\Gamma_{\rm cl}^{(2)}(t_1, t_2) \leq \Gamma_{\rm cl}^{(2)}(t_1, t_1), \quad g_{\rm cl}^{(2)}(t_1, t_2) \leq g_{\rm cl}^{(2)}(t_1, t_1). \tag{1.44}$$

For classical fields, the probability of detecting a second photoelectron is maximum for $t_2 = t_1$, immediately after the detection of the first one.

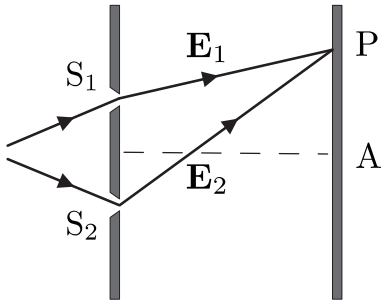

Figure 1.2: Schematic diagram of Young's double slit experiment. Two monochromatic light beams emerging from the slits S_1 and S_2 interfere to form on the observing screen an interference pattern, symmetrical about the point A. The visibility of the interference fringe on the screen point P at time t is described by the correlation function $\langle \hat{E}_1^{(-)}(\boldsymbol{r}_1, t-t_1)\hat{E}_2^{(+)}(\boldsymbol{r}_2, t-t_2)\rangle$.

Experimental evidence for this bunching effect has been first given by Hanbury-Brown and Twiss [73]. Bunching always occurs for chaotic light sources (such as stars or discharges) but there exist fields that violate inequality (1.44) and exhibit an "*antibunching*" behavior. Such fields are said to reveal non-classical properties since some observable signal cannot be reproduced by any classical field. We define the *nonclassical states* as the quantum states, whose quantum statistical properties cannot be described within the classical probability theory. For example, the antibunched light is nonclassical, since the violation of of Scwarz-type inequality (1.44) provides that the classical procedure of statistical averaging of the field correlation functions fails to describe correctly the outcomes of the measurements.

Before we discuss another intersting example of non-classical behavior of quantized optical radiation field we firstly consider the photodetection process. A photodetector measuring an electromegnetic mode converts photons in photoelectrons hence giving rise to an elctric current, called photocurrent $\hat{i}$. It is therefore natural to assume that the mean value of this photocurrent recorded during the (small) time interval $t, t+\Delta t$ is proportional to the normally ordered energy flow of the incident photons, i.e.,

$$\hat{i}(t,\Delta t)=\eta \int_t^{t+\Delta t} dt' \hat{I}(t') = 2\eta\varepsilon_0 c \int_t^{t+\Delta t} dt' \hat{E}^{(-)}(t')\hat{E}^{(+)}(t'). \tag{1.45}$$

where η is a constant depending on the detector called the quantum efficiency For a single mode field $\hat{E}^{(+)}$ is proportional to $\hat{a}$, so that $\hat{i}$ is proportional to $\hat{n}=\hat{a}^\dagger\hat{a}$. The probability that a photon detector registers n counting events when exposed Δt seconds to the light

is given by [75]

$$\mathcal{P}_n(t,\Delta t)=\frac{1}{n!}\Big\langle :\big[\hat{i}(t,\Delta t)\big]^n\exp\big[-\hat{i}(t,\Delta t)\big]:\Big\rangle. \tag{1.46}$$

We note that according to Eq. (1.46) the information lying in the phase of the field is completely lost in direct photodetection.

Let us now discuss the character of the photon distribution statistics. In the semiclassical model of photodetection the variance of the distribution $\mathcal{P}_n$ satisfies the following classical inequality

$$\overline{\Delta n^2}=\overline{n^2}-\overline{n}^2\geq\overline{n}, \tag{1.47}$$

where $\overline{n}$ is proportional to the classical intensity $\mathcal{I}$. In other words, the distribution $\mathcal{P}_n$ is always super-Poissonian for a classical field, i.e., the variance $\overline{\Delta n^2}$ greater than the variance $\bar{n}$ of the Poissonian distribution. In the particular case of the coherent light the random counts are distributed according to the Poissonian law. The observation of a sub-Poissonian distribution constitutes an experimental manifestation of the quantum nature of light. Let us rewrite the variance of the photocount distribution (1.46) as ($\hat{n}=\hat{a}^\dagger\hat{a}$)

$$\langle\Delta\hat{n}^2(t)\rangle=\langle\hat{n}(t)\rangle\big(1+Q(t)\big), \tag{1.48}$$

with [76]

$$Q(t)=\frac{\langle\Delta\hat{n}^2(t)\rangle-\langle\hat{n}(t)\rangle}{\langle\hat{n}(t)\rangle}=\frac{\langle\hat{n}(t)\rangle}{T^2}\int_{-T}^{T}d\tau(T-|\tau|)\Big\{g^{(2)}(t,t+\tau)-1\Big\}. \tag{1.49}$$

For the special case of a single-mode stationary field, Eq. (1.49) can be rewritten as

$$Q=\langle\hat{n}\rangle\big(g^{(2)}(0)-1\big). \tag{1.50}$$

The function Q characterizes the deviation of the variance from the Poissonian ones and is called the Mandel parameter. For nonclassical light one may get $Q<1$, which coincides with the requirement for $g^{(2)}(0)$ to be smaller than the corresponding coherence function, $g^{(2)}_{\rm coh}=1$, for the coherent light. Eq. (1.50) represents the special relationship between the sub-Poissonian statistics and the antibunching effect.

One should note, however, that sub-Poissonian photon-counting statistics need not imply photon antibunching, but can be accompanied by photon bunching [77]. This difference follows from the different nature of quantum measurements involved in the determination of the photon-counting statistics and bunching effects. A measurement of $g^{(2)}$, defined in Eq. (1.42), can focus on the few events where two photons are emitted close together. It provides an example of a conditional quantum measurement. In contrast to this, a nonconditional measurement, of the Mandel Q parameter, looks at the photon flux without regard to when a previous photon might have been emitted.

1.2.1 Quasi-probability distributions

So far we have considered the general theory of light interaction with bulk matter. Based on methods of Green's functions we are able to describe also other systems involved in usual optical experiments, such as photodetectors, interferometers, cavities and beam-splitters to name just a few. The object of interest in problems dealing with a radiation field interacting with these optical instruments is the reduced density matrix for the field. The reason is that usually we are dealing with a problem involving an infinite number of degrees of freedom, whereas measurements are in practice only made on a few of these. In the following discussion we will assume, just for simplicity, that measurements are made on the radiation field and not on the other systems with which it interacts. Mathematically we say that the observables of interest have the form

$$\hat{\mathcal{O}} = \hat{\mathcal{O}}_{\rm sys} \otimes \hat{\mathbf{1}}_{\rm ir}, \tag{1.51}$$

where the subscript "sys" refers to the system of the interest, e.g., radiation field or radiation field plus detector, etc., and the subscript "ir" refers to all other irrelevant systems; $\hat{\mathbf{1}}_{\rm ir}$ is the identity operator for these latter systems. Now the evaluation of the expectation value of the observable (1.51) reduces to the partial tracing of the product of $\hat{\mathcal{O}}_{\rm sys}$ with the reduced density matrix $\hat{\rho}_{\rm sys}= {\rm Tr}_{\rm ir}\{\hat{\rho}_{\rm sys} \otimes \hat{\rho}_{\rm ir}\}$. In the following we shall omit the subscript sys when we deal with optical fields and write simply $\hat{\rho}$. In terms of the functional integration the partial tracing operation, ${\rm Tr}_{\rm ir}$, is equivalent to the functional integration over all irrelevant fields. This integration can be easily performed since the functional integrals are merely Gaussian-type. In this way the exact action functional can be replaced with some effective action, which does not depend on the irrelevant variables.

In the previous section we have introduced the notion of nonclassicality. As we have seen the nonclassical radiation exhibits quantum statistical properties that cannot be explained in terms of classical probability theory. One rise the question how one can conveniently characterize these nonclassical fields. In this section we introduce the so-called quasi-probability distribution functions and their characteristic functions. These functions appear to be quite useful for the calculation of the moments of field operators with a certain ordering prescription.

Following R. Glauber it is convenient to introduce the so-called R-distribution, which is given by the matrix elements of the density matrix $\hat{\rho}$ in the coherent state basis as

$$R(\alpha,\alpha') = \langle\alpha|\hat{\rho}|\alpha'\rangle \exp\Big[\frac{1}{2}(|\alpha|^2 + |\alpha'|^2)\Big], \tag{1.52}$$

such that the density matrix can be written as

$$\hat{\rho} = \int \mathcal{D}[\alpha]\mathcal{D}[\alpha']|\alpha\rangle\langle\alpha'|R(\alpha,\alpha') \exp\Big[-\frac{1}{2}(|\alpha|^2 + |\alpha'|^2)\Big], \tag{1.53}$$

where the integration measure is defined as $\mathcal{D}[\alpha]=\frac{1}{2\pi i}d\alpha^* d\alpha$.

Since we are mostly interested in quantum statistical properties of the radiation, it is convenient to introduce the generating functions for field correlation functions with the certain ordering prescriptions for products of field operators. Using the definition of R-function (1.52) we introduce the so-called *quasi-probability functions*:

$$W(\alpha) = \frac{2}{\pi} e^{2|\alpha|^2} \int \mathcal{D}[\beta] R(-\beta,\beta) e^{-|\beta|^2+2(\beta^*\alpha-\beta\alpha^*)}, \tag{1.54a}$$

$$P(\alpha) = \frac{2}{\pi} e^{|\alpha|^2} \int \mathcal{D}[\beta] R(-\beta,\beta) e^{\beta^*\alpha-\beta\alpha^*}, \tag{1.54b}$$

$$Q(\alpha) = \frac{1}{\pi} R(\alpha,\alpha) e^{-|\alpha|^2}, \tag{1.54c}$$

known as the Wigner [78], Glauber-Sudarshan [1, 79], and Husimi-Kano [80, 81] quasi-probability functions, respectively. The notion "quasi-probability distributions" steams from the analogy with the classical probability theory. In contrast to the classical joint-distribution functions defined in the phase-space that should obey the standard Kolmogorov axioms for probabilities [82], the quasi-probability distributions are not restricted to be positive definite functions. This happens due to the Heisenberg's uncertainty principle. Indeed, the quantum analog of classical joint probability function that characterizes the probability to measure simultaneously the two orthogonal quadratures

$$\hat{x}(\phi)=\hat{a}e^{i\phi}+\hat{a}^\dagger e^{-i\phi}, \quad \hat{x}(\phi+\pi/2)=[\hat{a}e^{i\phi}-\hat{a}^\dagger e^{-i\phi}]/i \tag{1.55}$$

could become negative or ill-behaved and for these reasons we should call it quasi-probability distribution.

The quasi-probability functions (1.54) can also be obtained in the unified way from the so called s-parameterized distribution

$$P(\alpha,s) = \frac{1}{\pi} \int \mathcal{D}[\beta] C(\beta,s) e^{\beta^*\alpha-\beta\alpha^*}, \tag{1.56}$$

where

$$C(\beta,s) = \exp[s|\beta|^2/2] \int \mathcal{D}[\alpha] \langle\alpha|\hat{\rho} e^{\beta\hat{a}^\dagger-\beta^*\hat{a}}|\alpha\rangle \tag{1.57}$$

is the s-parameterized characteristic function. The s-parameterized distribution (1.56) with s=0, s=1, s=−1 correspond to $W(\alpha)$, $P(\alpha)$ and $Q(\alpha)$ functions, respectively. The s-parameterized functions can be expressed one through another as [57, 83]

$$P(\alpha,s) = \int \mathcal{D}[\beta] e^{\alpha\beta^*-\alpha^*\beta+\frac{1}{2}(s-s')|\beta|^2} \int \mathcal{D}[\gamma] e^{\beta\gamma^*-\beta^*\gamma} P(\gamma,s'). \tag{1.58}$$

The s-parameterized characteristic functions with s=0, s=1, s=−1 are called the *symmetric-* (denoted as C_W), *normal-* (C_P) and *antinormal-* (C_Q) *characteristic functions*. As it is clear from their names, by using these generation functions one obtains the

moments of photon-modes operators with the corresponding ordering of the field operators, namely

$$\langle\{(\hat{a}^\dagger)^k\hat{a}^l\}_{\rm sym}\rangle = \frac{\partial^k}{\partial\beta^k}\frac{\partial^l}{\partial(-\beta^*)^l}C_W(\beta)\Big|_{\beta=0}, \tag{1.59}$$

$$\langle(\hat{a}^\dagger)^k\hat{a}^l\rangle = \frac{\partial^k}{\partial\beta^k}\frac{\partial^l}{\partial(-\beta^*)^l}C_P(\beta)\Big|_{\beta=0}, \tag{1.60}$$

$$\langle\hat{a}^k(\hat{a}^\dagger)^l\rangle = \frac{\partial^k}{\partial\beta^k}\frac{\partial^l}{\partial(-\beta^*)^l}C_Q(\beta)\Big|_{\beta=0} \tag{1.61}$$

where $\{f(\hat{a},\hat{a}^\dagger)\}_{\rm sym}$ denotes the operations of the symmetric ordering of the given expression f. There are the following relations between the characteristic functions:

$$C_P(\beta) = C_W(\beta)e^{|\beta|^2/2}, \qquad C_Q(\beta) = C_W(\beta)e^{-|\beta|^2/2}, \tag{1.62}$$

which can be obtained from Eq. (1.57) using the Baker-Campbell-Hausdorff formula [84].

We have seen in Sec. 1.2 that the experimentally measured field correlation functions are the averages of normally-ordered products of field operators. Therefore, the P-function and its characteristic function are the natural object of study of nonclassicality. Indeed, similar to the characteristic function C_P the P-function can be used for the construction of the averages of normally-ordered polynomial functions of field operators. For example, the photodetection formula (1.46) can be written as

$$\mathcal{P}_n = \int\mathcal{D}[\alpha]\mathcal{P}_n(\alpha,\underline{\eta}) = \pi\int\mathcal{D}[\alpha]P(\alpha)\frac{(\underline{\eta}|\alpha|^2)^n}{n!}\exp\left[-\underline{\eta}|\alpha|^2\right], \tag{1.63}$$

where $P(\alpha)$ is the P-function of the detected field and $\underline{\eta}{=}\eta\hbar\omega$ is the dimensionless quantum efficiency of the detector. We note, that this expression can be inverted, i.e., the P-function can be expressed through $\mathcal{P}_n$, in the case of a diagonal density matrix in n-representation.

Another remarkable property of the P-function is that it diagonalizes the density matrix in coherent state basis, i.e.,

$$\hat{\rho} = \pi\int\mathcal{D}[\alpha]P(\alpha)|\alpha\rangle\langle\alpha|. \tag{1.64}$$

Because the operators $|\alpha\rangle\langle\alpha|$ do not constitute a complete set, the P-representation may not always exist as a regular function.

1.2.2 Example of squeezed light generation in parametric optical process

Usually the most useful experimental methods for generating nonclassical states rely on nonlinear optical techniques. The quantum state exhibiting classical statistical properties

can be transformed into the nonclassical state due to the nonlinear coupling with matter. For example, the nonclassical squeezed coherent light can be produced in a four-wave mixing process by pomping with the coherent light a $\chi^{(3)}$ nonlinear crystal [85].

Let us consider the time evolution of some definite classical state in a nonlinear medium. As an example, we consider the simple model for classical state that is known in quantum optics as *the model of signal-noise superposition* (SN model) and concentrate on the single mode case. The Hamiltonian of such system has the form [cf. with Eq. (1.9)]

$$\hat{H}^{\rm SN} = \hbar\omega\hat{a}^\dagger\hat{a} - \sqrt{\frac{\hbar\mu_0 c}{2\omega}}\big(J\hat{a}^\dagger + \hat{a}J^*\big). \tag{1.65}$$

Here we have assumed that the medium was excited by the coherent external currents $\boldsymbol{J}^{\rm ext}$ with large amplitude such that

$$J = \sum_{p=1,2}(\boldsymbol{e}_p\cdot\boldsymbol{J}); \qquad \boldsymbol{J} = \boldsymbol{J}^{\rm par} + \frac{1}{2}\boldsymbol{J}^{\rm dia} + \boldsymbol{J}^{\rm ext} \tag{1.66}$$

is a purely c-number total current density of the medium.

In thermal equilibrium with a thermostat at the temperature T and in the presence of the time-independent currents J, J^* the Gibbs canonical distribution function has the form

$$\hat{\rho}^{\rm SN} = \frac{1}{\mathcal{Z}^{\rm SN}}e^{-\beta\hat{H}^{\rm SN}}, \quad \beta{=}1/k_{\rm B}T \tag{1.67}$$

where the partition function $\mathcal{Z}^{\rm SN}{=}\,{\rm Tr}\{e^{-\beta\hat{H}^{\rm SN}}\}$ is given by

$$\mathcal{Z}^{\rm SN}{=}\int\mathcal{D}[z]\exp\Big(-\frac{1}{\hbar}\mathscr{S}^{\rm SN}[z]\Big){=}(\bar{N}_{\rm th}{+}1)\exp\Big[\beta|\tilde{J}|^2/\hbar\omega\Big], \tag{1.68}$$

where $\tilde{J}{=}\sqrt{\frac{\hbar\mu_0}{2\omega}}J$,

$$\mathscr{S}^{\rm SN}[z] = \int_0^{\hbar\beta}d\tau\{z^*\frac{\partial}{\partial\tau}z + \langle z|\hat{H}^{\rm SN}|z\rangle\} \tag{1.69}$$

is the action functional, and $\bar{N}_{\rm th}{=}(e^{\beta\hbar\omega}{-}1)^{-1}$ is the occupation number of the field mode in thermal equilibrium. It is easy to check by direct calculations that the statistical properties of the field described by the density matrix (1.67) are fully classical.

We assume that at time $t{=}0$ our model system starts to interact with a nonlinear media whose polarization is proportional to the square of the electric field. The interaction with the medium can be written than as

$$\hat{V}(t) = \hbar\frac{\lambda}{2}\big\{\hat{a}^2e^{2i\omega t-i\phi} + (\hat{a}^\dagger)^2e^{-2i\omega t+i\phi}\big\}. \tag{1.70}$$

This interaction describes parametric excitation of the medium and involves additional pumping field in the coherent state with amplitude proportional to $\lambda e^{i\phi}$ and frequency $\omega_p{=}2\omega$. We refer to this model as to the *degenerate parametric oscillator* (DPO) model.

The evolution of the system (1.67) is governed by the evolution operator

$$\hat{U}(t)=\mathcal{T}\exp\{-\frac{i}{\hbar}\int_0^t \hat{V}(t')dt'\}, \tag{1.71}$$

according the formula

$$\hat{\rho}^{\rm DPO}(t)=\hat{U}(t)\hat{\rho}^{\rm SN}(0)\hat{U}^{\dagger}(t). \tag{1.72}$$

Combining Eqs (1.72) and (1.52) we obtain the time dependent R-function for our problem

$$R_{\rm DPO}(\alpha,\alpha';t)=e^{(|\alpha|^2+|\alpha'|^2)/2}\int \mathcal{D}[\beta]\mathcal{D}[\beta']\langle\alpha|\hat{U}(t)|\beta\rangle\langle\beta|\hat{\rho}^{\rm SN}(0)|\beta'\rangle\langle\beta'|\hat{U}^{\dagger}(t)|\alpha'\rangle. \tag{1.73}$$

Using the functional integral techniques for imaginary time GFs (see Appendix B) one can easily obtain for the density matrix (1.67) the following expression for the matrix element

$$\begin{aligned}\langle\alpha|\hat{\rho}^{\rm SN}(0)|\alpha'\rangle&=\frac{1}{\mathcal{Z}^{\rm SN}}e^{-(|\alpha|^2+|\alpha'|^2)/2}\int\mathcal{D}[z]\exp\big[-\frac{1}{\hbar}\mathscr{S}^{\rm SN}[z]+\frac{1}{2}\{\alpha^* z(\hbar\beta)+\alpha' z(0)\}\big]\\&=\frac{1}{\bar{N}_{\rm th}+1}\langle\alpha|\alpha'\rangle\exp\Big[-\frac{1}{\bar{N}_{\rm th}+1}(\alpha'-\frac{\tilde{J}}{\hbar\omega})(\alpha^*-\frac{\tilde{J}}{\hbar\omega})\Big].\end{aligned} \tag{1.74}$$

The boundary conditions $z(0)=\alpha'$ and $z^*(\hbar\beta)=\alpha^*$ are accounted in Eq. (1.74) in the term added to the action [86], [64]. The matrix elements of the evolution operator in coherent-state basis are evaluated using the functional integral in real time representation:

$$\langle\alpha|\hat{U}(t)|\alpha'\rangle=e^{-(|\alpha|^2+|\alpha'|^2)/2}\int\mathcal{D}[z]\exp\big[-\frac{i}{\hbar}\mathscr{S}^{\rm DPO}[z;t]+\frac{1}{2}\{\alpha^* z(t)+\alpha' z^*(0)\}\big]. \tag{1.75}$$

The calculation of the matrix element of the evolution operator (1.75) was performed in [87] with the result

$$\langle\alpha|\hat{U}|\alpha'\rangle=\frac{e^{-(|\alpha|^2+|\alpha'|^2)/2}}{\sqrt{\cosh\lambda t}}\exp\Big[\frac{e^{-i\omega t}}{\cosh\lambda t}\Big\{\alpha'\alpha^*-\frac{i}{2}\sinh\lambda t(\alpha'^2e^{-i\phi+i\omega t}+(\alpha^*)^2e^{i\phi-i\omega t})\Big\}\Big]. \tag{1.76}$$

In order to explore the nonclassical properties of generated optical field such as sub-Poissonian statistics or antibunching, we calculate now the P-function for this field. We combine now Eqs. (1.73), (1.74), (1.76) and (1.54b). Performing the integration using successively the formula

$$\int\mathcal{D}[\beta]\exp[-s|\beta|^2+a\beta^*+b^*\beta+c(\beta^*)^2+d^*\beta^2]=\frac{1}{\sqrt{s^2-4cd^*}}\exp\frac{sab^*+c(b^*)^2+d^*a^2}{s^2-4cd^*}, \tag{1.77}$$

we finally obtain the P-function

$$P_{\rm DPO}(\alpha)=\frac{1}{\pi\sqrt{\mathscr{N}^2-\mathscr{M}^2}}\exp\Big[-\frac{\mathscr{N}\big|\alpha(t)-\tilde{\alpha}_0\big|^2+\mathscr{M}\,{\rm Im}\big\{e^{-i\phi}(\alpha(t)-\tilde{\alpha}_0)^2\big\}}{\mathscr{N}^2-\mathscr{M}^2}\Big], \tag{1.78}$$

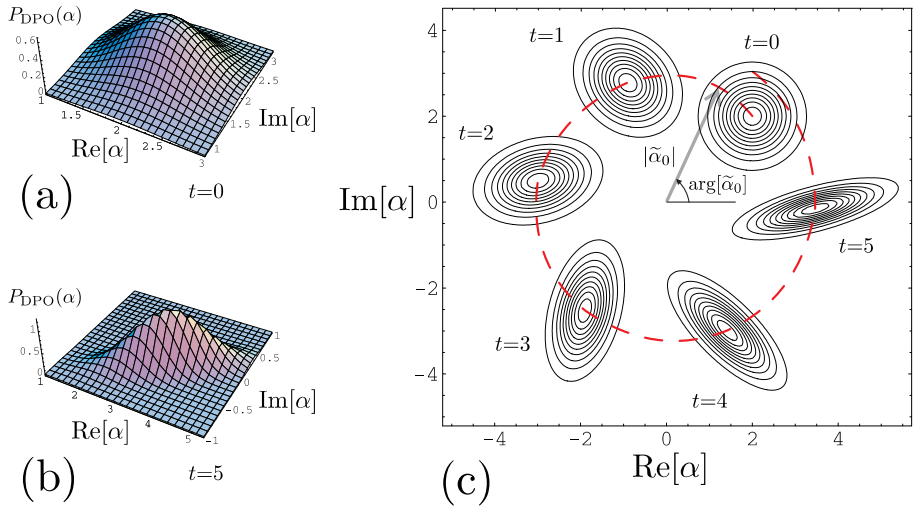

Figure 1.3: The P-function for DPO for t=0 (a); t=5 (b); countour plot of the time evolution of $P_{\rm PDO}(\alpha)$ for various times (c). The graphics are represented for the following parameters: $\bar{N}_{\rm th}$=0.2, λ=0.06,ω=$\pi/3$, α_0=$2\sqrt{2}e^{i\pi/4}$, and ϕ=$4\pi/3$.

where

$$\begin{aligned}\widetilde{\alpha}_0 &= \cosh\lambda t\alpha_0 - i\sinh\lambda t e^{i\phi}\alpha_0^*, \qquad \alpha_0{=}\tilde{J}/\hbar\omega \\ \mathscr{N} &= \bar{N}_{\rm th}\cosh 2\lambda t + \sinh^2\lambda t, \qquad \mathscr{M} = \left(\bar{N}_{\rm th}+1/2\right)\sinh 2\lambda t,\end{aligned} \tag{1.79}$$

and $\alpha(t)$=$\alpha e^{-i\omega t}$. Eq. (1.78) is valid if the condition

$$\mathscr{N}-\mathscr{M} = (2\bar{N}_{\rm th}+1)e^{-2\lambda t}-1 > 0, \tag{1.80}$$

is satisfied [88]. The violation of this condition will turn the P-function into a highly singular object. Fig. 1.3 shows the time evolution of the P-function (1.78) for parameters that satisfy this condition. Squeezing of the quasi-probability function along some direction (quadrature) means the reduction of quantum fluctuations in this quadrature with respect to the standard quantum limit, at the expense of increased fluctuations in the other one [89]. The light that exhibits these peculiar fluctuation properties is called a *squeezed light*. Thus, starting with the light field that exhibits classical behavior (SN model) at the initial moment of time we obtain the nonclassical squeezed light by the nonlinear process in DPO.

In order to investigate the nonclassical effects of the light generated in DPO, such as antibunching of photons and sub-Poissonian statistics of photocounts, with help of the P-function, we calculate the 2^{nd}-order correlation function

$$\begin{aligned}g^{(2)}(0){=}1{+}\frac{1}{\bar{n}^2}\Big[\bar{\mathscr{D}}&+\sinh^2\lambda t\cosh 2\lambda t \\ &+2\sinh\lambda t|\alpha_0|^2\Big\{\sinh 3\lambda t+\cosh 3\lambda t\sin(\phi{-}2\arg[\alpha_0])\Big\}\Big],\end{aligned} \tag{1.81}$$

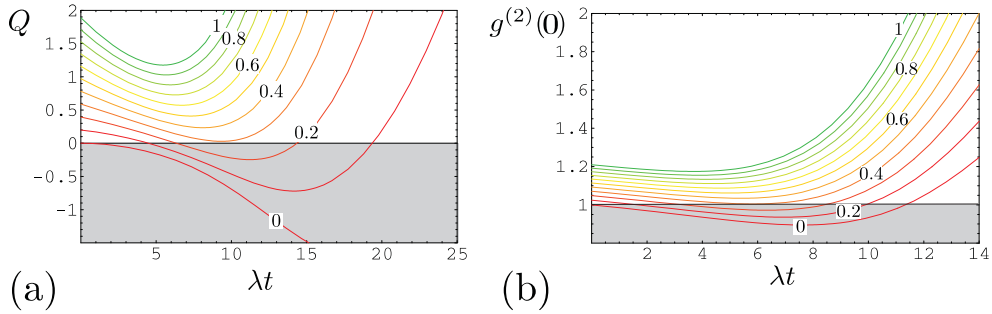

Figure 1.4: The Mandel parameter (a) and the normalized coherence function (b) are depicted for various values of $\bar{N}_{\rm th}$. The values of Q and $g^{(2)}(0)$ for which the output radiation field is nonclassical are indicated by the grey area.

where

$$\bar{n}{=}\langle\hat{a}^{\dagger}\hat{a}\rangle = \mathscr{N} + |\alpha_0|^2\big\{\cosh 2\lambda t + \sinh 2\lambda \sin(\phi - 2\arg[\alpha_0])\big\} \tag{1.82}$$

is the mean photon number and

$$\begin{aligned}\bar{\mathscr{D}} = \bar{N}_{\rm th}^2 \cosh 4\lambda t + 2\bar{N}_{\rm th}\sinh\lambda t \sinh 3\lambda t \\ + 2\bar{N}_{\rm th}|\alpha_0|^2\Big\{\cosh 4\lambda t + \sinh 4\lambda t \sin(\phi - 2\arg[\alpha_0])\Big\}.\end{aligned} \tag{1.83}$$

is the temperature dependent dispersion. Eqs (1.82) and (1.81) were firstly derived in [87] by using the technique of the thermodynamic generating functional. For vanishing temperature $\bar{N}_{\rm th}{\to}0$ and Eqs (1.82) and (1.81) coincide with the corresponding expressions derived in [90]. Setting $\alpha_0{=}0$ one obtains the result of [88] for the squeezed thermal state.

Using Eqs (1.82) and (1.81), we can calculate the Mandel parameter $Q{=}\bar{n}(g^{(2)}{-}1)$ [cf. Eq. (1.49)]. As it follows from the discussion in Sec. 1.2, light exhibits a sub-Poisson statistics if $Q{<}0$, i.e., the dispersion of photocount distribution is smaller than the mean photon number. This requirement is satisfied if the relation $\phi{-}2\arg[\alpha_0]{=}{-}\pi/2$ between the phases holds true. The increase of temperature, the positive term $\bar{\mathscr{D}}$ prevents a sub-Poissonian statistics. Similar to the case of sub-Poissonian statistics, the coherent field α_0 causes the antibunching effects characterized by negativity of $g^{(0)}{-}1$, whereas the thermal field $\bar{N}_{\rm th}$ destroys it. The functions Q and $g^{(2)}$ are shown in Fig. 1.4 for different temperatures and squeezing parameters λ. It is clearly seen that in the limiting case of a squeezed vacuum state (i.e., for $\alpha_0{=}0$ and $\bar{N}_{\rm th}{=}0$) light is bunched. The density matrix calculations for the squeezed vacuum yields $\rho_{nn}{=}\langle n|\hat{\rho}^{\rm DPO}|n\rangle{=}0$ for odd n, i.e., from the corpuscular point of view the squeezed vacuum consists of an even number of photons. Thus detected photons for this case tend to arrive on detector in pairs, which is the effect of bunching.

1.3 Conclusions

In the first part of this chapter we have summarized the basic methods used in the microscopic QED for the description of light interaction with matter. Starting from the microscopic Hamiltonian that describes light quanta coupled to the charged carriers (electrons, holes, etc.) and using the technique of functional integration we have derived the generating functional (S-matrix functional) for field and particle correlation functions. In this way, we have obtained the Green's functions as well as their equations of motion that describe the light-matter dynamics for both equilibrium and nonequilibrium situations. We have also considered the response of the system on the perturbation caused by interactions and we have related it to the self-energy contributions, charge-charge and density-density correlation functions.

In the second part of this chapter we have considered the coherence properties of ligh. We have introduced the notion of nonclassical light as an optical radiation field, which has the unusual (from the point of view of classical optics) quantum statistical properties. The effective method for the description of nonclassical light is based on the use of the so-called quasi-probability distributions. We have briefly introduced the quasi-probability distributions and their characteristic functions. Then we have discussed as an example the generation of nonclassical squeezed light in the parametric optical process. Using this example we discussed such nonclassical effects as sub-Poissonian statistics of photocounts and antibunching of photons. Here it has been demonstrated that the nonclassical properties can be suppressed or fully destoyed by increasing the thermal noise level in the system. In the next chapter we discuss the nonclassicality and its characterization by means of the P-function, its characteristic function, and normally-ordered correlation functions in more detail. The influence of the thermal fluctuations on the nonclassicality has been shown in Sec. 1.2.1 for the example of squeezed light. In the following chapter we proceed with the discussion of this subject and show that there exists some threshold for temperature, above which the system interacting with thermal bath looses its nonclassical features. The influence of the dispersion, absorption and amplification effects on the nonclassical properties of optical radiation propagating in complex material media will be considered in Chap. 3.

Chapter 2

Nonclassicality of Quantum Optical Systems with Losses

In the previous chapter we discussed that the electromagnetic field can be characterized by means of measurable field-field correlation functions such as intensity correlations and higher-order coherence functions. These correlation functions serve to a concise description of the statistical properties of the field spectra. Since there are nonclassical radiation fields, whose statistical properties cannot be described within the classical probability theory, it is desirable to obtain some nonclassicality criteria that allow one to distinguish between the classes of nonclassical and classical light fields.

The optical field correlation functions can be expressed through P-, Q- and Wigner quasi-probability functions and their corresponding characteristic functions in the form that closely resembles that of classical probability theory. In this context the quasi-probability functions are the closest analog of classical probability functions. Therefore, it is quite naturally to formulate the nonclassicality criteria as tests of quasi-probability functions for the violation of Kolmogorov axioms [82]. For example, one can consider the non-positive definite Wigner function as a candidate for testing nonclassicality. However, quadrature squeezing as well as sub-Poissonian statistics, being examples of nonclassicality, are still possible for some states with completely positive Wigner functions. This is explained by the fact that these features correspond to negative values of dispersions for some normally ordered observables, which are naturally determined via the Glauber-Sudarshan P-function.

Therefore, the class of states characterized by non-positive P-function is wider than the class of states characterized by non-positive Wigner function, sub-Poissonian statistics of photon counts and quadrature squeezing. Hence, following the works [91, 92], we will consider the nonclassicality as the non-positivity of the P-function. Unlike the case of the

Wigner function, this definition cannot be applied directly because of a strongly singular behavior of the P-function for nonclassical states.

Usually the quantum system cannot be isolated from the surrounding environment so that the nonclassical properties are affected by the presense of various noise sources. For example, the nonclassical light being brought in the contact with a large thermal reservoir evolves into the purely classical one after some definite time. On the other hand, if the nonclassical light propagates through the optical devices (e.g. mirrors, beam-splitters, cavities) its nonclassical properties are reduced due to the absorption, scattering, dephasing and damping processes in these devices. In this chapter we consider some models of such noisy systems.

This chapter is organized as follows. In Sec. 2.1 we reformulate the Bochner criterion for testing nonclassicality in terms of the P-function and its characteristic function. Then we investigate the influence of various noise sources on nonclassical properties of quantum systems. Firstly in Sec. 2.2, we discuss the influence of thermal noise on the nonclassicality of radiation fields interacting with a thermal bath. We present here two techniques for the calculation of quasi-probability distributions, namely the methods of functional integration and the input-output formalism. Some simple applications to quantum-optical systems are also discussed. Finally, in Sec. 2.3 we introduce the method of replacement schemes for the characterization of unwanted noise channels in realistic optical cavities. These beam-splitter-based schemes effectively describe the noise-induced mode coupling between intracavity and input modes. The application of this coupling effect to the problem of unbalanced and cascaded homodyne detection of the intracavity mode is discussed.

2.1 Characterization of nonclassicality

In this section we discuss the characterization of nonclassicality of arbitrary quantum systems taking into account that in many situations the P-function cannot be reconstructed experimentally. In order to make this characterization accessible to experimentators, the final expression of the criterion for nonclassicality should be formulated in terms of the Wigner function or its characteristic function, which can be reconstructed using the quantum tomography methods [71]. Thus, our strategy is the following: we firstly formulate the condition for a quantum state to be nonclassical in terms of the P-function and its characteristic function, then, using Eq. (1.58) which relates the P-function to the Wigner function (or alternatively Eq. (1.62), which relates their characteristic functions) we reformulate this condition in terms of measurable quantities.

The quasi-probability functions serve as the closest analogs of the classical joint probability functions. However the P- and Wigner functions could be nonpositive defined or

ill-behaved functions for the nonclassical quantum states and thus cannot be true classical joint probability distributions. One can consider this feature of quasi-probability functions as a test on nonclassicality. Hence, it is natural to adopt the so-called Bochner criterion [93] for testing the nonclassicality [92]. Arguing in this way, we conclude that the P-function is positive-definite (in other words, it can be interpret as probability function) if and only if for any function $f(\alpha) \in \mathbb{C}$ with compact support the following inequality is satisfied

$$\int \mathcal{D}[\alpha]\mathcal{D}[\beta]\, C_N(\alpha-\beta) f(\alpha) f^*(\beta) \geq 0. \tag{2.1}$$

Thus, the necessary and sufficient condition for the P-function of some nonclassical state to violate the Kolmogorov axioms for probability functions can be reformulated in terms of its characteristic function. In order to test quantum states with respect to nonclassicality, it is sufficient to find such a function $f(\alpha)$ that violates the inequality (2.1).

An important example is the discrete variant of the Bochner criterion, when this function is taken in the form

$$f(\alpha) = \sum_k \xi_k\, \delta(\alpha - \alpha_k), \tag{2.2}$$

where ξ_k, α_k are some arbitrary complex numbers. The experimental implementation of this criterion for optical fields was described in [94].

The inequality (2.1) can be rewritten in another equivalent form. For this purpose we introduce the object $\mathcal{W}(\alpha)$, which following [95] we will refer as *the witness function* and define it as

$$\mathcal{W}(\alpha) = |g(\alpha)|^2 \geq 0, \tag{2.3}$$

where $g(\alpha)$ is the Fourier image of $f(\alpha)$. It is easy to see, that the inequality (2.1) takes now the following form

$$\overline{\mathcal{W}} = \int \mathcal{D}[\alpha]\, P(\alpha)\mathcal{W}(\alpha) \geq 0. \tag{2.4}$$

Put it differently, the expression (2.4) means that the mean value, $\overline{\mathcal{W}}$, of some operator $\hat{\mathcal{W}}$ must be greater or equal to zero. This operator is defined in such a way that its normally-ordered symbol is the witness function $\mathcal{W}(\alpha)$, i.e.

$$\mathcal{W}(\alpha) = \langle \alpha | \hat{\mathcal{W}} | \alpha \rangle. \tag{2.5}$$

Hence, if we succeed to find the operator $\hat{\mathcal{W}}$ satisfying (2.5) and (2.3), such that its mean value is less than zero (or the condition (2.4) fails to obey), then we can assert that nonclassicality is inherent for the given state. As it was noted in [95], the concept of the witness function can be used for testing other kinds of nonclassicality as well.

As the next step, we rewrite the criteria (2.1) and (2.4) in terms of the Wigner function and its characteristic function, C_W. To this end, we use Eqs. (2.1) and (1.62) to reformulate

the Bochner condition in terms of C_W

$$\int \mathcal{D}[\alpha]\mathcal{D}[\beta]\, C_W(\alpha-\beta)e^{|\alpha|^2/2}f(\alpha)f^*(\beta) \geq 0. \tag{2.6}$$

This inequality we can bring in the form equivalent to Eq. (2.1) by redefying the complex-valued functions as $\tilde{f}(\alpha)\equiv f(\alpha)e^{|\alpha|^2/4}$. Therefore, the criterion for nonclassicality can be formulated fully in terms of the measurable quantities such as the characteristic function of Wigner distribution.

Another way to formulate the nonclassicality criterion in terms of measurable quantities relies on the methods of normally-ordered moments of field operators. Similar to classical probability theory the characteristic function C_P determines fully through its moments (1.60). The violation of inequality (2.1) is equivalent to negativity of determinants constructed from these moments [96]. In Ref. [72] the experimental setup for measurements of the normally-ordered moments has been proposed.

2.2 Nonclassicality of noisy quantum states

The number of thermal photons in the optical domain of the electromagnetic radiation is negligibly small. Hence, in this case the environment can be regarded as being in the vacuum state. The main problem is that the modern technologies in many cases do not afford to produce the optical devices with small interaction of the electromagnetic field and the absorbing medium. Especially this is apparent for optical high-Q (high-quality) cavities, where the resulting outgoing pulse includes just near by 50% of the initial intracavity mode [35]. Somewhat the microwave cavities are devoid of this shortcoming. In this case the constant of interaction between field and absorption system is comparatively small (see the discussion in [35]). However, the microwave domain is characterized by the presence of a great number of thermal photons. This causes more serious difficulties in testing nonclassical properties of quantum states. Thus, there arises a natural question about a balance between the constant of interaction and the temperature of the environment for the optimal detection of the nonclassicality. This is the subject of the present section.

2.2.1 Quantum state of a noisy system

Let us consider the system of interest being put into contact with a thermal reservoir at time t=0. If we adopt the notations α for the dynamical variables characterizing the system of interest and $\boldsymbol{\beta}$=$(\beta_1, \beta_2, ...\beta_N)$ as the bath variables (of N degrees of freedom),

then the system-bath interaction in RWA approximation can be written as

$$\hat{V} = \hbar \sum_{i=1}^{N} \left[\kappa_i \hat{a}^\dagger \hat{b}_i + \text{H.c.} \right] \tag{2.7}$$

where κ_i characterizes the coupling of system to the i-th thermal mode. Here $\hat{a}$ and $\hat{b}_i$ are mode operators of the signal and reservoir, respectively. From the form of the interaction it is clear that we focus on a class of linear systems only. It gives us a possibility to consider a wide enough class of experiments with a quantum electromagnetic field of low intensity.

We suppose that at the initial time, before the interaction is switched on, the density matrix can be decomposed as $\hat{\rho} = \hat{\rho}_{\text{in}} \otimes \hat{\rho}_{\text{bath}}$, where the bath is supposed to be in a thermal state

$$\hat{\rho}_{\text{th}} = \frac{1}{\mathcal{Z}} \prod_{i}^{N} e^{-\hbar\omega_i \hat{b}_i^\dagger \hat{b}_i / k_{\text{B}} T}, \qquad \mathcal{Z} = \text{Tr}\{ \prod_{i}^{N} e^{-\hbar\omega_i \hat{b}_i^\dagger \hat{b}_i / k_{\text{B}} T} \}, \tag{2.8}$$

so that $\hat{\rho}_{\text{bath}} = \hat{\rho}_{\text{th}}$. From Eq. (1.73) it follows than that the R-function of the system in contact with reservoir reads as

$$\begin{aligned} R_{\text{out}}(\alpha_f, \alpha_f', t) = e^{\frac{|\alpha_f|^2}{2} + \frac{|\alpha_f'|^2}{2}} \int \mathcal{D}[\boldsymbol{\beta}_f] e^{|\boldsymbol{\beta}_f|^2} \int \mathcal{D}[\alpha_i] \mathcal{D}[\alpha_i'] \mathcal{D}[\boldsymbol{\beta}_i] \mathcal{D}[\boldsymbol{\beta}_i'] \langle \alpha_f, \boldsymbol{\beta}_f | \hat{U}(t) | \alpha_i, \boldsymbol{\beta}_i \rangle \\ \times \langle \alpha_i | \hat{\rho}_{\text{in}}(0) | \alpha_i' \rangle \langle \boldsymbol{\beta}_i | \hat{\rho}_{\text{th}} | \boldsymbol{\beta}_i' \rangle \langle \alpha_i', \boldsymbol{\beta}_i' | \hat{U}^\dagger(t) | \alpha_f', \boldsymbol{\beta}_f' \rangle, \end{aligned} \tag{2.9}$$

where we have performed the integration over the irrelevant (bath) degrees of freedom. Here the subscripts i and f refer to the initial (at time t_0) and final (at time t) states of the system and the bath. Using the functional integral representation for the matrix elements of evolution operators and density matrices, we recast Eq. (2.9) into the following expression:

$$\begin{aligned} R_{\text{out}}(\alpha_f, \alpha_f', t) = e^{\frac{|\alpha_f|^2}{2} + \frac{|\alpha_f'|^2}{2}} \int \mathcal{D}[\alpha_i] \mathcal{D}[\alpha_i'] \langle \alpha_i | \hat{\rho}_{\text{in}}(0) | \alpha_i' \rangle \int \mathcal{D}[z] \mathcal{D}[z'] \mathcal{F}_{\text{FV}}[z, z'] \\ \times \exp\Big[-\frac{i}{\hbar} \mathscr{S}_S[z, t] + \frac{i}{\hbar} \mathscr{S}_S[z', t] + \frac{1}{2} \{ \alpha_f^* z(t) + \alpha_i z^*(0) + \alpha_f' z'^*(t) + \alpha_i' z'(0) \} \Big], \end{aligned} \tag{2.10}$$

where $\mathscr{S}_S$ is the action functional of the system of interest and

$$\begin{aligned} \mathcal{F}_{\text{FV}}[z, z'] = \int \mathcal{D}[\boldsymbol{\beta}_f] e^{|\boldsymbol{\beta}_f|^2} \int \mathcal{D}[\boldsymbol{\beta}_i] \mathcal{D}[\boldsymbol{\beta}_i'] e^{-\frac{|\boldsymbol{\beta}_i|^2}{2} - \frac{|\boldsymbol{\beta}_i|^2}{2}} R_{\text{th}}(\boldsymbol{\beta}_i, \boldsymbol{\beta}_i') \int \mathcal{D}[\boldsymbol{z}] \mathcal{D}[\boldsymbol{z}'] \\ \times \exp\Big[-\frac{i}{\hbar} \big(\mathscr{S}_B[\boldsymbol{z}] - \mathscr{S}_B[\boldsymbol{z}'] + \mathscr{S}_I[\boldsymbol{z}, z] - \mathscr{S}_I[\boldsymbol{z}', z'] \big) + \frac{1}{2} \{ \boldsymbol{\beta}_f^* \boldsymbol{z}(t) + \boldsymbol{\beta}_i \boldsymbol{z}^*(0) + \boldsymbol{\beta}_f' \boldsymbol{z}(t) + \boldsymbol{\beta}_i' \boldsymbol{z}(0) \} \Big] \end{aligned} \tag{2.11}$$

is the so-called Feynman-Vernon influence functional [97]. In Eq. (2.11) $R_{\rm th}$ is the R-function of the thermal state

$$R_{\rm th}(\beta,\beta')=\frac{1}{\bar{N}_{\rm th}+1}\exp\Big[-\frac{\bar{N}_{\rm th}}{\bar{N}_{\rm th}+1}\beta^*\beta'\Big] \quad \bar{N}_{\rm th}=(e^{\hbar\omega/k_{\rm b}T}-1)^{-1}, \tag{2.12}$$

$\mathscr{S}_B$ is the bath action and $\mathscr{S}_I$ is the interaction term that originates from (2.7). Let us use the Wick's theorem in the form it is given in Eq. (B.8) of Appendix B and order the time variables along the countor of Fig. 1.1 such that $t{=}t_+$ and $t'{=}t_-$. Then we can rewrite the influence functional Eq. (2.11) as

$$\begin{aligned}
&\mathcal{F}_{\rm FV}[z,z']=\mathcal{F}_{\rm FV}[J,J']=\exp\{-\frac{i}{\hbar}\mathscr{S}_{\rm FV}[J,J']\},\\
&\mathscr{S}_{\rm FV}[J,J']{=}\frac{1}{2}\sum_i\int_0^t dt'\int_0^{t'}dt''\big[J_i(t'){-}J_i'(t')\big]^*\big\{D_{i,\rm th}^{(0)>}(t'{-}t'')J_i(t'')-D_{i,\rm th}^{(0)<}(t'{-}t'')J_i'(t'')\big\}
\end{aligned} \tag{2.13}$$

where $J_i{=}\kappa_i z\sqrt{2\varepsilon_0\hbar\omega_i}$ is the source term of thermal fluctuations in the ith mode and the reservoir GFs $D_{\rm th}^{(0)\gtrless}$ are defined in Eq. (E.4) of Appendix E. From Eq. (2.13) one sees that $D_{i,\rm th}^{(0)>}$ represents an act of emission of a thermal photon by the sources and the reabsorption is represented by $D_{i,\rm th}^{(0)<}$. In thermal equilibrium for an isolated system, the number of thermal photons excited from the heat bath according to the Kubo-Martin-Schwinger conditions [98] is distributed according to the Boltzmann distribution $D_{i,\rm th}^{(0)>}(\omega_i)/D_{i,\rm th}^{(0)<}(\omega_i){=}\exp[\beta\hbar\omega_i]$.

Therefore, the Feynman-Vernon functional (2.13) describes the influence of the reservoir degrees of freedom on the dynamical properties of a system brought in contact with the thermal bath. Particularly, the real and imaginary parts of the reservoir GF (E.4) that enters the influence functional are responsible for the friction and decoherence effects of the relevant system. If one uses the analogy with the Brownian particle moving in viscous medium than the friction term describes the damping of the particle trajectory [32]. The contribution of the decoherence term to the influence functional (2.13) eliminates the quantum interference properties of the system under study and collapses its wave function [99, 100].

So far we have considered the system interacting with a bath on the microscopic level. In order to find out the nonclassicality criterion for such a system it is instructive to adopt the input-output formalism of macroscopic QED (Appendix C). In this approach the coupling of the system with the reservoir can be modeled by the set of N partially transmitting plates (mirrors) which mix the signal field incoming in one arm of a plate with the beam of thermal photons incoming on the other arm. The reflection coefficient of the i-th plate is related with the coupling parameter κ_i of Eq. (2.7) as $\mathrm{r}_i{=}\sin(|\kappa_i|t_i)$

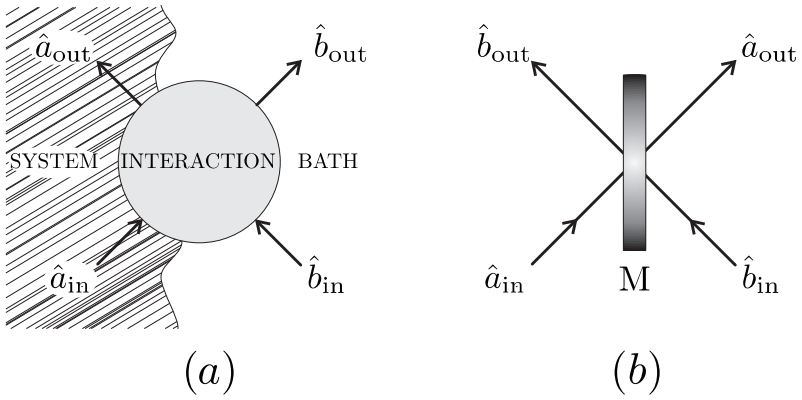

Figure 2.1: (a) The model of an open quantum system in terms of the input-output formalism. $\hat{a}_{\rm in}$ and $\hat{b}_{\rm in}$ are operators of the system and the environment before interaction, $\hat{a}_{\rm out}$ and $\hat{b}_{\rm out}$ correspond to these operators after interaction. (b) The equivalent to (a) scheme, where the system-reservoir interaction is modelled with the help of a semitransparent mirror M.

with t_i being the propagation time of the signal mode through the i-th plate. As the final step due to the linearity of the problem one can replace the whole set of beam-splitters with the single BS with the effective reflection coefficient

$$\mathcal{R} \equiv \prod_i \mathrm{r}_i \, \exp\Big\{ i \arg[\kappa_i] - i\frac{\pi}{2} \Big\}.$$

In this case the set of bath operators $\hat{b}_i$ is replaced with the collective operator $\hat{b}$.

Following this idea, let us consider an open quantum system as a device with two input-output ports. One of them corresponds to a system and another one corresponds to the bath (see. Figure 2.1). Let the operator $\hat{a}_{\rm in}$ describes a system before the interaction. For example, it can be an operator of the input-field mode. The operator $\hat{b}_{\rm in}$ describes the degrees of freedom of an environment before interaction, e.g. at the initial moment of time. In the same manner we will describe the system after interaction in terms of the operator $\hat{a}_{\rm out}$, which can be interpreted as the output field-mode operator. We also suppose that these operators satisfy the usual bosonic commutation relations.

We describe the evolution of the system in terms of a linear input-output relation between these operators

$$\hat{a}_{\rm out} = \mathcal{T}\hat{a}_{\rm in} + \mathcal{R}\hat{b}_{\rm in}. \tag{2.14}$$

where we have introduced for convenience the transmission coefficient $\mathcal{T}$ ($|\mathcal{T}|^2 + |\mathcal{R}|^2 = 1$). As the next step we will rewrite the input-output relation (2.14) in the Schrödinger picture of motion, i.e. we will consider the transformation of the density operator under the

noise influence. As it was mentioned already in Sec. 2.1, it is convenient to describe nonclassicality by using the Glauber-Sudarshan P-representation (1.54b). The characteristic function of the output field can be written as

$$C_P^{\rm out}(\beta) = {\rm Tr}\Big\{\hat{\rho}\,\exp\big[\hat{a}_{\rm out}^{\dagger}\beta - \hat{a}_{\rm out}\beta^{*} + \frac{|\beta|^2}{2}\big]\Big\}, \tag{2.15}$$

where $\hat{\rho}$ is the density operator of the system and the bath.

Substituting the input-output relations (2.14) into Eq. (2.15), one obtains for the characteristic function of the output state the expression

$$C_P^{\rm out}(\beta) = C_P^{\rm in}(\mathcal{T}^{*}\,\beta)e^{-|\beta|^2\bar{N}_{\rm th}(1-|\mathcal{T}|^2)} \tag{2.16}$$

where $\bar{N}_{\rm th} = \prod_i \bar{N}_{\rm th}(\omega_i)$ is the effective occupation number of thermal photons. One can easily see that for

$$\bar{N}_{\rm th} = \frac{|\mathcal{T}|^2}{1-|\mathcal{T}|^2} \tag{2.17}$$

the characteristic function (2.16) turns into a characteristic function for the Q-distribution of a certain state. Thus, for such values of $\bar{N}_{\rm th}$ the P-function is always positive. The same one can say if the number of thermal photons is greater than the value determined by the criterion (2.17). Therefore, Eq. (2.17) defines *thermal threshold of the nonclassicality*. In other words, if the number of thermal photons in the bath is greater than the value, given by Eq. (2.17), the nonclassicality in the sense of negative values of P-function always vanishes. However only the fact, that the number of thermal photons is less than the thermal threshold defined by Eq. (2.17), can not be considered as sufficient condition of the nonclassicality.

Using the inverse Fourier transform we get from (2.16) the relation for the P-function of the state in the form [I]

$$P_{\rm out}(\alpha) = \frac{1}{|\mathcal{T}|^2}\exp[\bar{N}_{\rm th}(1-|\mathcal{T}|^2)\Delta_{\alpha}]P_{\rm in}\left(\frac{\alpha}{\mathcal{T}}\right), \tag{2.18}$$

where $\Delta_{\alpha} = \frac{\partial^2}{\partial({\rm Re}\,\alpha)^2} + \frac{\partial^2}{\partial({\rm Im}\,\alpha)^2}$. This means that the P-function for the output state satisfies the diffusion-like differential equation

$$\frac{\partial}{\partial\bar{N}_{\rm th}}P_{\rm out}(\alpha,\bar{N}_{\rm th}) = (1-|\mathcal{T}|^2)\Delta_{\alpha}P_{\rm out}\left(\alpha,\bar{N}_{\rm th}\right), \tag{2.19}$$

with the "initial" condition

$$P_{\rm out}(\alpha,0) = \frac{1}{|\mathcal{T}|^2}P_{\rm in}\left(\frac{\alpha}{\mathcal{T}}\right). \tag{2.20}$$

Therefore, we can conclude that under the thermal noise influence the P-function of the system transforms according to the diffusion-like differential equation (2.19), where the

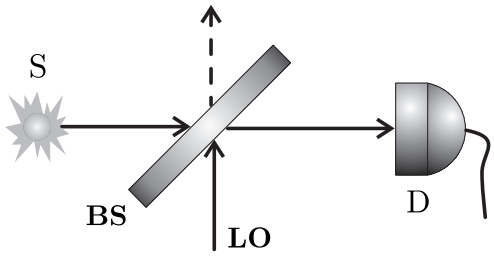

Figure 2.2: The scheme of unbalanced homodyne detection. The signal field generated by the source S is mixed by the beam-splitter BS with the local oscillator LO field and then is detected by the detector D.

mean number of thermal photons plays formally the role of the "time variable". This means that with a growing number of thermal photons in the environment, the P-function of the system is smoothed. For a certain value of $\bar{N}_{\rm th}$, which is less or equal to the thermal threshold (2.17), the domains of its negative values disappear as well as singular behavior.

Using the Bochner criterion (2.4) along with Eq. (2.19), one can derive the relation between the witness functions defined on the input ($\mathcal{W}$) and output ($\mathcal{W}_{\rm th}$)

$$\mathcal{W}_{\rm th}(\alpha,\bar{N}_{\rm th})=\exp[-\bar{N}_{\rm th}(1-|\mathcal{T}|^2)\Delta_\alpha]\mathcal{W}\left(\frac{\alpha}{\mathcal{T}}\right), \tag{2.21}$$

such that the inequality

$$\int\mathcal{D}[\alpha]P_{\rm out}(\alpha)\mathcal{W}_{\rm th}(\alpha,\bar{N}_{\rm th})<0 \tag{2.22}$$

implies that the nonclassical input field remains to be nonclassical in the output. This means that we can find the new witness function as a solution of diffusion-like differential equation with a negative diffusion coefficient

$$\frac{\partial}{\partial\bar{N}_{\rm th}}\mathcal{W}_{\rm th}(\alpha,\bar{N}_{\rm th})=-(1-|\mathcal{T}|^2)\Delta_\alpha\mathcal{W}_{\rm th}(\alpha,\bar{N}_{\rm th}), \tag{2.23}$$

and the following "initial" condition

$$\mathcal{W}_{\rm th}(\alpha,0)=\mathcal{W}\left(\frac{\alpha}{\mathcal{T}}\right). \tag{2.24}$$

Therefore, for a noisy state the witness function can be redefined in such a way that testing the nonclassicality gives a result equal to the noiseless case. The fact that Eq. (2.23) is a diffusion-like equation with negative diffusion coefficient means that with growing a number of thermal photons $\bar{N}_{\rm th}$ one has to choose a sharper witness function for obtaining the same result. This possibility exists up to a certain temperature threshold only, which however can be less than the value defined by Eq. (2.17) but cannot be greater.

2.2.2 Testing the nonclassicality with unbalanced homodyning

Unbalanced homodyning, proposed in [101], allows one to test the nonclassicality with an important class of witness functions, which have a form of the Gauss distribution

$$\mathcal{W}(\alpha) = \frac{1}{\pi a^2}\ \exp\Big[-\frac{|\alpha-\gamma|^2}{a^2}\Big], \tag{2.25}$$

where the width of this distribution can be controlled by changing values of its dispersion a. Unbalanced homodyning represents itself the simplified homodyning scheme described in Appendix C (see also Fig 2.2). In this method the photon-counting distributions $\mathcal{P}_n^{\rm in}(\gamma,\eta_{\rm h})$ [cf. Eq. (1.63)] are detected in one output channel by the photodetector D. The photon-counting distributions depend on the coherent amplitude γ and the overall efficiency of the homodyning, $\eta_{\rm h}$, which are expressed in terms of the amplitude of the local oscillator $\gamma_{\rm LO}$, the transmission $\sqrt{1-{\rm r}^2}$ and the reflection coefficient r of the beam splitter and the dimensionless efficiency of photon counting $\underline{\eta}$,

$$\gamma = -\frac{\rm r}{\sqrt{1-{\rm r}^2}}\gamma_{\rm LO}, \quad \eta_{\rm h} = \underline{\eta}\sqrt{1-{\rm r}^2}. \tag{2.26}$$

As shown in [101] the value of $\overline{\mathcal{W}}$, obtained by inserting Eq. (2.25) in Eq. (2.4), can be reconstructed from the probabilities of photon counts as:

$$\overline{\mathcal{W}} = \frac{1}{\pi a^2}\sum_{n=0}^{\infty}\Big[-\frac{1-\eta_{\rm h}a^2}{\eta_{\rm h}a^2}\Big]^n \mathcal{P}_n^{\rm in}(\gamma,\eta_{\rm h}). \tag{2.27}$$

This gives us a possibility to find such a witness function, which tests the nonclassicality for the corresponding noisy state. It can be obtained by resolving the diffusion-like equation (2.23), with "initial" condition (2.24) specified by the function (2.25). The solution is written as :

$$\mathcal{W}_{\rm th}(\alpha) = \frac{1}{\pi\big(a^2-\bar{N}_{\rm th}\frac{|\mathcal{T}|^2}{1-|\mathcal{T}|^2}\big)}\ \exp\Bigg[-\frac{\big|\frac{\alpha}{\mathcal{T}}-\gamma\big|^2}{a^2-\bar{N}_{\rm th}\frac{|\mathcal{T}|^2}{1-|\mathcal{T}|^2}}\Bigg]. \tag{2.28}$$

It is worth noting that this solution is defined just for

$$\bar{N}_{\rm th} \le a^2\Big(\frac{|\mathcal{T}|^2}{1-|\mathcal{T}|^2}\Big)^{-1} = a^2\frac{|\mathcal{R}|^2}{|\mathcal{T}|^2}. \tag{2.29}$$

For other values of $\bar{N}_{\rm th}$, it is not positive definite and has strong singularities. This is a typical property for the solution of the diffusion equation with negative diffusion coefficient. The last expression defines the thermal threshold for the scheme of unbalanced homodyning. Taking into account that the maximal value of a^2 is 1, one immediately obtains Eq. (2.17).

Corresponding value of $\overline{\mathcal{W}}_{\rm th}$ as well as the s-parameterized P-distribution for the noiseless signal can be reconstructed from the probabilities of photon counts for the noisy signal $P_n^{\rm out}(\gamma,\eta_{\rm h})$ using the following expression [I]:

$$\overline{\mathcal{W}}_{\rm th}=P_{\rm in}(\gamma,s)=\frac{|\mathcal{T}|^2}{\pi\left(a^2-\bar{N}_{\rm th}\frac{|\mathcal{T}|^2}{1-|\mathcal{T}|^2}\right)}\sum_{n=0}^{+\infty}\left[-\frac{1-\eta_{\rm h}\left(a^2-\bar{N}_{\rm th}\frac{|\mathcal{T}|^2}{1-|\mathcal{T}|^2}\right)}{\eta_{\rm h}\left(a^2-\bar{N}_{\rm th}\frac{|\mathcal{T}|^2}{1-|\mathcal{T}|^2}\right)}\right]^n\mathcal{P}_n^{\rm out}(\mathcal{T}\gamma,\eta_{\rm h}),\quad(2.30)$$

where $s{=}1-2a^2$. A disadvantage of this method is the fact that for some quantum states the series defined by Eqs. (2.27), (2.30) may diverge (see [101]). This gives some restrictions for the application of this method. Recently this approach has been generalized in order to describe the signal field coupled to multimode noise [102].

2.2.3 An example: Fock state

A single-photon Fock state with the density operator $\hat{\rho}_{\rm in}=|1\rangle\langle 1|$ is a good candidate for the experimental realization of the proposed method. The generation of this state by using the frequency down-conversion process and testing it for the nonclassicality with the application of the balanced homodyne detection is reported in [94]. The s-parameterized distribution (1.56) for the single-photon Fock state has the following form:

$$P_{\rm in}\left(\alpha,s\right)=\begin{cases}\frac{2}{\pi(1-s)^3}\left(4\left|\alpha\right|^2-1+s^2\right)\exp\left[-\frac{2|\alpha|^2}{1-s}\right], & -1\leq s<1\\ \left(1+\partial^2_{\alpha^*\alpha}\right)\delta(\alpha), & s=1\end{cases},\quad(2.31)$$

This is a regular function for $-1\leq s<1$, and a distribution with very strong singularity for $s=1$, i.e. for the Glauber-Sudarshan P-function. It is clear that this state has nonclassical properties and non-positive-definite phase-space distributions for all values of the parameter $s\neq -1$.

Different losses in experimental set-up lead to admixing the vacuum state into the density operator $|1\rangle\langle 1|$. Hence, the resulting state has the form of the following statistical mixture:

$$\hat{\rho}_{\rm out}=|\mathcal{T}|^2|1\rangle\langle 1|+|\mathcal{R}|^2\,|0\rangle\langle 0|.\quad(2.32)$$

This is a result of interaction between the field mode and zero-temperature bath (where the mean number of thermal photons $\bar{N}_{\rm th}$ is negligible). As it was shown in [94], the nonclassicality can be tested, at least in principle, for any value of the efficiency η. Such a situation is usual for the optical domain. We consider a more general case, when the bath does have non-zero temperature, that is typical for the microwave domain, the vibrational motion of trapped atom, etc.

The Glauber-Sudarshan P-function for the thermal noisy state can be obtained from Eq. (2.18) and is written as follows:

$$P_{\rm out}(\alpha) = \frac{1}{|\mathcal{T}|^2} P_{\rm in}\left(\frac{\alpha}{\mathcal{T}}, s'\right), \tag{2.33}$$

where

$$s' = 1 - 2\bar{N}_{\rm th}\frac{|\mathcal{R}|^2}{|\mathcal{T}|^2}. \tag{2.34}$$

The right-hand side of this equation in the case of a single-photon Fock state has non-positive values for $s' > -1$. Therefore, taking into account Eq. (2.34) we conclude that this state under the thermal noise influence preserves nonclassical properties up to the thermal threshold given by Eq. (2.17).

The application of the unbalanced homodyning scheme means testing the nonclassicality with the witness function $\mathcal{W}(\alpha)$ given by Eq. (2.25). Hence, according to Eq. (2.4) for single-photon (noiseless) Fock state one has the following value for the quantity $\overline{\mathcal{W}}$:

$$\overline{\mathcal{W}} = P_{\rm in}\left(\gamma, 1-2a^2\right) = \frac{1}{\pi a^6}\left\{|\gamma|^2 + a^2\left(a^2-1\right)\right\}\exp\Big[-\frac{|\gamma|^2}{a^2}\Big]. \tag{2.35}$$

It has negative values for any $a^2 < 1$ and, moreover, shows non-positivity of the phase-space distribution with $s = 1 - 2a^2$.

Applying the same witness function for the single-photon Fock state under thermal noise influence, one obtains the following value:

$$\overline{\mathcal{W}}' = \frac{1}{a^2}\int \mathcal{D}[\alpha] P_{\rm out}(\alpha)\ \mathcal{W}(\alpha) = \frac{1}{|\mathcal{T}|^2} P_{\rm in}\left(\frac{\gamma}{\mathcal{T}}, s'\right), \tag{2.36}$$

where

$$s' = 1 - 2\frac{\bar{N}_{\rm th}|\mathcal{R}|^2 + a^2}{|\mathcal{T}|^2}. \tag{2.37}$$

This procedure can test the nonclassicality only if $s' > -1$. In other words, testing the nonclassicality with the witness function (2.25) is impossible if $a^2 \geq |\mathcal{T}|^2 - \bar{N}_{\rm th}|\mathcal{R}|^2$.

However, in the case when the mean number of thermal photons $\bar{N}_{\rm th}$ is less than the thermal threshold, one can apply the witness function $\mathcal{W}_{\rm th}(\alpha)$ that is given by Eq. (2.28). In an experiment, the value of $\overline{\mathcal{W}}_{\rm th}$ can be reconstructed by using Eq. (2.30). This gives a numerical result, which is equal to Eq. (2.35), that indicates both the presence of nonclassicality and non-positive values for the phase-space distribution with $s = 1 - 2\left(a^2|\mathcal{T}|^2 - \bar{N}_{\rm th}|\mathcal{R}|^2\right)$.

2.3 Realistic optical cavities and nonclassicality

This section is devoted to the description of light propagation in high-Q cavities with the correct accounting of various losses. We shall distinguish cavities operating in the

optical and the microwave domain. It has been already mentioned in the previous section, that in the microwave domain one can neglect absorption effects of cavity mirrors and consider the dephasing and damping of cavity field due to its interaction with a thermal reservoir. In this case one should expect that the results of Sec. 2.2 hold true for microwave cavities operating in a linear regime. Indeed, let us consider the process of quantum-state extraction from a high-Q cavity [35]. In this case, the operator $\hat{a}_{\rm in}$ can be interpreted as the operator of an intracavity mode at the initial time. The operator $\hat{a}_{\rm out}$ of Eq. (2.14) corresponds to the non-monochromatic mode leaking from the cavity. The process of absorption and scattering by the mirrors can be considered as an interaction between the system and the bath. Hence, the operator $\hat{c}_{\rm in}$ corresponds to the absorption system of the mirror and the scattering modes of field. The corresponding input-output relations were considered in the previous chapter. The efficiency η of this process is closely related with two components of the cavity decay rate: $\gamma_{\rm rad}$, which is responsible for the output and $\gamma_{\rm abs}$, which is responsible for the absorption and scattering, so that $\eta{=}\gamma_{\rm rad}/(\gamma_{\rm rad}{+}\gamma_{\rm abs})$. The nonclassicality of the outcoupled field is characterized then by Eqs (2.21) and (2.30), where one substitutes $\mathcal{T}{=}\sqrt{\eta}$.

For cavities operating in the optical domain, the most important of losses are scattering and absorption. In the framework of quantum noise theories (QNT), a high-Q cavity mode is usually considered as a harmonic oscillator interacting through the coupling mirror with a number of external modes. This leads to the description of the cavity mode in terms of a quantum Langevin equation and input-output relations [33]. A quantum-field theoretical approach [34, 103, 104] for such a system leads to the same results in appropriate limits.

2.3.1 Unwanted noise and replacement schemes

In the following we will derive the input-output relations and the Langevin equation for a high-Q cavity, taking into account all possible loss channels. There are several relevant loss channels, namely losses due to the scattering and absorption losses on the two mirrors of a cavity and additional unwanted noise channels inside the cavity due to the coupling to the thermal reservoir modes, scattering by the active medium placed in the cavity, to name just a few.

Let us consider the quantum state being prepared outside the cavity. We send the prepared state on an optical cavity composed of the semitransparent mirror M_1 and the perfectly reflecting mirror M_2 (see Fig. 2.3). We also assume that a proper mode of electromagnetic waves is established along the cavity axis. The evolution of the externally prepared quantum state in cavity can be decomposed into the following steps. Firstly it propagates through the mirror M_1, enters the cavity, couples to the intracavity filed,

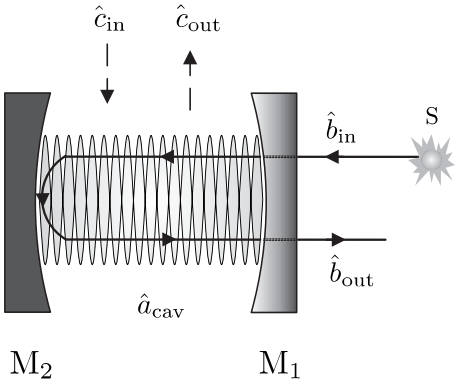

Figure 2.3: One-sided cavity composed of the semitransparent mirror M_1 and the perfectly reflecting mirror M_2. The evolution of the electromagnetic field mode externally prepared by source S is shown by arrows. The annihilation mode operators of the intracavity field ($\hat{a}_{\rm cav}$), the input field ($\hat{b}_{\rm in}$) and the unwanted noise channels ($\hat{c}_{\rm in/out}$) are also indicated.

reflects from the mirror M_2 and finally outcouples from the cavity passing again the mirror M_1. We will describe the cavity in the presence of unwanted losses by means of the quantum Langevin equation

$$\begin{aligned}\dot{\hat{a}}_{\rm cav}(t) = &-\big[i\omega_{\rm cav} + \frac{1}{2}\Gamma\big]\hat{a}_{\rm cav}(t_1) \\ &+ \mathcal{T}^{(\rm c)}\hat{b}_{\rm in}(t) + \mathcal{A}^{(\rm c)}_{(1)}\hat{c}^{(1)}_{\rm in}(t) + \mathcal{A}^{(\rm c)}_{(2)}\hat{c}^{(2)}_{\rm in}(t) + \mathcal{A}\hat{c}_{\rm in}(t)\end{aligned} \tag{2.38}$$

and the input-output relations

$$\hat{b}_{\rm out} = \mathcal{T}^{(0)}\hat{a}_{\rm cav} + \mathcal{R}^{(0)}\hat{b}_{\rm in} + \mathcal{A}^{(0)}_{(1)}\hat{c}^{(1)}_{\rm in} + \mathcal{A}^{(0)}_{(2)}\hat{c}^{(2)}_{\rm in} \tag{2.39}$$

obtained from the corresponding replacement scheme [II] (see Fig. 2.4), or, equivalently, from the field-theoretical approach [105]. Here $\hat{a}_{\rm cav}$ is the intracavity-mode operator, $\hat{b}_{\rm in}$ is the input-mode operator, $\hat{b}_{\rm out}$ is the output-mode operator, $\hat{c}_{\rm in}$, $\hat{c}^{(1)}_{\rm in}$, $\hat{c}^{(2)}_{\rm in}$ are input operators associated with unwanted noise. The c-number coefficients in the quantum Langevin equation and the input-output relations are expressed in terms of the transmission and reflection coefficients $\mathcal{T}^{(i)}$ and $\mathcal{R}^{(i)}$ (i=1, 2, 3) of the beam-splitters BS_1, BS_2 and the semi-transparent plate M_3, the phase factor $\phi^{(3)}$ of the semi-transparent plate M_3, the resonance frequency ω_0, the radiation and absorption decay rates of the "primary" cavity in the scheme, γ and $|\mathcal{A}|^2$ respectively, as follows [II]:

$$\Gamma = \gamma\,\frac{1 - \left|\mathcal{R}^{(3)}\right|^2\left|\mathcal{T}^{(1)}\right|^2\left|\mathcal{T}^{(2)}\right|^2}{\left|1 - \mathcal{R}^{(3)*}\mathcal{T}^{(1)}\mathcal{T}^{(2)}\right|^2} + |\mathcal{A}|^2\,, \tag{2.40}$$

$$\omega_{\rm cav} = \omega_0 - i\frac{\gamma}{2}\frac{\mathcal{R}^{(3)*}\mathcal{T}^{(1)}\mathcal{T}^{(2)} - \mathcal{R}^{(3)}\mathcal{T}^{(1)*}\mathcal{T}^{(2)*}}{\left|1 - \mathcal{R}^{(3)*}\mathcal{T}^{(1)}\mathcal{T}^{(2)}\right|^2}, \tag{2.41}$$

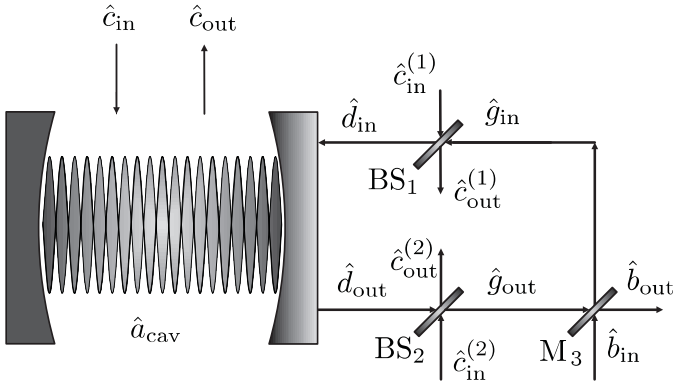

Figure 2.4: Replacement scheme for modeling the unwanted noise in a one-sided cavity. The beam-splitters $\rm BS_1$ and $\rm BS_2$ model the unwanted noise in the coupling mirror, and the semitransparent plate $\rm M_3$ simulates some feedback.

$$\mathcal{T}^{(\rm c)} = \sqrt{\gamma}\,\frac{\mathcal{T}^{(1)}\mathcal{T}^{(3)*}}{1-\mathcal{R}^{(3)*}\mathcal{T}^{(1)}\mathcal{T}^{(2)}}\,, \tag{2.42}$$

$$\mathcal{A}^{(\rm c)}_{(1)} = \sqrt{\gamma}\,\frac{\mathcal{R}^{(1)}}{1-\mathcal{R}^{(3)*}\mathcal{T}^{(1)}\mathcal{T}^{(2)}}\,, \tag{2.43}$$

$$\mathcal{A}^{(\rm c)}_{(2)} = -\sqrt{\gamma}\,\frac{\mathcal{T}^{(1)}\mathcal{R}^{(2)}\mathcal{R}^{(3)*}}{1-\mathcal{R}^{(3)*}\mathcal{T}^{(1)}\mathcal{T}^{(2)}}\,, \tag{2.44}$$

$$\mathcal{T}^{(0)} = \sqrt{\gamma}\,e^{i\varphi^{(3)}}\,\frac{\mathcal{T}^{(2)}\mathcal{T}^{(3)}}{1-\mathcal{R}^{(3)*}\mathcal{T}^{(1)}\mathcal{T}^{(2)}}\,, \tag{2.45}$$

$$\mathcal{R}^{(0)} = e^{i\varphi^{(3)}}\,\frac{\mathcal{R}^{(3)}-\mathcal{T}^{(1)}\mathcal{T}^{(2)}}{1-\mathcal{R}^{(3)*}\mathcal{T}^{(1)}\mathcal{T}^{(2)}}\,, \tag{2.46}$$

$$\mathcal{A}^{(0)}_{(1)} = -e^{i\varphi^{(3)}}\,\frac{\mathcal{T}^{(2)}\mathcal{R}^{(1)}\mathcal{T}^{(3)}}{1-\mathcal{R}^{(3)*}\mathcal{T}^{(1)}\mathcal{T}^{(2)}}\,, \tag{2.47}$$

$$\mathcal{A}^{(0)}_{(2)} = e^{i\varphi^{(3)}}\,\frac{\mathcal{R}^{(2)}\mathcal{T}^{(3)}}{1-\mathcal{R}^{(3)*}\mathcal{T}^{(1)}\mathcal{T}^{(2)}}\,. \tag{2.48}$$

The coefficients (2.42)-(2.48) together with the cavity absorption coefficient $\mathcal{A}$ obey definite constraints [II, III], which follow from the requirement of preserving the commutation rules for operators involved in the replacement scheme.

2.3.2 Noise-induced mode coupling

Assuming that the state of the intracavity mode is generated at time t=0, the solution of the quantum Langevin equation (2.38) can be written as [II]

$$\hat{a}_{\rm cav}(t) = \left[\mathcal{T}^{(0)}\right]^{-1} F^{*}(t)\hat{a}_{\rm cav}(0) + \mathcal{T}^{(\rm c)}\int_0^t dt'\mathscr{D}_{\rm s}^{\rm ret}\,(t,t')\,\hat{b}_{\rm in}\,(t') + \hat{\tilde{C}}\,(t)\,, \tag{2.49}$$

where

$$F^{*}(t) = \theta(t)\,\mathcal{T}^{(0)} \exp\Big[-\big(i\omega_{\mathrm{cav}} + \Gamma/2\big)t\Big], \tag{2.50}$$

$$\mathscr{D}_{\mathrm{s}}^{\mathrm{ret}}(t,t') = \theta(t)\,\theta(t-t') \exp\Big[-\big(i\omega_{\mathrm{cav}} + \Gamma/2\big)(t-t')\Big], \tag{2.51}$$

$\theta(t)$ is a unit step function, and $\hat{\tilde{C}}(t)$ is a linear integral expression for the operators of unwanted noise. Since we assume that the absorption system and the scattering modes are in the vacuum state, the explicit form of this operator plays no role for our further consideration. Substituting Eq. (2.49) into the input-output relation (2.39), one obtains the relation

$$\hat{b}_{\mathrm{out}}(t) = \hat{a}_{\mathrm{cav}}(0)F^{*}(t) + \int_{-\infty}^{\infty} dt'\,\mathscr{D}^{\mathrm{ret}}(t,t')\,\hat{b}_{\mathrm{in}}(t') + \hat{C}(t)\,. \tag{2.52}$$

Hence the output-mode operator is expressed by the input-mode operator, the intracavity mode operator at the initial time and the operators of unwanted noise. Here the intracavity photon propagator $\mathscr{D}^{\mathrm{ret}}$ should not be confused with the photon GF though there is an ultimate connection between the both functions. The propagator $\mathscr{D}^{\mathrm{ret}}(t,t')$ splits into two parts, $\mathcal{R}^{(0)}\delta(t-t') + \mathscr{D}_{\mathrm{s}}^{\mathrm{ret}}(t,t')$, that correspond to a free field and a source field, respectively [106]. In Eq. (2.49) $\hat{C}(t)$ is again a linear integral expression containing the operators of unwanted noise, whose explicit form is not needed for the further consideration. The first term in Eq. (2.52) describes the extraction of the intracavity mode into the *cavity-associated output mode* (CAOM). The second term describes the reflection of the input field, where $\mathscr{D}^{\mathrm{ret}}(t,t')$ is the integral kernel of the corresponding mode transformation. It is worth noting that non-Hermitian properties of this integral transformation lead to changing (decreasing) the norm of the reflected pulse compared with the input one. This corresponds to the partial absorption/scattering during reflection at the cavity.

It is convenient to use another (equivalent) representation of Eq. (2.52). Let $\big\{U_n^{\mathrm{in}}(t)\,, n{=}0\ldots{+}\infty\big\}$ and $\big\{U_n^{\mathrm{out}}(t)\,, n{=}0\ldots{+}\infty\big\}$ be two different complete sets of orthogonal functions associated with input and output fields respectively, i.e.

$$\hat{b}_{\mathrm{in(out)}}(t) = \sum_{n=0}^{+\infty} U_n^{\mathrm{in(out)}}(t)\,\hat{b}_{\mathrm{in(out)}}(n), \tag{2.53}$$

$$\hat{b}_{\mathrm{in(out)}}(n) = \int_{-\infty}^{\infty} \mathrm{d}t\big[U_n^{\mathrm{in(out)}}(t)\big]^{*}\hat{b}_{\mathrm{in(out)}}(t)\,. \tag{2.54}$$

Here $\hat{b}_{\mathrm{in(out)}}(n)$ is the annihilation operator of an input (output) photon in the non-monochromatic mode corresponding to the function $U_n^{\mathrm{in(out)}}(t)$.

We choose the function $U_0^{\mathrm{out}}(t)$ in the form of the pulse extracted from the cavity (CAOM)

$$U_0^{\mathrm{out}}(t) = \frac{F^{*}(t)}{\sqrt{\eta_{\mathrm{ext}}}}, \tag{2.55}$$

where

$$\eta_{\rm ext} = \int_{-\infty}^{\infty} dt\, |F(t)|^2 = \frac{\left|\mathcal{T}^{(0)}\right|^2}{\Gamma} \tag{2.56}$$

can be interpreted as the efficiency of the intracavity-field extraction into the CAOM [35].

The function $U_0^{\rm in}(t_1)$, defined by using the propagator $\mathscr{D}^{\rm ret}(t,t')$ as

$$U_0^{\rm in}(t) = \frac{1}{\sqrt{\underline{\eta}_{\rm ref}}} \int_{-\infty}^{\infty} dt'\, \mathscr{D}^{\rm ret}(t,t')\, U_0^{\rm out}(t') = U_0^{\rm out}(t)\, e^{-i\varphi}, \tag{2.57}$$

corresponds to the *nonmonochromatic matched input mode* (MIM), which only makes a contribution, among the other orthogonal input modes of this set, into the CAOM under reflection at the cavity. Here

$$\underline{\eta}_{\rm ref} = \left|\mathscr{D}^{\rm ret}(0,0)\right|^2 = \left|\frac{\mathcal{T}^{(0)}\mathcal{T}^{(\rm c)}}{\Gamma} + \mathcal{R}^{(0)}\right|^2 \tag{2.58}$$

is the efficiency of the MIM reflection into the CAOM, which can be found through the condition of normalization for the function $U_0^{\rm in}(t_1)$, Eq. (2.57). The phase φ is defined as

$$\varphi = \arg\left[\frac{\mathcal{T}^{(0)}\mathcal{T}^{(\rm c)}}{\Gamma} + \mathcal{R}^{(0)}\right]. \tag{2.59}$$

Along with the CAOM, the MIM is reflected into another nonmonochromatic output mode as well, see Fig. 2.5. This *additional output mode* (AOM) results in noise effects when one measures some properties of the quantum state of the CAOM. To analyze it, we need the total response of the cavity on the MIM, that can be obtained by using the integral kernel $\mathscr{D}^{\rm ret}(t_1,t_2)$ as

$$\begin{aligned} U^{\rm out}(t) &= \int_{-\infty}^{\infty} dt'\, \mathscr{D}^{\rm ret}(t,t')\, U_0^{\rm in}(t') \\ &= \theta(t)\sqrt{\Gamma}\left(\mathcal{T}^{(\rm c)}\mathcal{T}^{(0)}t + \mathcal{R}^{(0)}\right)\; e^{-\left(i\omega_{\rm cav}+\frac{\Gamma}{2}\right)t + i\left(\arg\mathcal{T}^{(0)}-\varphi\right)}. \end{aligned} \tag{2.60}$$

Since the total reflected pulse $U^{\rm out}(t)$ is a superposition of the CAOM with the AOM, i.e.

$$U^{\rm out}(t) = \sqrt{\underline{\eta}_{\rm ref}}U_0^{\rm out}(t) + \sqrt{\overline{\eta}_{\rm ref}}U_1^{\rm out}(t)\,, \tag{2.61}$$

the form of the AOM, denoted as $U_1^{\rm out}(t)$, can be found as

$$U_1^{\rm out}(t) = \frac{1}{\sqrt{\overline{\eta}_{\rm ref}}}\left[U^{\rm out}(t) - \sqrt{\underline{\eta}_{\rm ref}}\,U_0^{\rm out}(t)\right] = \theta(t)\sqrt{\Gamma}e^{i\chi}(\Gamma t - 1)\, e^{-\left(i\omega_{\rm cav}+\frac{\Gamma}{2}\right)t}. \tag{2.62}$$

Here

$$\chi = \arg\frac{\mathcal{T}^{(0)}\mathcal{T}^{(\rm c)}}{\Gamma} + \arg\mathcal{T}^{(0)} - \varphi, \tag{2.63}$$

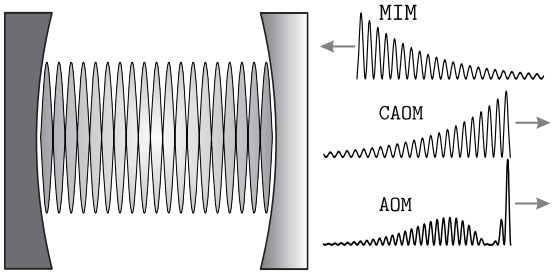

Figure 2.5: The mode structure of the external field: cavity-associated output mode (CAOM), additional output mode (AOM) and matched input mode (MIM).

and

$$\overline{\eta}_{\rm ref} = \frac{\left|\mathcal{T}^{(0)}\right|^2 \left|\mathcal{T}^{(c)}\right|^2}{\Gamma^2} \tag{2.64}$$

is the efficiency of the reflection of the MIM into the AOM, which is found via the normalization of the function $U_0^{\rm out}(t)$.

One can check by direct calculations that in the new representation, Eq. (2.52), is rewritten as

$$\hat{b}_{\rm out}(n=0) = \sqrt{\eta_{\rm ext}}\,\hat{a}_{\rm cav}(0) + \sqrt{\underline{\eta}_{\rm ref}}\,\hat{b}_{\rm in}(n=0) + \hat{C}_0, \tag{2.65}$$

$$\hat{b}_{\rm out}(n=1) = \sqrt{\overline{\eta}_{\rm ref}}\,\hat{b}_{\rm in}(n=0) + \sum_{m=1}^{\infty} \mathscr{D}^{\rm ret}_{m,1}\,\hat{b}_{\rm in}(m) + \hat{C}_1, \tag{2.66}$$

$$\hat{b}_{\rm out}(n) = \sum_{m=1}^{\infty} \mathscr{D}^{\rm ret}_{m,n}\,\hat{b}_{\rm in}(m) + \hat{C}_n \text{ for } n = 2, 3\ldots, \tag{2.67}$$

where

$$\mathscr{D}^{\rm ret}_{m,n} = \int_{-\infty}^{\infty} dt dt' U_n^{\rm out*}(t)\,\mathscr{D}^{\rm ret}\left(t,t'\right) U_m^{\rm in}\left(t'\right), \tag{2.68}$$

$$\hat{C}_n = \int_{-\infty}^{\infty} dt U_n^{\rm out*}(t)\,\hat{C}\left(t\right). \tag{2.69}$$

The first term of Eq. (2.65) describes the intracavity-field extraction into the CAOM with the efficiency $\eta_{\rm ext}$ [35]. This mode corresponds to the function $U_0^{\rm out}(t)$. The second term of Eq. (2.65) demonstrates a possibility to combine input and intracavity fields in the nonmonochromatic output mode (CAOM) with the efficiency $\underline{\eta}_{\rm ref}$ given by Eq. (2.58). As it follows from the Eqs. (2.66, 2.67), the field extracted from the cavity does not give a contribution into other nonmonochromatic output modes. Moreover according to Eq. (2.65), only the MIM described by the function $U_0^{\rm in}(t)$ contributes into the CAOM via reflection at the cavity. It is worth noting that the MIM can be easily prepared in an experiment since it has the form of a pulse extracted from another cavity.

The frequency representation of the CAOM and the AOM have a very similar form. Their Fourier images, denoted as $U_0^{\rm out}(\omega)$ and $U_1^{\rm out}(\omega)$ respectively, have equal absolute values, i.e.

$$\left|U_0^{\rm out}(\omega)\right|^2 = \left|U_1^{\rm out}(\omega)\right|^2 = \frac{\Gamma}{2\pi\left[\left(\omega-\omega_{\rm cav}\right)^2+\frac{\Gamma^2}{4}\right]}. \tag{2.70}$$

Hence, these two orthogonal modes are irradiated in the same frequency domain. They differ only in the phases. Hence, an additional noise contributed by AOM should be considered in all applications dealing with combining intracavity and input fields in CAOM.

A special case is a cavity, which does not include any additional channel of losses. For such a type of cavities the efficiency of the MIM reflection into CAOM given by Eq. (2.58) is equal to zero. In other words, the input field is completely reflected into AOM. Hence, for such cavities the combination of the intracavity and the input field in the nonmonochromatic output mode becomes impossible. This is a quite nontrivial result, that means that the presence of unwanted losses in cavities provides us a possibility to extract from the cavity coupled intracavity and input fields. From the previous section we have learned that noise usually spoils nonclassical properties of quantum systems. In this chapter we have considered a counterexample. It appears that without unwanted noise one cannot sufficiently extract for further detection the nonclassical state, generated in the cavity or/and prepared outside and incoupled to the cavity on the input port.

However, there exists a class of degenerate cavities with losses, but for which it is also impossible to outcouple the combination of MIM and CAOM. The replacement scheme for such a type of cavities includes neither internal losses nor additional feedback inside the semitransparent mirror [II]. In contrast to non-degenerate schemes, where the parametrization completely describes cavities with unwanted losses, degenerate schemes do not describe all possible cavities but only special classes. The condition

$$\frac{\mathcal{T}^{(0)}\mathcal{T}^{(c)}}{\Gamma}+\mathcal{R}^{(0)}=0, \tag{2.71}$$

that follows from Eq. (2.58) by setting $\underline{\eta}_{\rm ref}$=0, can be considered as an additional constraint, which in contrast to other constraints does not follow from the requirement that the commutation relations hold true. The constraint (2.71) also restricts the class of cavities suitable for quantum state manipulation of nonclassical optical radiation.

2.3.3 Unbalanced and cascaded homodyne detection and quantum-state reconstruction

The peculiar property which plays the unwanted noise in quantum state extraction from realistic cavities can be applied for the unbalanced homodyning of the intracavity field.

The scheme of the corresponding experiment is presented in Fig. 2.2 with the signal mode S being extracted from the cavity. Let us assume that a quantum state of light has been generated inside the cavity at the initial moment of time. The local oscillator field with the coherent amplitude β is prepared in another cavity in the form of MIM. The photodetector with the quantum efficiency $\underline{\eta}$ counts the photon number of the total outgoing field, i.e.

$$\hat{n}_{\rm out} = \hat{b}^{\dagger}_{\rm out}(0)\hat{b}_{\rm out}(0) + \hat{b}^{\dagger}_{\rm out}(1)\hat{b}_{\rm out}(1) + ... \tag{2.72}$$

We can adapt the procedure described in [101] for the reconstruction of s-parameterized phase-space distribution (1.56) of the intracavity field via the measured values of photocount probabilities. The most sufficient difference from [101] in the present case relies on a non-trivial contribution of AOM described by the second term in Eq. (2.72).

Using an argumentation similar to the one in [101] and utilizing the input-output relations (2.65) and (2.66) one can write the s-parameterized phase space distribution $P_{\rm cav}(\alpha, s)$ for the intracavity field mode in the following form [II]:

$$P_{\rm cav}(\alpha, s) = \frac{2}{\pi(1-s)} \exp\Big[\frac{2}{1-s}\frac{\overline{\eta}_{\rm ref}}{\underline{\eta}_{\rm ref}}|\alpha|^2\Big] \sum_{n=0}^{\infty}\Big[-\frac{2-\eta(1-s)}{\eta(1-s)}\Big]^n \mathcal{P}_n(\alpha, \eta), \tag{2.73}$$

where $\mathcal{P}_n(\alpha, \eta)$ is the photocount probability defined in Eq. (1.63), $\eta{=}\eta_{\rm ext}\underline{\eta}$ is the overall efficiency of detection, and

$$\alpha = -\sqrt{\frac{\underline{\eta}_{\rm ref}}{\eta_{\rm ext}}}\beta \tag{2.74}$$

is the effective coherent amplitude. One can use Eq. (2.73) for the reconstruction of the s-parameterized phase-space distribution of the intracavity field. The exponential factor in front of the sum, which does not occur in [101], is responsible for reducing the influence of the AOM.

It is worth noting that such a measurement is impossible for cavities associated with the degenerate replacement scheme and, particularly, for cavities without channels of unwanted noise. As it follows from Eq. (2.74) and the fact that for such cavities $\underline{\eta}_{\rm ref} = 0$, this measurement procedure is possible only for $\alpha = 0$, i.e. for the origin of the phase space. On the other hand, due to the presence of unwanted noise the complete information about a quantum state of the intracavity field can be obtained directly.

The efficiency of the scheme can be sufficiently improved by using the related scheme of cascaded homodyning [107]. In this scheme the balanced homodyne detection is used for counting photons [108], see Fig. 2.6. The first local oscillator (LO1) is prepared in the form of the MIM similar to the case of unbalanced homodyning. The phase randomized second local oscillator (LO2) is prepared in the form of the CAOM and it can be derived from the MIM, cf. Eq. (2.57). In this case the influence of the AOM disappears completely.

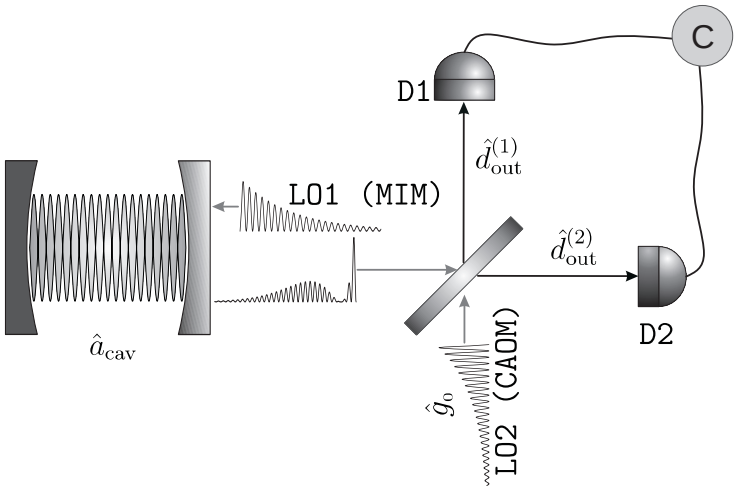

Figure 2.6: Cascaded homodyne detection of the intracavity field.

Hence the results of the work [107] with the overall efficiency η can be directly applied to this case. A detailed treatment of this cascaded homodyne detection scheme has been given in [II].

2.4 Conclusions

In this chapter we have considered the simple model of open quantum systems, namely the model of a thermal bath coupled to the quantum system of interest. Using the functional integral technique one can derive the Glauber R-function as well as the P-function and use them for the test of nonclassicality of the signal field. The contribution due to the thermal noise in these quasi-probability functions can be recast into the Feynman-Vernon influence functional, which describes the damping and dephasing (decoherence) effects due to the interaction with the reservoir.

On the other hand, using the input-output formalism the effective criterion for testing nonclassicality for noisy quantum systems has been obtained in terms of the witness function. In the case if the temperature is less than the thermal threshold and the noiseless state is tested for the nonclassicality with the witness function $\mathcal{W}(\alpha)$, then there exit (but not always) other witness functions $\mathcal{W}_{\rm th}(\alpha)$, which have the same mean value for the noisy state as $\mathcal{W}(\alpha)$ for the noiseless one. This new witness function can be obtained as a solution of a diffusion-like equation with negative diffusion coefficient. This feature explains both the existence of the thermal threshold of the nonclassicality and the restrictions for the application of the proposed method. Indeed, if the mean number of thermal photons $\bar{N}_{\rm th}$, that plays a role of "time variable" in this equation, is greater than a certain value,

then the corresponding solution may not be a positive-definite one and, moreover, has strong singularities.

An example is the witness function chosen in a form of the Gauss distribution with dispersion a^2. The corresponding mean, that is a value of the phase space distribution with $s{=}1{-}2a^2$ in a certain point, can be reconstructed in an experiment using the procedure of unbalanced homodyne detection. The evolution of this witness function according to the diffusion-like equation with negative diffusion coefficient results in a decreasing dispersion. It is clear that there exists a value of $\bar{n}$ when it degenerates into the δ-function. Beyond this value, the solution is defined in the space of distributions which, moreover, are not positive-definite ones. Hence, testing the nonclassicality beyond a certain threshold is impossible.

Our general model of open quantum system has a vast majority of applications in quantum optics. For example, it can be effectively adopted to the description of optical high-Q cavities operating both in microwave and optical domain. In the latter case one must however replace the thermal photons of the reservoir with appropriate by chosen channels of absorptive and scattering losses. For realistic cavities this can be achieved by constructing the so called replacement schemes. The concept of replacement schemes is a very helpful tool to study, within the framework of quantum noise theory, the effect of unwanted noise associated with absorption and scattering in realistic high-Q cavities, which leads to the appearance of additional noise terms in both the standard quantum Langevin equations and the input-output relations attributed to them.

The method of replacement schemes in fact allows one to distinguish, with respect to the unwanted noise, between qualitatively different cavity models. Roughly speaking, one can distinguish between non-degenerate and degenerate schemes. In contrast to non-degenerate schemes, where the parametrization completely describes cavities with unwanted losses, degenerate schemes do not describe all possible cavities but only special classes.

In the next chapter we shall consider the influence of the effects connected with dispersion, absorption and amplification on nonclassical properties of radiation that propagates in structured semiconductor media. Again, the input-output methods successfully applied in the present chapter play also an important role in the description of more complex material systems.

Chapter 3

Propagation of Nonclassical Light in Semiconductors

In Chap. 1 we have seen that a complete characterization of quantum states requires the knowledge of the correlation properties of the considered quantum system, in principle up to arbitrarily high orders. Hence the theoretical description of the observed phenomena requires also calculations of high-order correlation properties. In the field of quantum optics such calculations are usually based on models for the light-matter interaction of limited complexity or on concepts of effective interaction Hamiltonians for the light-matter interaction [57].

In the field of semiconductor physics on the other hand, much effort has been spent on the development of theoretical methods for describing the complex interactions within the many-particle systems. This includes the description of coherent optical interactions by semiconductor Bloch equations and semiconductor luminescence equations as well as the devolvement of nonequilibrium Green's function methods [59, 109]. In principle these methods also include infinite hierarchies of correlations, but they are usually treated by properly developed methods of truncations and/ or decorrelations. Altogether, the theoretical methods of quantum optics and semiconductor physics have been widely developed independently of each other.

One of the basic problems is a proper description of the propagation of nonclassical radiation fields through complex matter system. For this purpose a description of high-order correlation properties of the radiation field is needed, which takes into account the influence of the many-particle quantum properties of the matter system as well. The description of light propagation in quantum optics has been first developed for inhomogeneous and non-dispersive dielectrics [110]. Later on, the methods have been generalized for describing correctly the quantum noise effects of light during propagation in dispersive

and absorbing dielectrics [111,112]. By these methods high-order field correlations can be studied, based on the given dielectric properties of the matter system. On the other hand, the non-equilibrium description of semiconductor physics allows one to calculate the dielectric properties within some approximations of the many-particle theory. Such methods have been successfully applied to the description of light propagation including amplification and lasing [113–115], with the restriction to lower-order correlation properties such as the light intensity and the emission spectrum.

In present chapter we compare the methods developed independently in quantum optics and semiconductor physics for describing light propagation in steadily excited media with significant dispersion and absorption effects. We start our discussion by introducing a two band model of a semiconductor medium. Starting from the microscopic Hamiltonian we derive the equation of motion for carrier GFs as well as the semiconductor Bloch equation. In sections 3.2, 3.3 it is shown that in this manner one can easily extend the quantum optical approach to include gain in the medium, leading to light amplification and lasing. In Sec. 3.4 we show that using the splitting property of the photon GFs one can describe propagation of arbitrary, even nonclassical light in bounded media in terms of the classical wave propagation problem. In Sec. 3.5 we discuss the influence of the nonclassical squeezed light on the carrier kinetics in a semiconductor. Finally, in Sec. 3.6 we discuss the squeezing spectra of light propagated through a semiconductor slab.

3.1 Microscopic theory of light interacting with semiconductor medium

In this section we calculate the polarization that an optical field induces in a semiconductor material. In order to derive the microscopic theory of light interaction with semiconductor media, the Hamiltonian (1.1) should be rewritten in order to include the effects of band structure. This can be done by appending indices v and c to electronic operators $\hat{\psi}(\boldsymbol{r})$ in order to distinguish valence and conduction electrons, respectively. For many model calculations one can assume that electrons only with wavevectors, lying in the vicinity of k=0 (Γ symmetry point), contribute directly to the optical transitions. Near the band extremum we can use the parabolic approximation for band structure and write

$$\varepsilon^{\mathrm{c}}_{\boldsymbol{k}} = \frac{\hbar^2 k^2}{2m^*_{\mathrm{c}}} + E_g, \quad \varepsilon^{\mathrm{v}}_{\boldsymbol{k}} = \frac{\hbar^2 k^2}{2m^*_{\mathrm{v}}} \tag{3.1}$$

where m^*_{c} and m^*_{v} are the effective masses of electrons in the conduction and valence bands, respectively, and E_g is the band gap energy.

A transition of the valence electron into the conduction band caused by light absorption leads to a vacancy in the valence band. One usually refers to the conduction electrons simply as electrons and the missing valence-band electrons as positively charged holes. The electron and hole energies, $\varepsilon^{\rm e}_{\boldsymbol{k}}$ and $\varepsilon^{\rm h}_{\boldsymbol{k}}$, are given by Eq. (3.1) with the effective masses $m^*_{\rm c}$ and $m^*_{\rm v}$ being replaced with the effective masses of the electron and hole, in such a way that $m^*_{\rm e}{=}m^*_{\rm c}$ and $m^*_{\rm h}{=}{-}m^*_{\rm v}$. For further references we define also the reduced electron-hole mass $\mu{=}m^*_{\rm e}m^*_{\rm h}/(m^*_{\rm e}{+}m^*_{\rm h})$.

The microscopic Hamiltonian (1.1) in the dipole approximation can be rewritten as the sum of four terms $\hat{H}(t){=}\hat{H}^0_{\rm ph}+\hat{H}^{(1)}_{\rm ph}+\hat{H}^0_{\rm ch}+\hat{H}_{\rm Coul}+\hat{V}^{\rm ext}(t)$ where $\hat{H}^0_{\rm ph}$ is the free radiation Hamiltonian of Eq. (1.2) and

$$\hat{H}^{(1)}_{\rm ph}=-\hat{\boldsymbol{J}}^{\rm par}_{\rm cv}{\cdot}\hat{\boldsymbol{A}}=-\frac{e}{\mu}\sum_{\boldsymbol{k}}\Big[\hat{\boldsymbol{p}}_{\rm cv}{\cdot}\hat{\boldsymbol{A}}^{(-)}\hat{\psi}^{\rm v\dagger}_{\boldsymbol{k}}\hat{\psi}^{\rm c}_{\boldsymbol{k}}+{\rm H.c.}\Big], \tag{3.2a}$$

$$\hat{H}^0_{\rm ch}=\sum_{\boldsymbol{k}}\big[\varepsilon^{\rm e}_{\boldsymbol{k}}\hat{\psi}^{\rm c\dagger}_{\boldsymbol{k}}\hat{\psi}^{\rm c}_{\boldsymbol{k}}+\varepsilon^{\rm h}_{\boldsymbol{k}}\hat{\psi}^{\rm v\dagger}_{\boldsymbol{k}}\hat{\psi}^{\rm v}_{\boldsymbol{k}}\big], \tag{3.2b}$$

$$\hat{H}_{\rm Coul}=\frac{1}{2}\sum_{\boldsymbol{k},\boldsymbol{k}',\boldsymbol{q}}\sum_{\rm i,j=c,v}v_{\boldsymbol{q}}\;\hat{\psi}^{\rm i\dagger}_{\boldsymbol{k}+\boldsymbol{q}}\hat{\psi}^{\rm j\dagger}_{\boldsymbol{k}'-\boldsymbol{q}}\hat{\psi}^{\rm j}_{\boldsymbol{k}'}\hat{\psi}^{\rm i}_{\boldsymbol{k}} \tag{3.2c}$$

are the light-matter interaction, carrier kinetic, and Coulomb interaction parts of the full Hamiltonian, respectively. In addition we assume the influence of the external time-dependent classical field (coherent pump) on the system

$$\hat{V}^{\rm ext}(t)=-\hat{\boldsymbol{J}}^{\rm ext}_{\rm cv}\cdot\boldsymbol{A}^{\rm ext}(t)=-\sum_{\boldsymbol{k}}\big[\boldsymbol{J}^{\rm ext}{\cdot}\boldsymbol{A}^{\rm ext(-)}(t)\hat{\psi}^{\rm v\dagger}_{\boldsymbol{k}}\hat{\psi}^{\rm c}_{\boldsymbol{k}}+{\rm H.c.}\big] \tag{3.3}$$

If one approximates the time dependence of the vector potential by a plane wave with frequency $\omega_0(\boldsymbol{k}){=}(E_g+\varepsilon^{\rm e}_{\boldsymbol{k}}+\varepsilon^{\rm h}_{\boldsymbol{k}})/\hbar$, the interaction term $\boldsymbol{J}^{\rm ext}{\cdot}\boldsymbol{A}^{\rm ext}(t)$ can be approximated by the dipole coupling $\boldsymbol{d}_{\rm cv}{\cdot}\boldsymbol{E}^{(-)}e^{i\omega_0 t}{+}\boldsymbol{d}_{\rm vc}{\cdot}\boldsymbol{E}^{(+)}e^{-i\omega_0 t}$ [116]. The dipole transition matrix element is expressed through the lattice periodic part of the Bloch functions, $u_{{\rm v}\boldsymbol{k}}$ and $u_{{\rm c},\boldsymbol{k}}$ and the dipole operator $e\hat{\boldsymbol{r}}$ as $\boldsymbol{d}_{\rm cv}{=}-\int d^3\boldsymbol{r}u^*_{{\rm c},\boldsymbol{k}}\langle e\hat{\boldsymbol{r}}\rangle u_{{\rm v},\boldsymbol{k}}$. Within the effective mass approximation the projection of the dipole matrix in the field direction $\boldsymbol{e}_{\boldsymbol{E}}$ is given by

$$d_{\rm cv}=\boldsymbol{d}_{\rm cv}{\cdot}\boldsymbol{e}_{\boldsymbol{E}}{=}e\sqrt{E_g/4\mu}\big[E_g+k^2/2\mu\big]^{-1}. \tag{3.4}$$

In the following we neglect intraband optical transitions, since they are not observed in the visible part of the spectrum.

In order to calculate the light-induced polarization, we use the technique of the nonequilibrium Green functions that has been outlined in Sec. 1.1.1. The electronic GFs depend now on band indices and are defined as

$$\begin{aligned}&G^{\rm ret}_{\rm ij}(\boldsymbol{k},\boldsymbol{k}',t,t'){=}{-}\frac{i}{\hbar}\theta(t{-}t')\langle\{\hat{\psi}^{\rm i}_{\boldsymbol{k}}(t),\hat{\psi}^{\rm j\dagger}_{\boldsymbol{k}'}(t')\}\rangle,\quad G^{<}_{\rm ij}(\boldsymbol{k},\boldsymbol{k}',t,t'){=}\frac{i}{\hbar}\langle\hat{\psi}^{\rm j\dagger}_{\boldsymbol{k}}(t')\hat{\psi}^{\rm i}_{\boldsymbol{k}'}(t)\rangle,\\&G^{>}_{\rm ij}(\boldsymbol{k},\boldsymbol{k}',t,t'){=}-\frac{i}{\hbar}\langle\hat{\psi}^{\rm i}_{\boldsymbol{k}}(t')\hat{\psi}^{\rm j\dagger}_{\boldsymbol{k}'}(t)\rangle,\quad G^{\rm adv}_{\rm ij}(\boldsymbol{k},\boldsymbol{k}',t,t'){=}\frac{i}{\hbar}\theta(t'{-}t)\langle\{\hat{\psi}^{\rm i}_{\boldsymbol{k}}(t),\hat{\psi}^{\rm j\dagger}_{\boldsymbol{k}'}(t')\}\rangle\end{aligned} \tag{3.5}$$

where $\hat{\psi}^{\rm i}_{\boldsymbol{k}}$ is the annihilation operator of an electron in the band i=v, c with the wavevector $\boldsymbol{k}$. The diagonal elements are the electron and hole GFs, the non-diagonal (interband) elements describe the polarization. These Green's functions can be evaluated from the corresponding contour-ordered S-matrix functional [cf. Eqs (1.20b), (1.30a)]. For example, starting from Eq. (1.30a) and using Eq. (1.27), one obtains the Dyson's equations for the particle propagator $G^{<}_{\rm ij}$,

$$G^{(0)-1}({\rm i},1)G^{<}_{\rm ij}(1,1') = \int d2\big[\Sigma^{\rm ret}_{\rm ik}(1,2)G^{<}_{\rm kj}(2,1') + \Sigma^{<}_{\rm ik}(1,2)G^{\rm adv}_{\rm kj}(2,1')\big], \tag{3.6a}$$

$$\big[G^{(0)-1}({\rm j},1')\big]^{*}G^{<}_{\rm ij}(1,1') = -\int d2\big[G^{\rm ret}_{\rm ik}(1,2)\Sigma^{<}_{\rm kj}(2,1') + G^{<}_{\rm ik}(1,2)\Sigma^{\rm adv}_{\rm kj}(2,1')\big], \tag{3.6b}$$

where $G^{(0)-1}({\rm c},1){=}i\hbar\partial/\partial t_1{+}\nabla^2_{\boldsymbol{r}_1}/2m^{*}_{\rm c}{-}E_g$ and $G^{(0)-1}({\rm v},1){=}i\hbar\partial/\partial t_1{+}\nabla^2_{\boldsymbol{r}_1}/2m^{*}_{\rm v}$. For simplicity in the following we shall assume that $|m^{*}_{\rm v}|{=}m^{*}_{\rm c}{=}\mu/2$. We now add Eqs (3.6a) and (3.6b) and rewrite them in terms of center of mass coordinates

$$\boldsymbol{r} = \boldsymbol{r}_1 - \boldsymbol{r}_2, \quad \boldsymbol{R} = (\boldsymbol{r}_1 + \boldsymbol{r}_2)/2.$$

The Dyson equation for the nondiagonal in band indices GF reads then as ($T{=}(t_1{+}t'_1)/2$)

$$\begin{aligned}\Big\{i\hbar\frac{\partial}{\partial T} + \frac{\nabla_{\boldsymbol{r}}{\cdot}\nabla_{\boldsymbol{R}}}{2\mu} - E_g\Big\}G^{<}_{\rm ij}(\boldsymbol{r},\boldsymbol{R},t_1,t'_1) = \sum_{\rm k=i,j}\int_{-\infty}^{t_1}dt_2\int d^3\boldsymbol{r}' \\ \times\Big[\Sigma^{\rm ret}_{\rm ik}(\boldsymbol{r}{-}\boldsymbol{r}',\boldsymbol{R},t_1,t_2)G^{<}_{\rm kj}(\boldsymbol{r}',\boldsymbol{R},t_2,t'_1){-}G^{\rm ret}_{\rm ik}(\boldsymbol{r}',\boldsymbol{R},t_1,t_2)\Sigma^{<}_{\rm kj}(\boldsymbol{r}{-}\boldsymbol{r}',\boldsymbol{R},t_2,t'_1) \\ {+}\Sigma^{<}_{\rm ik}(\boldsymbol{r}{-}\boldsymbol{r}',\boldsymbol{R},t_1,t_2)G^{\rm adv}_{\rm kj}(\boldsymbol{r}',\boldsymbol{R},t_2,t'_1){-}G^{<}_{\rm ik}(\boldsymbol{r}',\boldsymbol{R},t_1,t_2)\Sigma^{\rm adv}_{\rm kj}(\boldsymbol{r}{-}\boldsymbol{r}',\boldsymbol{R},t_2,t'_1)\Big],\end{aligned} \tag{3.7}$$

where we have used the variable replacement according to $\boldsymbol{r}'{=}\boldsymbol{r}_2{-}(\boldsymbol{R}{-}\boldsymbol{r}/2)$ and we have approximated $\boldsymbol{R}{+}\frac{1}{2}(\boldsymbol{r}{-}\boldsymbol{r}'){\equiv}\boldsymbol{R}$ since microscopic variables $\boldsymbol{r}$, $\boldsymbol{r}'$ are neglictible comparative to the macroscopic $\boldsymbol{R}$ [60]. Performing the Fourier transformation with respect to variables $\boldsymbol{r}$, $\boldsymbol{R}$ we obtain the following equation for $G^{<}_{\rm ij}$

$$\begin{aligned}\Big\{i\hbar\frac{\partial}{\partial T} - \varepsilon^{\rm v}_{\bar{\boldsymbol{k}}+\frac{1}{2}\boldsymbol{K}} + \varepsilon^{\rm c}_{\bar{\boldsymbol{k}}-\frac{1}{2}\boldsymbol{K}}\Big\}G^{<}_{\rm ij}(\bar{\boldsymbol{k}}{-}\frac{1}{2}\boldsymbol{K},\bar{\boldsymbol{k}}{+}\frac{1}{2}\boldsymbol{K},t_1,t'_1) = \frac{1}{\upsilon}\sum_{\boldsymbol{q}}\sum_{\rm k}\int_{-\infty}^{t_1}dt_2 \\ \times\Big[\Sigma^{\rm ret}_{\rm ik}(\bar{\boldsymbol{k}}{+}\frac{1}{2}\boldsymbol{K},\bar{\boldsymbol{k}}{-}\boldsymbol{q}{+}\frac{1}{2}\boldsymbol{K},t_1,t_2)G^{<}_{\rm kj}(\bar{\boldsymbol{k}}{-}\frac{1}{2}\boldsymbol{K},\bar{\boldsymbol{k}}{-}\boldsymbol{q}{+}\frac{1}{2}\boldsymbol{K},t_2,t'_1) \\ {-}G^{\rm ret}_{\rm ik}(\bar{\boldsymbol{k}}{-}\boldsymbol{q}{+}\frac{1}{2}\boldsymbol{K},\bar{\boldsymbol{k}}{-}\frac{1}{2}\boldsymbol{K},t_1,t_2)\Sigma^{<}_{\rm kj}(\bar{\boldsymbol{k}}{-}\boldsymbol{q}{+}\frac{1}{2}\boldsymbol{K},\bar{\boldsymbol{k}}{+}\frac{1}{2}\boldsymbol{K},t_2,t'_1) \\ {+}\Sigma^{<}_{\rm ik}(\bar{\boldsymbol{k}}{+}\frac{1}{2}\boldsymbol{K},\bar{\boldsymbol{k}}{-}\boldsymbol{q}{+}\frac{1}{2}\boldsymbol{K},t_1,t_2)G^{\rm adv}_{\rm kj}(\bar{\boldsymbol{k}}{-}\frac{1}{2}\boldsymbol{K},\bar{\boldsymbol{k}}{-}\boldsymbol{q}{+}\frac{1}{2}\boldsymbol{K},t_2,t'_1) \\ {-}G^{<}_{\rm ik}(\bar{\boldsymbol{k}}{-}\boldsymbol{q}{+}\frac{1}{2}\boldsymbol{K},\bar{\boldsymbol{k}}{-}\frac{1}{2}\boldsymbol{K},t_1,t_2)\Sigma^{\rm adv}_{\rm kj}(\bar{\boldsymbol{k}}{-}\boldsymbol{q}{+}\frac{1}{2}\boldsymbol{K},\bar{\boldsymbol{k}}{+}\frac{1}{2}\boldsymbol{K},t_2,t'_1)\Big].\end{aligned} \tag{3.8}$$

We note also the relations $\boldsymbol{k}{=}\bar{\boldsymbol{k}}{-}\frac{1}{2}\boldsymbol{K}$, $\boldsymbol{k}'{=}\bar{\boldsymbol{k}}{+}\frac{1}{2}\boldsymbol{K}$ where the momenta variables $\boldsymbol{k}$, $\boldsymbol{k}'$ have early appeared in Eq. (3.5).

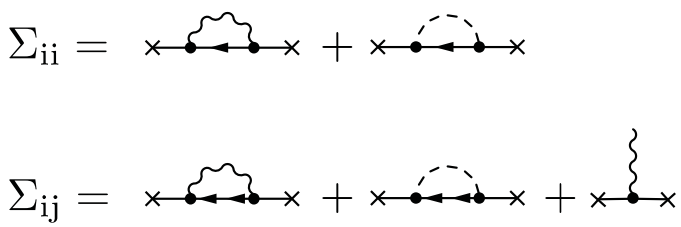

Figure 3.1: Intraband ($\Sigma_{\rm ii}$) and interband ($\Sigma_{\rm ij}$) self-energy contributions to the carrier Green's functions in Hartree-Fock approximation. The lines with one and two arrows represent the diagonal and non-diagonal in band indices carrier GFs, respectively. The wavy lines denote the photon propagators and the dashed lines represent the Coulomb interaction. The last term in the second line originates from the coherent pump.

For a microscopic description of the interaction of the electron-hole system and an external electromagnetic field it is usually enough to consider the equation of motion for the Green's functions $G^{\gtrless}$ with equal time argument. According to the definitions, the one-particle distribution functions and the excitonic transition amplitude (excitonic polarization) are related to the Green's functions (3.5) by

$$f^{\rm e}_{\boldsymbol{k},\boldsymbol{k}'}(t)=\varrho^{\rm cc<}_{\boldsymbol{k},\boldsymbol{k}'}(t),\quad f^{\rm h}_{\boldsymbol{k},\boldsymbol{k}'}(t)=\delta_{\boldsymbol{k},\boldsymbol{k}'}-\varrho^{\rm vv<}_{\boldsymbol{k},\boldsymbol{k}'}(t) \tag{3.9}$$

and

$$p^{\rm cv}_{\boldsymbol{k},\boldsymbol{k}'}(t)=\varrho^{\rm cv<}_{\boldsymbol{k},\boldsymbol{k}'}(t),\quad p^{\rm vc}_{\boldsymbol{k},\boldsymbol{k}'}(t)=p^{\rm cv*}_{\boldsymbol{k},\boldsymbol{k}'}(t)=\varrho^{\rm vc<}_{\boldsymbol{k},\boldsymbol{k}'}(t). \tag{3.10}$$

where for convenience we have introduced the following notation: $\varrho^{\rm ij<}_{\boldsymbol{k},\boldsymbol{k}'}(t)=\delta_{\rm ij}\delta_{\boldsymbol{k},\boldsymbol{k}'}+\varrho^{\rm ij>}_{\boldsymbol{k},\boldsymbol{k}'}(t)$ $=-i\hbar G^{<}_{\rm ij}(\boldsymbol{k},\boldsymbol{k}',t,t)$. Let us consider now the low-density of electron-hole pair states. For self energies of particles in the screened Hartree-Fock approximation (see Fig 3.1), from Eq. (3.8) we obtain

$$\begin{aligned}
&i\hbar\frac{\partial}{\partial t}p^{\rm cv}_{\boldsymbol{k},\boldsymbol{k}'}+\frac{1}{\upsilon}\sum_{\boldsymbol{q}}\Big[\mathfrak{e}^{\rm c}_{\boldsymbol{k}',\boldsymbol{k}'-\boldsymbol{q}}p^{\rm cv}_{\boldsymbol{k},\boldsymbol{k}'-q}-\mathfrak{e}^{\rm v}_{\boldsymbol{k}'-q,\boldsymbol{k}'}p^{\rm cv}_{\boldsymbol{k}'-\boldsymbol{q},\boldsymbol{k}}+\hbar\Omega_{\rm cv}(\boldsymbol{k}',\boldsymbol{k}'-\boldsymbol{q})N_{\boldsymbol{k},\boldsymbol{k}'-\boldsymbol{q}}\Big]\\
&\qquad=\sum_{\rm k=c,v}\sum_{\boldsymbol{q}}\int dt_2\Big[\Sigma^{\rm ph<}_{\rm ck}(\boldsymbol{k}',\boldsymbol{k}'-\boldsymbol{q},t,t_2)G^{>}_{\rm kv}(\boldsymbol{k},\boldsymbol{k}'-\boldsymbol{q},t_2,t)\\
&\qquad\qquad+G^{>}_{\rm ck}(\boldsymbol{k}'-\boldsymbol{q},\boldsymbol{k},t,t_2)\Sigma^{\rm ph<}_{\rm kv}(\boldsymbol{k}'-\boldsymbol{q},\boldsymbol{k}',t_2,t)-\{>\longleftrightarrow<\}\Big],
\end{aligned}\tag{3.11}$$

where

$$\mathfrak{e}^{\rm c,v}_{\boldsymbol{k},\boldsymbol{k}'}=\varepsilon^{\rm c,v}_{\boldsymbol{k}}\delta_{\boldsymbol{k},\boldsymbol{k}'}-\frac{1}{\upsilon}\sum_{\boldsymbol{q}}\Big[v_{\boldsymbol{q}}f^{\rm e,h}_{\boldsymbol{k}'-\boldsymbol{q},\boldsymbol{k}-\boldsymbol{q}}\mp v_{\boldsymbol{k}-\boldsymbol{k}'}\big(f^{\rm e}_{\boldsymbol{q},\boldsymbol{k}-\boldsymbol{k}'-\boldsymbol{q}}-f^{\rm h}_{\boldsymbol{q},\boldsymbol{k}-\boldsymbol{k}'+\boldsymbol{q}}\big)\Big], \tag{3.12}$$

$$N_{\boldsymbol{k},\boldsymbol{k}'}=\delta_{\boldsymbol{k},\boldsymbol{k}'}-f^{\rm e}_{\boldsymbol{k},\boldsymbol{k}'}-f^{\rm h}_{\boldsymbol{k},\boldsymbol{k}'} \tag{3.13}$$

$$\hbar\Omega_{\rm ij}(\boldsymbol{k},\boldsymbol{k}') = \boldsymbol{d}_{\rm ij}(\frac{1}{2}[\boldsymbol{k}+\boldsymbol{k}'])\cdot\boldsymbol{E}_{\boldsymbol{k}-\boldsymbol{k}'} + 2\frac{1}{\upsilon}\sum_{\boldsymbol{q}} v_{\boldsymbol{q}} p^{\rm ij}_{\boldsymbol{k}'-\boldsymbol{q},\boldsymbol{k}-\boldsymbol{q}}, \tag{3.14}$$

$$\Sigma^{\rm ph\gtrless}_{\rm ij}(\boldsymbol{k},\boldsymbol{k}',t,t') = i\hbar\frac{1}{\upsilon}\sum_{\boldsymbol{q}} D^{\gtrless}(\boldsymbol{q},t,t')G^{\gtrless}_{\rm ij}(\boldsymbol{k}'-\boldsymbol{q},\boldsymbol{k}-\boldsymbol{q},t,t'). \tag{3.15}$$

Here Eq. (3.12) represents the density-dependent band-gap renormalization due to the Coulomb interaction $v_{\boldsymbol{q}}$. Equation (3.13) defines the phase space blocking factor (Pauli blocking). The coherent excitation together with the interband Coulomb interaction define the Rabi frequency (3.14) that characterizes the rate of the interband transitions. Finally, Eq. (3.15) is the particle self-energy induced by the interaction with the quantized radiation field that also contributes to the energy shift and Rabi-frequency. We also note, that $\Sigma^{\rm ph\gtrless}_{\rm ij}$ for i$\neq$j is negligibly small unless the radiation field is in resonance with interband transition frequency. The resonance condition can be achieved by placing the interaction system in a resonator tuned to the resonance frequency.

For translational invariant system it is easy to see that $f^{\rm i}_{\boldsymbol{k},\boldsymbol{k}'}=f^{\rm i}_{\boldsymbol{k}}\delta_{\boldsymbol{k},\boldsymbol{k}'}$ and $p^{\rm cv}_{\boldsymbol{k},\boldsymbol{k}'}=p^{\rm cv}_{\boldsymbol{k}}\delta_{\boldsymbol{k},\boldsymbol{k}'}$. In this case Eq. (3.11) reduces to the well-known semiconductor Bloch equation for microscopic polarization $p^{\rm cv}_{\boldsymbol{k}}$ [55, 116, 117].

From Eqs (3.8) and (3.15) it is seen that the electron-hole kinetics is closely linked with the electromagnetic field dynamics expressed in terms of the photon GF. We shall return to this point in Sec. 3.5 where we describe the influence of the nonclassical light on dielectric properties of a medium. The next sections 3.2 – 3.4 are devoted to the description of light propagation in bounded media. In particular we will obtain the expression for the photon GFs needed later on for the calculations of the self-energy given in Eq. (3.15).

3.2 Light propagation in bounded semiconductor media

In this section we shall describe the influence of the dispersion and absorption (or amplification) effects on the nonclassical properties of light propagating in semiconductor media with boundaries. This problem can be formulated in terms of the Maxwell wave equation for the effective field given in Eq. (1.22) with the appropriate spatial boundary conditions. Indeed, we start from the microscopic Hamiltonian

$$\hat{H}^{\rm ph}(t)=\hat{H}^{0}_{\rm ph} + \hat{H}^{(1)}_{\rm ph} + \hat{V}^{\rm ext}(t)$$

that described the dynamics of the electromagnetic field being coupled to the media (term $\hat{H}^{(1)}_{\rm ph}$) and to the external perturbation $\boldsymbol{J}_{\rm ext}$ (term $\hat{V}^{\rm ext}(t)=-\boldsymbol{J}^{\rm ext}(t)\cdot\hat{\boldsymbol{A}}$). Then we define with the help of the Hamiltonian functional $\mathcal{H}_{\rm ph}[\mathcal{A}_\mu;t]=\langle\mathcal{A}_\mu|\hat{H}_{\rm ph}(t)|\mathcal{A}_\mu\rangle$ the canonical

action $\mathscr{S}_{\mathcal{C}}^{\rm ph}=\int_{\mathcal{C}} dt\big\{(\dot{\mathcal{A}}_\mu)^2-\mathcal{H}^{\rm ph}[\mathcal{A}_\mu;t]\big\}$ defined on the Keldysh contour $\mathcal{C}$. Varying this action with respect to the vector potential variable, $\mathcal{A}_\mu\equiv\langle\hat{A}_\mu\rangle_{\mathcal{C}}\equiv\langle\hat{A}_\mu\rangle$, we finally obtain the Maxwell wave equation for the effective field [in the following we shall omit the band indices for simplicity]

$$\Box\langle\hat{\boldsymbol{A}}(\boldsymbol{r},t)\rangle=-\mu_0\big[\boldsymbol{J}^{\rm med}(\boldsymbol{r},t)+\boldsymbol{J}^{\rm ext}(\boldsymbol{r},t)\big]. \tag{3.16}$$

where $\boldsymbol{J}^{\rm med}=\langle\hat{\boldsymbol{J}}_{\rm cv}^{\rm par}\rangle_{\mathcal{C}}$ is the effective medium current density induced by the external perturbation. The solution of this equation in terms of the photon GFs (in the Fourier domain) reads as

$$\langle\hat{A}_\mu(\boldsymbol{r},\omega)\rangle=-\mu_0\int d^3\boldsymbol{r}'\,D^{\rm ret}_{\mu\nu}(\boldsymbol{r},\boldsymbol{r}',\omega)J^{\rm ext}_\nu(\boldsymbol{r}',\omega), \tag{3.17}$$

where the inverse of the retarded photon GF $D^{\rm ret}(\boldsymbol{r},\boldsymbol{r}',\omega)$ resolves Eq. (1.37) and in linear approximation it is given by

$$D^{{\rm ret},-1}_{\mu\nu}(\boldsymbol{r},\boldsymbol{r}',\omega)=\Big(D^{(0){\rm ret},-1}_{\mu\nu}(\boldsymbol{r},\boldsymbol{r}')-P^{\rm ret}_{\mu\nu}(\boldsymbol{r},\boldsymbol{r}',\omega)\Big)=\Box\delta_{\mu\nu}\delta(\boldsymbol{r}-\boldsymbol{r}')-P^{\rm ret}_{\mu\nu}(\boldsymbol{r},\boldsymbol{r}',\omega). \tag{3.18}$$

Here the retarded polarization function $P^{\rm ret}_{\mu\nu}(\boldsymbol{r},\boldsymbol{r}',\omega)$ being related to the complex (dielectric) susceptibility tensor $\chi_{\mu\nu}(\boldsymbol{r},\boldsymbol{r}',\omega)=\chi'_{\mu\nu}(\boldsymbol{r},\boldsymbol{r}',\omega)+i\chi''_{\mu\nu}(\boldsymbol{r},\boldsymbol{r}',\omega)$ of the medium according to

$$P^{\rm ret}_{\mu\nu}(\boldsymbol{r},\boldsymbol{r}',\omega)=-\frac{\omega^2}{c^2}\,\chi_{\mu\nu}(\boldsymbol{r},\boldsymbol{r}',\omega). \tag{3.19}$$

Inverting Eq. (3.17) by applying on both sides the inverted GF (3.18) we can rewrite the solution of Eq. (1.22) in the integral form of the Lippmann-Schwinger equation

$$\langle\hat{A}_\mu(\boldsymbol{r},\omega)\rangle=A^{\rm ext}_\mu(\boldsymbol{r},\omega)+\int d^3\boldsymbol{r}_1d^3\boldsymbol{r}_2D^{(0){\rm ret}}_{\mu\rho}(\boldsymbol{r},\boldsymbol{r}_1,\omega)P^{\rm ret}_{\rho\sigma}(\boldsymbol{r}_1,\boldsymbol{r}_2,\omega)\langle\hat{A}_\sigma(\boldsymbol{r}_2,\omega)\rangle. \tag{3.20}$$

Eq. (3.20) can be rewritten more compactly as

$$\langle\hat{A}_\mu(\boldsymbol{r},\omega)\rangle=\int d^2\boldsymbol{r}_1\varepsilon^{\perp{\rm ret},-1}_{\mu\nu}(\boldsymbol{r},\boldsymbol{r}_1,\omega)A^{\rm ext}_\nu(\boldsymbol{r}_1,\omega) \tag{3.21}$$

where $\varepsilon^{\perp}_{\mu\nu}$ is the transverse dielectric tensor

$$\begin{aligned}\varepsilon^{\perp,-1}_{\mu\nu}(\underline{1},\underline{2})=\frac{\delta\langle\hat{A}_\mu(\underline{1})\rangle}{\delta A^{\rm ext}_\nu(\underline{2})}&=\int d\underline{3}D_{\mu\rho}(\underline{1},\underline{3})D^{(0),-1}_{\rho\nu}(\underline{3},\underline{2})\\&=\delta^{\perp}_{\mu\nu}(\underline{1}-\underline{2})+\int d\underline{3}D_{\mu\rho}(\underline{1},\underline{3})P_{\rho\nu}(\underline{3},\underline{1}),\end{aligned} \tag{3.22}$$

$$\begin{aligned}\varepsilon^{\perp}_{\mu\nu}(\underline{1},\underline{2})=\frac{\delta A^{\rm ext}_\mu(\underline{1})}{\delta\langle\hat{A}_\nu(\underline{2})\rangle}&=\int d\underline{3}D^{(0)}_{\mu\rho}(\underline{1},\underline{3})D^{-1}_{\rho\nu}(\underline{3},\underline{2})\\&=\delta^{\perp}_{\mu\nu}(\underline{1}-\underline{2})-\int d\underline{3}D^{(0)}_{\mu\rho}(\underline{1},\underline{3})P_{\rho\nu}(\underline{3},\underline{2}).\end{aligned} \tag{3.23}$$

In Refs. [113, 114, 118] the following generalization of the Optical Theorem (1.36) for the medium with boundaries has been given:

$$D^{\gtrless}_{\mu\nu}(\boldsymbol{r},\boldsymbol{r}',\omega) = \int d^3\boldsymbol{r}_1 \int d^3\boldsymbol{r}_2\, D^{\rm ret}_{\mu\rho}(\boldsymbol{r},\boldsymbol{r}_1,\omega) \times \Big[P^{\gtrless}_{\rho\lambda}(\boldsymbol{r}_1,\boldsymbol{r}_2,\omega) \mp i\epsilon\frac{4\omega}{c^2} n^{\gtrless}(\omega)\delta_{\rho\lambda}\delta(\boldsymbol{r}_1-\boldsymbol{r}_2)\Big]\, D^{\rm adv}_{\lambda\nu}(\boldsymbol{r}_2,\boldsymbol{r}',\omega). \tag{3.24}$$

Here $P^{\gtrless}_{\mu\nu}$ are the corresponding Keldysh components of the polarization tensor, and summation over repeated indices is understood. It is noteworthy, that in Eq. (3.24), beside the polarization function $P^{\gtrless}_{\mu\nu}$ of the medium an additional contribution appears, which is induced by the surrounding vacuum. Such a contribution would already formally result in Eq. (3.18), if $\Box{=}\Delta{+}(\omega+i\epsilon)^2/c^2$ is used for the retarded GF. There it disappears in the limit $\epsilon{\to}0$. In the integral representation (3.24), however, that term leads to an improper integral over $D^{\rm ret}_{\mu\rho}D^{\rm adv}_{\rho\nu}$, which is just proportional to $1/\epsilon$. Hence, a well-defined vacuum-induced contribution to the propagating fluctuations and thus to the spectral function appears. The function $n^{<}{=}n^{>}{-}1$ describes the nonequilibrium distribution of photons owing to external preparation, e.g., due to interaction with a heat bath or incoherent radiation incident from outside.

Within the framework of macroscopic QED, the Maxwell wave equation (1.22) is regarded as being the operator-valued inhomogeneous wave equation

$$\Box\hat{\boldsymbol{A}}(\boldsymbol{r},t) = -\mu_0\big[\,\hat{\boldsymbol{J}}^{\rm med}(\boldsymbol{r},t) + \boldsymbol{J}^{\rm ext}(\boldsymbol{r},t)\big] \tag{3.25}$$

that corresponds to the Maxwell equations of the transverse part of the macroscopic electromagnetic field in a linear dielectric medium. Hence, the current density $\hat{\boldsymbol{J}}^{\rm med}(\boldsymbol{r},\omega)$ associated with the medium under consideration must have the form

$$\hat{J}^{\rm med}_{\mu}(\boldsymbol{r},\omega){=}{-}\varepsilon_0\omega^2\int d^3\boldsymbol{r}'\,\chi_{\mu\nu}(\boldsymbol{r},\boldsymbol{r}',\omega)\hat{A}_{\nu}(\boldsymbol{r}',\omega) + \hat{J}_{\mu,{\rm N}}(\boldsymbol{r},\omega), \tag{3.26}$$

and in place of Eq. (3.17) we obtain the operator-valued equation

$$\hat{A}_{\mu}(\boldsymbol{r},\omega){=}{-}\mu_0\int d^3\boldsymbol{r}'\,D^{\rm ret}_{\mu\nu}(\boldsymbol{r},\boldsymbol{r}',\omega)\,\Big[\hat{J}_{\nu,{\rm N}}(\boldsymbol{r}',\omega){+}J^{\rm ext}_{\nu}(\boldsymbol{r}',\omega)\Big]\,, \tag{3.27}$$

where the noise current density operator $\hat{\boldsymbol{J}}_{\rm N}(\boldsymbol{r},\omega)$ obeys the commutation relation

$$\begin{aligned}\big[\hat{J}_{\mu,{\rm N}}(\boldsymbol{r},\omega),\hat{J}^{\dagger}_{\nu,{\rm N}}(\boldsymbol{r}',\omega')\big]&{=}\frac{i\hbar}{\mu_0}\Big\{P^{\rm ret}_{\mu\nu}(\boldsymbol{r},\boldsymbol{r}',\omega){-}P^{\rm adv}_{\mu\nu}(\boldsymbol{r},\boldsymbol{r}',\omega)\Big\}\delta(\omega{-}\omega')\\ &{=}\frac{i\hbar}{\mu_0}\Big\{P^{>}_{\mu\nu}(\boldsymbol{r},\boldsymbol{r}',\omega){-}P^{<}_{\mu\nu}(\boldsymbol{r},\boldsymbol{r}',\omega)\Big\}\delta(\omega{-}\omega')\end{aligned} \tag{3.28}$$

$[\hat{\boldsymbol{J}}_{\rm N}(\boldsymbol{r},-\omega){=}\hat{\boldsymbol{J}}^{\dagger}_{\rm N}(\boldsymbol{r},\omega)]$, which ensures the validity of the commutation relation given by Eq. (1.5). We note here also that the consistency of the microscopic and macroscopic

QED theories relies on the equality $\boldsymbol{J}^{\rm med}=\langle\hat{\boldsymbol{J}}^{\rm med}\rangle$ that follows from the stochastic nature of noise currents, i.e., from the vanishing of $\langle\hat{\boldsymbol{J}}_{\rm N}\rangle$.

With the analog of the optical theorem (3.24) in macroscopic QED, which one obtains by inserting Eq. (3.27) in (1.34) and by using for $D^{\rm ret}_{\mu\nu}(\boldsymbol{r},\boldsymbol{r}',\omega)=D^{\rm adv}_{\nu\mu}(\boldsymbol{r}',\boldsymbol{r},-\omega)$, $\omega>0$, the relation [IV]

$$P^{>}_{\mu\nu}(\boldsymbol{r},\boldsymbol{r}',t-t')=P^{<}_{\nu\mu}(\boldsymbol{r}',\boldsymbol{r},t'-t)=\frac{\mu_0}{i\hbar}\big\langle\hat{J}_{\mu,{\rm N}}(\boldsymbol{r},t)\hat{J}_{\nu,{\rm N}}(\boldsymbol{r}',t')\big\rangle \tag{3.29}$$

can be derived. Within the framework of microscopic QED the correlation functions of noise currents with the use of (3.29) can be related to the measurable correlation functions of the medium current densities

$$L^{>}_{\mu\nu}(\boldsymbol{r},\boldsymbol{r}',t-t')=\frac{\mu_0}{i\hbar}\big\langle\hat{J}^{\rm med}_{\mu}(\boldsymbol{r},t)\hat{J}^{\rm med}_{\nu}(\boldsymbol{r}',t')\big\rangle. \tag{3.30}$$

Taking the time variable along the Keldysh contour $\mathcal{C}$ (see Fig. 1.1), we can write the correlation function (3.30) as

$$L_{\mu\nu}(\underline{1},\underline{1}')=-\mu_0\frac{\delta\langle\hat{J}^{\rm med}_{\mu}(\underline{1})\rangle}{\delta A^{\rm ext}_{\nu}(\underline{1}')}, \tag{3.31}$$

where $\boldsymbol{A}^{\rm ext}$ is the vector potential of the external electromagnetic field. Applying the chain rule for the variational derivatives, one gets the Bethe-Salpeter equation for $L_{\mu\nu}$

$$L_{\mu\nu}(\underline{1},\underline{1}')=P_{\mu\nu}(\underline{1},\underline{1}')+\int d\underline{2}d\underline{3}P_{\mu\rho}(\underline{1},\underline{2})D^{(0)}_{\rho\lambda}(\underline{2},\underline{3})L_{\lambda\nu}(\underline{3},\underline{1}'), \tag{3.32}$$

where we have used the definition

$$D^{(0)}_{\mu\nu}(\underline{1},\underline{1}')=-\frac{1}{\mu_0}\frac{\delta A^{\rm ext}_{\mu}(\underline{1})}{\delta j^{\rm ext}_{\nu}(\underline{1}')} \tag{3.33}$$

of the free photon GF and the formula (1.33) for the polarization $P_{\mu\nu}$. We refer to Eq. (1.31) for the definition of the transversal current density $\boldsymbol{j}^{\rm ext}$ that enters Eq. (3.33).

The $\gtrless$-components of the polarization tensor one obtains from (3.32) by using the Langreth theorem (1.1.1). After some algebra we arrive after Fourier transformation at

$$\begin{aligned}P^{\gtrless}_{\mu\nu}(\boldsymbol{r},\boldsymbol{r}',\omega)=\int d^3\boldsymbol{r}_1\int d^3\boldsymbol{r}_2\Big\{&\varepsilon^{\perp{\rm ret}}_{\mu\rho}(\boldsymbol{r},\boldsymbol{r}_1,\omega)L^{\gtrless}_{\rho\lambda}(\boldsymbol{r}_1,\boldsymbol{r}_2,\omega)\varepsilon^{\perp{\rm adv}}_{\lambda\nu}(\boldsymbol{r}_2,\boldsymbol{r}',\omega)\\&-P^{\rm ret}_{\mu\rho}(\boldsymbol{r},\boldsymbol{r}_1,\omega)D^{(0)\gtrless}_{\rho\lambda}(\boldsymbol{r}_1,\boldsymbol{r}_2,\omega)P^{\rm adv}_{\lambda\nu}(\boldsymbol{r}_2,\boldsymbol{r}',\omega)\Big\}.\end{aligned} \tag{3.34}$$

From Eq. (3.34) we see that, as expected, the correlation function of the noise current density in macroscopic QED, cf. Eq. (3.29), is directly related to the microscopically well-defined and observable correlation function of the medium current density as given by Eq. (3.30).

3.3 Restriction to the slab geometry

In the following we will deal with the propagation of TE-polarized radiation along the x axis, through a semiconductor slab of thickness L which is infinitely extended in the y-z–plane (see Fig. 3.2). For simplicity, we assume that the electric field is polarized along the z-axis $\hat{\boldsymbol{A}}=(0,0,\hat{A})$. Then, neglecting spatial dispersion, the complex refractive index inside the medium, $n=n'+in''$, is obtained from $n^2(\omega)=1+\chi(\omega)$.

Using Green's function technique, the spontaneous emission of the slab is studied in Ref. [113,114,119]. A generalization of the results including spatial dispersion and providing exact relations between (spontaneous and stimulated) emission and linear absorption can be found in Ref. [118]. The intensity of the (spontaneously) emitted radiation can be obtained from the Poynting theorem for the medium in the steady state (see Appendix D). Combining Eqs (3.24), (D.7), and (D.10) we find for the energy flow through the slab surface, i.e., intensity of spontaneous emission, the following expression [IV]:

$$I_{\rm em}(\omega)\equiv\Delta\mathcal{S}_{\rm em}(\omega)=\frac{Lc}{4}\hbar\omega b(\omega)\widehat{P}(\omega)\widehat{D}_L^{\rm vac}(\omega)\,, \tag{3.35}$$

where

$$\widehat{D}_L^{\rm vac}(\omega)=-i\epsilon\frac{4\omega}{c^2L}\int\limits_{-L/2}^{L/2}dxdx'D^{\rm ret}(x,x',\omega)D^{\rm adv}(x',x,\omega) \tag{3.36}$$

is the vacuum-induced contribution to the photon spectral function resulting from the ones in the optical theorem (3.24), $\widehat{P}=2i\,{\rm Im}\,P^{\rm ret}$ is, according to (3.19), related to χ'' associated with linear absorption/amplification, and b is defined as the ratio between the recombination rate $P^<$ of electron–hole pairs and $\widehat{P}$. The function $b(\omega)$ characterizes globally (i. e., inside and outside the slab) the emitted radiation and, as such, b is accessible to direct observation in experiments. It generalizes Planck's formula for the black body radiation to nonequilibrium radiation of an excited medium in the steady state. We also note, that Eq. (3.35), in contrast to our approach, was obtained in [119] from the requirement for the Poynting vector to be a normally-ordered correlation function of the field operators for the case of quasi-equilibrium.

Evaluating the integral in Eq. (3.36) with the GFs defined in Appendix E, one obtains

$$\widehat{D}_L^{\rm vac}(\omega)=\frac{8c}{\omega}\frac{|\,\mathscr{r}(\omega)|}{|1-\mathscr{r}^2(\omega)|^2}\frac{1}{|n^2(\omega)-1|}\mathscr{I}_L(\omega), \tag{3.37}$$

where

$$\mathscr{I}_L(\omega)=\big\{1+|\,\mathscr{r}(\omega)|^2\big\}\frac{\sinh[\omega n''(\omega)L/c]}{\omega n''(\omega)L/c}+\big\{\,\mathscr{r}(\omega)+\mathscr{r}^*(\omega)\big\}\frac{\sin[\omega n'(\omega)L/c]}{\omega n'(\omega)L/c}, \tag{3.38}$$

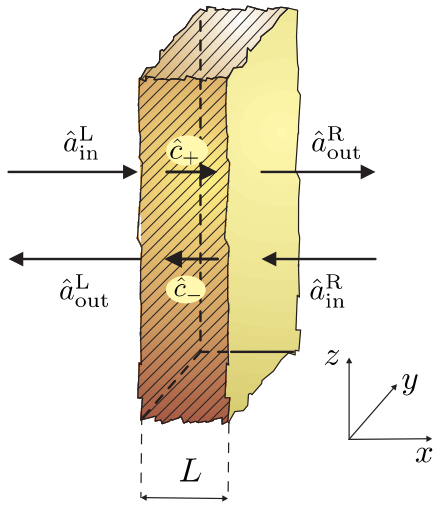

Figure 3.2: Illustration of the considered semiconductor medium in a slab geometry. The directions of propagating modes are shown by arrows and the operators involved in the input-output relations (3.40) are indicated.

and

$$\mathscr{r}(\omega)=[1-n(\omega)]/[1+n(\omega)]e^{i\omega n(\omega)L/c} \tag{3.39}$$

is the internal reflectivity.

On the basis of Eq. (3.27), by setting $J_{\mathrm{ext}}=0$, the input–output relations

$$\begin{pmatrix}\hat{a}^{\mathrm{L}}_{\mathrm{out}}(-\frac{L}{2},\omega)\\ \hat{a}^{\mathrm{R}}_{\mathrm{out}}(+\frac{L}{2},\omega)\end{pmatrix}=\mathbf{T}\cdot\begin{pmatrix}\hat{a}^{\mathrm{L}}_{\mathrm{in}}(-\frac{L}{2},\omega)\\ \hat{a}^{\mathrm{R}}_{\mathrm{in}}(+\frac{L}{2},\omega)\end{pmatrix}+\mathbf{A}\cdot\begin{pmatrix}\hat{c}_+(\omega)\\ \hat{c}_-(\omega)\end{pmatrix} \tag{3.40}$$

can be derived [112], where $\mathbf{T}$ and $\mathbf{A}$ are 2×2 transmission and absorption matrices, respectively with elements defined as

$$\begin{aligned}&T_{11}(\omega)=T_{22}(\omega)=\mathcal{R}(\omega);\ T_{12}(\omega)=T_{21}(\omega)=\mathcal{T}(\omega);\\ &A_{11}(\omega)=A_{21}(\omega)=\big\{\mathcal{V}_-(\omega)+\mathcal{V}_+(\omega)\big\}/\mathcal{N}_+(\omega);\\ &A_{12}(\omega)=-A_{22}(\omega)=\big\{\mathcal{V}_-(\omega)-\mathcal{V}_+(\omega)\big\}/\mathcal{N}_-(\omega),\end{aligned} \tag{3.41}$$

where functions $\mathcal{T}$, $\mathcal{R}$ and $\mathcal{V}_\pm$ are defined in Eqs (E.14), (E.15) of Appendix E and

$$\mathcal{N}_\pm(\omega)=\Big[\frac{\omega}{c}n'(\omega)n''(\omega)\Big\{\frac{\sinh[n''(\omega)\omega L/c]}{n''(\omega)}\pm\frac{\sin[n'(\omega)\omega L/c]}{n'(\omega)}\Big\}\Big]^{-1/2}. \tag{3.42}$$

These matrices in general fulfill the matrix relation $\mathbf{T}\mathbf{T}^*+\mathbf{A}\mathbf{A}^*=\mathbf{1}$, that is just the requirement for the output operators $\hat{a}^{\mathrm{R,L}}_{\mathrm{out}}$ in (3.40) to obey the bosonic commutation relations.

The input-output relation (3.40) relates the input field $\hat{a}^{\mathrm{R}}_{\mathrm{in}}$ ($\hat{a}^{\mathrm{L}}_{\mathrm{in}}$),

$$\hat{a}^{\mathrm{R,L}}_{\mathrm{in}}(\pm\frac{L}{2},\omega)=i(\hbar\omega\varepsilon_0)^{-1/2}\int_{-\infty}^{\mp L/2}dx'e^{-i\omega x'/c}\hat{J}_{\mathrm{N}}(\mp x',\omega), \tag{3.43}$$

incoming on the right (left) side of the slab, with the corresponding output fields. In the following we omit the arguments $\pm L/2$ for simplicity.

The absorption/amplification effects are calculated by bosonic quasiparticle annihilation operators

$$\hat{c}_{\pm}(\omega)=\frac{i}{2}(\hbar\omega\varepsilon_0)^{-1/2}\mathcal{N}_{\pm}(\omega)\int\limits_{-L/2}^{L/2}dx'\left(e^{in(\omega)\omega x'/c}\pm e^{-in(\omega)\omega x'/c}\right)\hat{J}_{\mathrm{N}}(x',\omega) \tag{3.44}$$

expressed in terms of the noise current density operator and associated with the slab–radiation excitations. The poles of D^{ret} yield the polaritonic dispersion relations of the slab, which allows one to relate the operators $\hat{c}_{\pm}$ to the polaritonic annihilation operators. Assuming that the input field is in the vacuum state, the spectrum of the output field detected on the right side of the slab

$$\begin{aligned}&2\varepsilon_0 c\langle\hat{E}^{(-)\mathrm{R}}(x,\omega)\hat{E}^{(+)\mathrm{R}}(x,\omega)\rangle\equiv I_{\mathrm{em}}(\omega),\\&\hat{E}^{(+)\mathrm{R}}(x,\omega)=i\sqrt{\frac{\hbar\omega}{2\varepsilon_0}}\left[\hat{a}^{\mathrm{R}}_{\mathrm{in}}(\omega)e^{-i\omega x/c}+\hat{a}^{\mathrm{R}}_{\mathrm{out}}(\omega)e^{i\omega x/c}\right]\end{aligned} \tag{3.45}$$

is obtained in just the same form as in Eq. (3.35), by identifying $\langle\hat{c}^{\dagger}(\omega)\hat{c}(\omega)\rangle\equiv b(\omega)$, where $\hat{c}(\omega)=[\hat{c}_{+}(\omega)+\hat{c}_{-}(\omega)]/\sqrt{2}$. Note that the relation of photon operators to polaritonic ones was already considered in [111], for the absorptive case and a harmonic oscillator model for the medium. In our treatment this result is not only generalized to include amplification, it is also valid for arbitrary non-equilibrium media under steady-state excitation.

Steadily excited semiconductors in quasi-equilibrium are of particular interest, such as exciton gases generated at low up to moderate excitation and light-emitting diodes working at high excitation. For quasi-equilibrium, due to the Kubo-Martin-Schwinger condition [98], the function $b(\omega)$ develops into a Bose distribution

$$b(\omega)=\left\{\exp\left[\beta(\hbar\omega-\mu)\right]-1\right\}^{-1}.$$

On the experiment one can continuously vary the chemical potential μ by applying an external optical excitation (pumping) to the semiconductor medium. The chemical potential starts at $\mu=0$ for complete thermal equilibrium and characterizes the degree of excitation beyond the thermal one for $\mu>0$. The crossover from absorption ($\chi''>0$) to gain ($\chi''<0$) appears at $\hbar\omega=\mu$. By expanding the product $b(\omega)\chi''(\omega)$ in Eq. (3.35) at $\hbar\omega=\mu$, it is seen that the spontaneous emission remains finite at the crossover, it is given by the slope of the absorption function χ''. Since both χ'' and b switch their signs, the spontaneous emission stays positive in the whole frequency region, as it should be. We also note, that the operators $\hat{c}(\omega)$ preserve their algebraic properties at the crossover. The vanishing prefactor $\chi''=2n'n''$, that appears in the commutator for $\hat{c}(\omega)$, by using Eqs. (3.19) and (3.28),

cancels with the analogous one in the normalization $\mathcal{N}_\pm$ in Eq. (3.44), cf. Eq. (3.42). Thus we obtain a unified description of absorption and amplification in semiconductors.

The results we obtain for the emission spectra are, in the case of absorption, similar to those derived by Artoni and Loudon [120]. In our method the correlation function of the noise current is related to the Bose distribution for polaritonic quasi-particles in quasi-equilibrium. In the former approach, however, the same correlation functions had been related to some artificially introduced Bose distribution function of thermal photons. Besides the differences in the physical interpretation, the polaritonic Bose distribution includes the chemical potential, which allows us to study the continuous transition from absorptive behavior of the medium to amplification, as discussed above. This is impossible in the model using thermal photons as the origin of the noise currents. Moreover, in our approach we could also study in detail the response of the system under conditions far from equilibrium, by a more detailed treatment of the polariton kinetics.

Let us now calculate the squeezing spectrum of light prepared in squeezed vacuum state incident on the left-hand side of the semiconductor slab. We restrict our consideration to the two mode squeezed vacuum state $|\psi\rangle_{\rm sv}$ (see for details Appendix E). The input field on the right-hand side is assumed to be in the vacuum state. Using Eqs (3.27), (3.35), (E.8), and (E.9), the normally ordered electromagnetic energy flow through the medium surface,

$$\Delta\mathcal{S}_{\rm sv}(\omega)=2\varepsilon_0 c\int d\omega'\Big\{\langle:\hat{E}^{\rm R}(\frac{L}{2},\omega)\hat{E}^{\rm R}(\frac{L}{2},\omega'):\rangle_{\rm sv}-\langle:\hat{E}^{\rm L}(-\frac{L}{2},\omega)\hat{E}^{\rm L}(-\frac{L}{2},\omega'):\rangle_{\rm sv}\Big\},$$

is derived as

$$\begin{aligned}\Delta\mathcal{S}_{\rm sv}(\omega)=I_{\rm em}(\omega)-\hbar\omega_0 c\Big\{&\big(1-|\mathcal{T}(\omega)|^2-|\mathcal{R}(\omega)|^2\big)|\nu|^2\\&-2\mu|\nu|\ {\rm Re}\big(1-[\mathcal{T}(\omega)]^2-[\mathcal{R}(\omega)]^2\big)e^{2i\omega_0 L/2c+i\phi}\Big\},\end{aligned}\tag{3.46}$$

where $\mu=\cosh|\xi|$, $\nu=\sinh|\xi|e^{i\phi}$ and $\xi=|\xi|e^{i\phi}$ is the squeezing strength parameter. Here, we have assumed that the detector is placed on the right-hand side of the slab.

The measured squeezing spectrum reads then as $\mathcal{S}_{\rm sv}(x,\omega)=2\varepsilon_0 c\int d\omega'\langle:\hat{E}^{\rm R}(x,\omega)\hat{E}^{\rm R}(x,\omega'):\rangle_{\rm sv}$ and is calculated to be

$$\mathcal{S}_{\rm sv}(x,\omega)=I_{\rm em}(\omega)+\hbar\omega_0 c\Big\{|\mathcal{T}(\omega)|^2|\nu|^2+2\mu|\nu|\ {\rm Re}\,[\mathcal{T}(\omega)]^2\,e^{2i\omega_0 x/c+i\phi}\Big\},\quad x\geq\frac{L}{2},\tag{3.47a}$$

$$\mathcal{T}(\omega)=\frac{\varkappa}{[1-\varkappa^2(\omega)]}\frac{4n(\omega)}{[n^2(\omega)-1]}e^{-i\omega L/c}.\tag{3.47b}$$

From Eqs (3.35), (3.37) and (3.46) it is evident that the behavior of the functions (3.46) and (3.47) strongly depends on the behavior of the denominator $1-\varkappa^2(\omega)$ in the transmission coefficient $\mathcal{T}(\omega)$. In particular, the squeezing spectrum shows an oscillating behavior with the maxima at the Fabry-Perot resonances with the frequencies $\omega_s=2\pi cs/Ln'(\omega)$, with integer s.

3.4 An exact property of photon Green's function for bounded semiconductor media

In the previous section the macroscopic QED formalism of input-output relations has been constructed for bounded medium of a slab geometry. In Appendix C the paradigm for obtaining input-output relations from the S-matrix functional is outlined. Similar to the scattering theory of quantum electrodynamics based on S-matrix the input-output relations are well-suited just for characterization of the output and input fields defined on large distances from the scatterer. This asymptotic requirement leads to the failure of input-output formalism in the description the near-field effects and effects connected with spatial dispersion. In the present section we develop a method that allows one to describe the light propagation in bounded media without any restrictions or assumptions peculiar to input-output approach.

Let us start from the integral form of the Dyson equation for the photon GF given in Eq. (B.24b) of Appendix B. Using the Langreth rules (1.27) and resolving the Dyson equation with respect to $D^{\gtrless}$ we obtain, in short-hand notation, the *generalized Optical Theorem* [121]:

$$D^{\gtrless} = D^{\gtrless}_{\rm med} + D^{\rm vac\gtrless}, \tag{3.48a}$$

$$D^{\gtrless}_{\rm med} = D^{\rm ret} P^{\gtrless} D^{\rm adv}, \tag{3.48b}$$

$$D^{\rm vac\gtrless} = \varepsilon^{\perp {\rm ret},-1}\, D^{(0)\gtrless}\, \varepsilon^{\perp {\rm adv},-1}, \tag{3.48c}$$

where $\epsilon^{\perp,-1}$ is defined in Eq. (3.2). It is easy to see that Eq. (3.24) is a special form of Eq. (3.48) and is valid only for to the stationary excited medium.

Substituting Eq. (1.7) in Eq. (1.34) one obtains the following structure of the free photon GF:

$$\begin{aligned} D^{(0)\gtrless}_{\mu\nu}(1,2) =& \frac{c}{i\mathfrak{v}} \sum_{p,\boldsymbol{k}} \sum_{p',\boldsymbol{k}'} \frac{1}{\sqrt{kk'}} \Big[\mathcal{C}^{\gtrless} \mathrm{F}_{\mu,p,\boldsymbol{k}}(1) \mathrm{F}^*_{\nu,p',\boldsymbol{k}'}(2) + \mathcal{C}^{\lessgtr} \mathrm{F}^*_{\mu,p,\boldsymbol{k}}(1) \mathrm{F}_{\nu,p',\boldsymbol{k}'}(2) \\ &+ \mathfrak{C}\, \mathrm{F}_{\mu,p,\boldsymbol{k}}(1) \mathrm{F}_{\nu,p',\boldsymbol{k}'}(2) + \mathfrak{C}^* \mathrm{F}^*_{\mu,p,\boldsymbol{k}}(1) \mathrm{F}^*_{\nu,p',\boldsymbol{k}'}(2) \Big] \end{aligned} \tag{3.49}$$

where

$$\mathbf{F}_{p,\boldsymbol{k}}(\boldsymbol{r},t) = \boldsymbol{e}_p \exp[i(\boldsymbol{k}\cdot\boldsymbol{r} - c|\boldsymbol{k}|t)] = \mathbf{F}^*_{p,\boldsymbol{k}}(-\boldsymbol{r},-t) \tag{3.50}$$

describes classical plane waves with polarization $\boldsymbol{e}_p$ and wave vector $\boldsymbol{k}$. The prefactors $\mathcal{C}^{\gtrless}$ and $\mathfrak{C}$ are normal and anomalous correlation functions of field operators, namelly

$$\mathcal{C}^{<}_{p\boldsymbol{k}p'\boldsymbol{k}'} = \delta_{p,p'}\delta_{\boldsymbol{k},\boldsymbol{k}'} - \mathcal{C}^{>}_{p\boldsymbol{k}p'\boldsymbol{k}'} = \langle \hat{a}^\dagger_{p\boldsymbol{k}}; \hat{a}_{p'\boldsymbol{k}'} \rangle, \tag{3.51a}$$

$$\mathfrak{C}_{p\boldsymbol{k}p'\boldsymbol{k}'} = \langle \hat{a}_{p\boldsymbol{k}}; \hat{a}_{p'\boldsymbol{k}'} \rangle, \quad \mathfrak{C}^*_{p\boldsymbol{k}p'\boldsymbol{k}'} = \langle \hat{a}^\dagger_{p\boldsymbol{k}}; \hat{a}^\dagger_{p'\boldsymbol{k}'} \rangle \tag{3.51b}$$

where the notation rule (1.14) has been used. Using Eq. (3.48c) it easy to show that after propagating in the medium the vacuum fluctuations of the input field appear renormalized according to

$$D^{\mathrm{vac}\gtrless}(1,2) = D^{(0)\gtrless}(1,2)\Big|_{\mathbf{F}\to\mathbf{A}}, \tag{3.52}$$

i.e., with $\mathbf{F}$ replaced by the effective fields

$$\begin{aligned} \mathrm{A}_{\mu,p\boldsymbol{k}}(1) &= \int d2\, \varepsilon^{\perp\mathrm{ret},-1}_{\mu\nu}(1,2)\mathrm{F}_{\nu,p\boldsymbol{k}}(2) \\ \mathrm{A}^{*}_{\mu,p\boldsymbol{k}}(1) &= \int d2\, \varepsilon^{\perp\mathrm{ret},-1}_{\mu\nu}(1,2)\mathrm{F}^{*}_{\nu,p\boldsymbol{k}}(2), \end{aligned} \tag{3.53}$$

which describe propagation (i.e., reflection, absorption, and transmission) of a classical plane wave in a bounded medium. In fact, these effective fields are normal mode expansions of the vector potential $\hat{A}_\mu(1)$ and, hence, are also solutions of Eq. (3.20).

The general structure of Eqs (3.49), (3.52), and (3.51) suggest to figure out in the photon GFs $D^{(0)}$ and D^{vac} two contributions, namely

$$D^{(0)}(1,2)=D^{(0)}_{\mathrm{sp}}(1-2)+D^{(0)}_{\mathrm{stim}}(1,2), \quad D^{\mathrm{vac}}(1,2)=D^{\mathrm{vac}}_{\mathrm{sp}}(1-2)+D^{\mathrm{vac}}_{\mathrm{stim}}(1,2). \tag{3.54}$$

Here the spontaneous contributions D_{sp} arise from the ground state fluctuations of electromagnetic vacuum. Explicitly these contributions are defined as

$$D^{(0)>}_{\mu\nu,\mathrm{sp}}(1-2) = D^{(0)<}_{\mu\nu,\mathrm{sp}}(2-1) = \frac{c}{2i\mathfrak{v}}\sum_{p,\boldsymbol{k}}\frac{1}{k}\mathrm{F}_{\mu,p,\boldsymbol{k}}(1)\mathrm{F}^{*}_{\nu,p',\boldsymbol{k}'}(2), \tag{3.55a}$$

$$D^{\mathrm{vac}>}_{\mu\nu,\mathrm{sp}}(1-2) = D^{\mathrm{vac}<}_{\mu\nu,\mathrm{sp}}(2-1) = \frac{c}{2i\mathfrak{v}}\sum_{p,\boldsymbol{k}}\frac{1}{k}\mathrm{A}_{\mu,p,\boldsymbol{k}}(1)\mathrm{A}^{*}_{\nu,p',\boldsymbol{k}'}(2). \tag{3.55b}$$

On the other hand, the photons prepared in definite quantum state outside of media give rise to the stimulated field-field fluctuations D_{stim}.

We now derive the squeezing spectrum in order to compare it with the result of macroscopic input-output calculations given in Eq. (3.46). To this end, we shall use extensively the results of Appendices D and E. Combining Eqs (D.14) and (E.13) and inserting them in Eq. (D.10) we obtain [VI]

$$I_{\mathrm{em}} \equiv \Delta\mathcal{S}_{\,\mathrm{em}} = -\frac{\hbar c^2}{2\mathfrak{v}}\sum_{\boldsymbol{k}} k_\perp b(k_\perp)\Big\{1-\big|\mathcal{R}_{\boldsymbol{k}}\big|^2-\big|\mathcal{T}_{\boldsymbol{k}}\big|^2\Big\} \tag{3.56}$$

$$I_{\mathrm{sp}} \equiv \Delta\mathcal{S}_{\,\mathrm{sp}} = -\frac{\hbar c^2}{2\mathfrak{v}}\sum_{\boldsymbol{k}} k_\perp\Big\{1-\big|\mathcal{R}_{\boldsymbol{k}}\big|^2-\big|\mathcal{T}_{\boldsymbol{k}}\big|^2\Big\} \tag{3.57}$$

where $\mathcal{T}$ and $\mathcal{R}$ are transmission and reflection coefficients. Performing the transition to the continuous limit and using the relation $\int dk_\perp = \int d\omega\omega/c^2k_\perp$ we obtain for the

medium-induced spontaneous emission spectrum:

$$I_{\rm em}=\int\frac{d\omega}{2\pi}\frac{d^2\boldsymbol{k}_\parallel}{(2\pi)^2}I_{\rm em}(\omega,\boldsymbol{k}_\parallel)=-\int\frac{d\omega}{2\pi}\frac{d^2\boldsymbol{k}_\parallel}{(2\pi)^2}\frac{\hbar\omega c}{2}b(\omega)\Big\{1-\big|\mathcal{R}(\omega,\boldsymbol{k}_\parallel)\big|^2-\big|\mathcal{T}(\omega,\boldsymbol{k}_\parallel)\big|^2\Big\}. \quad (3.58)$$

For the spatially homogeneous case and for radiation incident normally to the slab boundary ($\boldsymbol{k}_\parallel$=0), the expressions for $I_{\rm sp}(\omega)$ defined in Eqs (3.35) and (3.58) are equivalent due to the relation derived in Refs [118, 122]:

$$1-\big|\mathcal{R}_{\boldsymbol{k}}\big|^2-\big|\mathcal{T}_{\boldsymbol{k}}\big|^2=\frac{ic}{2\omega}\int dxdx'\mathcal{A}^*_{\boldsymbol{k}}(x)\widehat{P}(x,x',\omega)\mathcal{A}_{\boldsymbol{k}}(x'), \quad (3.59)$$

where $\mathcal{A}_{\boldsymbol{k}}(x)$ is defined in Eq. (D.12). Finally, computing the contribution to spectrum from $D^{\rm vac}_{\rm stim}$ from Eqs (D.10) and (D.16) we obtain

$$\begin{aligned}\Delta\mathcal{S}_{\rm stim}(\omega,\boldsymbol{k}_\parallel)=-\hbar\omega_0 c\Big\{&\big(1-|\mathcal{T}(\omega,\boldsymbol{k}_\parallel)|^2-|\mathcal{R}(\omega,\boldsymbol{k}_\parallel)|^2\big)|\mathfrak{v}|^2\\&-2\mu|\mathfrak{v}|\ {\rm Re}\big(1-\big[\mathcal{T}(\omega,\boldsymbol{k}_\parallel)\big]^2-\big[\mathcal{R}(\omega,\boldsymbol{k}_\parallel)\big]^2\big)e^{2i\sqrt{\omega_0^2/c^2-\boldsymbol{k}_\parallel^2}L/2+i\phi}\Big\}.\end{aligned} \quad (3.60)$$

Here we have used the evident relations $\mathcal{C}^<=\langle\hat{a}^{\rm R,L\dagger}_{\rm in};\hat{a}^{\rm R,L}_{\rm in}\rangle_{\rm sv}=|\mathfrak{v}|^2$ and $\mathfrak{C}=\langle\hat{a}^{\rm R,L}_{\rm in};\hat{a}^{\rm R,L}_{\rm in}\rangle_{\rm sv}=-\mu\mathfrak{v}$. We see that the sum $I_{\rm em}(\omega,\boldsymbol{k}_\parallel=0)+\Delta\mathcal{S}_{\rm stim}(\omega,\boldsymbol{k}_\parallel=0)$ coinsides with the normally-ordered energy flow $\Delta\mathcal{S}_{\rm sv}(\omega)$ given by Eq. (3.46). The vacuum induced spontaneous emission $I_{\rm sp}$ is here ignored since we are interested in the normally-ordered quantities only. Thus, we can see that both approaches yield the same results for optical spectra detected far from the slab. There is, however, one crucial difference. Namely, the theory developed in the present section describes light propagation in bounded media *exactly* in all spatial regions, including boundaries. This can be seen from Eq. (3.59), which is valid for a medium with spatial inhomogeneity, including spatial dispersion. The application of the input-output formalism, in contrast, is limited by an assumption concerning the absence of spatial dispersion so that $\widehat{P}(x,x',\omega)=\widehat{P}(x,\omega)\delta(x-x')$, which is not justified near media boundaries.

3.5 Influence of nonclassical radiation on the dielectric properties of a medium

It is instructive to consider as an example the influence of quantum radiation in squeezed vacuum state, incident on semiconductor material, on the electron-hole kinetics. We concentrate on this particular quantum state due to its peculiar phase dependent noise properties. We note that the presented here method can be applied for the case of incident light being prepared in arbitrary quantum state. Using the results of Appendix E one

writes the vacuum photon GF (E.7) after the Fourier transform with respect to $\boldsymbol{r}_1-\boldsymbol{r}_2$, $(\boldsymbol{r}_1+\boldsymbol{r}_2)/2$, t_1-t_2, and $(t_1+t_2)/2$ as

$$\begin{aligned}D_{\rm sv}^{(0)\gtrless}(\boldsymbol{k},\boldsymbol{K},\omega,\Omega)=\frac{-i}{2\sqrt{(\omega_0/c)^2-k^2}}\Big\{&\mathcal{C}_k^{\gtrless}\big[\delta(\boldsymbol{k}+\boldsymbol{k}_0)\delta(\omega-\omega_0-ck)+\delta(\boldsymbol{k}-\boldsymbol{k}_0)\delta(\omega-\omega_0+ck)\big]\\&+\mathcal{C}_k^{\lessgtr}\big[\delta(\boldsymbol{k}+\boldsymbol{k}_0)\delta(\omega+\omega_0+ck)+\delta(\boldsymbol{k}-\boldsymbol{k}_0)\delta(\omega+\omega_0-ck)\big]\\+\delta(\boldsymbol{k})\big[\delta(\omega-ck)+\delta(\omega+ck)\big]&\big[\mathfrak{C}_k\delta(\boldsymbol{K}+\boldsymbol{k}_0)\delta(\Omega-\omega_0)+\mathfrak{C}_k^*\delta(\boldsymbol{K}-\boldsymbol{k}_0)\delta(\Omega+\omega_0)\big]\Big\}.\end{aligned} \tag{3.61}$$

In the following we will neglect the $\boldsymbol{K}$ dependence since in semiconductor materials for optical excitation $\boldsymbol{K}\ll\boldsymbol{k}$. The right hand side of Eq. (3.11) can be simplified by using the generalized Kadanoff-Baym ansatz [123]

$$G_{\rm ij}^{\gtrless}(\boldsymbol{k},t,t')=\mp\Big\{G_{\rm ik}^{\rm ret}(\boldsymbol{k},t,t')\varrho_{\boldsymbol{k}}^{\rm kj\gtrless}(t')-\varrho_{\boldsymbol{k}}^{\rm ik\gtrless}(t)G_{\rm kj}^{\rm adv}(\boldsymbol{k},t,t')\Big\}. \tag{3.62}$$

The photon self-energy contribution in RPA approximation for bounded media has, similar to Eq. (3.15), structure and reads as

$$\Sigma_{\rm sv,ij}^{\rm ph\gtrless}(\boldsymbol{k},\omega,\Omega)=i\hbar\frac{1}{\upsilon}\sum_{\boldsymbol{q}}D_{\rm sv}^{\rm vac\gtrless}(\boldsymbol{q},\omega,\Omega)G_{\rm ij}^{\gtrless}(\boldsymbol{k}-\boldsymbol{q},\omega,\Omega), \tag{3.63}$$

where the vacuum-induced photon GF is connected with the free GF (3.61) by means of Eq. (3.52).

Let us now consider Eq. (3.11). Since we neglected here the $\boldsymbol{K}$-dependence in photon and particle GFs, i.e., we assume that we deal with translational invariant system, we can reduce Eq. (3.11) by setting $f_{\boldsymbol{k},\boldsymbol{k}'}^{\rm i}=f_{\boldsymbol{k}}^{\rm i}\delta_{\boldsymbol{k},\boldsymbol{k}}$ and $p_{\boldsymbol{k},\boldsymbol{k}'}^{\rm cv}=f_{\boldsymbol{k}}^{\rm cv}\delta_{\boldsymbol{k},\boldsymbol{k}}$. The particle GF we write in the quasi-particle approximation as

$$G_{\rm ii}^{\rm ret}(\boldsymbol{k},\omega,\Omega)=\frac{1}{\hbar\omega-\mathfrak{E}_{\boldsymbol{k}}^{\rm i}(\Omega)+i\Gamma_{\boldsymbol{k}}^{\rm i}(\Omega)/2},\quad\begin{aligned}\mathfrak{E}_{\boldsymbol{k}}^{\rm i}&=\mathfrak{e}_{\boldsymbol{k}}^{\rm i}-\operatorname{Re}\Sigma_{\rm sv,ii}^{\rm ph\,ret}(\mathfrak{E}_{\boldsymbol{k}}^{\rm i})\\\Gamma_{\boldsymbol{k}}^{\rm i}&=-2\operatorname{Im}\Sigma_{\rm sv,ii}^{\rm ph\,ret}(\mathfrak{E}_{\boldsymbol{k}}^{\rm i}),\end{aligned} \tag{3.64}$$

where the diagonal part of photon self-energy (3.15) reads as

$$\Sigma_{\rm sv,ii}^{\rm ph\,ret}(\boldsymbol{k},\mathfrak{E}_{\boldsymbol{k}}^{\rm i},\Omega)=\frac{1}{\upsilon}\sum_{\boldsymbol{q}}\int\frac{d\omega}{2\pi}\frac{\big[1-f_{\boldsymbol{q}}^{\rm i}(\omega)\big]D_{\rm sv}^{\rm vac>}(\boldsymbol{k}-\boldsymbol{q},\omega,\Omega)+f_{\boldsymbol{k}}^{\rm i}(\omega)D_{\rm sv}^{\rm vac<}(\boldsymbol{k}-\boldsymbol{q},\omega,\Omega)}{\mathfrak{E}_{\boldsymbol{k}}^{\rm i}(\Omega)-\mathfrak{E}_{\boldsymbol{q}}^{\rm i}(\Omega)-\omega+i\Gamma_{\boldsymbol{q}}^{\rm i}(\Omega)/2}. \tag{3.65}$$

After some algebra Eq. (3.11) can be rewritten as

$$\begin{aligned}&\big\{\omega+\mathfrak{e}_{\boldsymbol{k}}^{\rm c}-\mathfrak{e}_{\boldsymbol{k}}^{\rm v}-\Sigma_{\rm sv}^{\rm ph\,ret}(\boldsymbol{k},\omega,\Omega)\big\}p_{\boldsymbol{k}}^{\rm cv}(\omega)\\&\qquad+\frac{1}{\upsilon}\sum_{\boldsymbol{q}}\big\{2N_{\boldsymbol{k}}v_{\boldsymbol{k}-\boldsymbol{q}}+\Theta_{\rm sv}(\boldsymbol{k},\boldsymbol{q},\omega,\Omega)\big\}p_{\boldsymbol{q}}^{\rm cv}(\omega)=N_{\boldsymbol{k}}d_{\rm cv}E(\omega)\end{aligned} \tag{3.66}$$

where $\Sigma^{\rm ph}_{\rm sv}=\Sigma^{\rm ph}_{\rm sv,cc}+\Sigma^{\rm ph}_{\rm sv,vv}$. In Eq. (3.66) we have defined the interaction matrix

$$\Theta_{\rm sv}(\boldsymbol{k},\boldsymbol{q},\Omega)=\frac{1}{\upsilon}\sum_{\rm i\neq j}\int\frac{d\omega}{2\pi}\frac{\left[1-f^{\rm i}_{\boldsymbol{k}}(\omega)\right]D^{\rm vac>}_{\rm sv}(\boldsymbol{k}-\boldsymbol{q},\omega,\Omega)+f^{\rm i}_{\boldsymbol{k}}(\omega)D^{\rm vac<}_{\rm sv}(\boldsymbol{k}-\boldsymbol{q},\omega,\Omega)}{\Omega-\mathfrak{E}^{\rm i}_{\boldsymbol{k}}(\Omega)+\mathfrak{E}^{\rm j}_{\boldsymbol{k}}(\Omega)-\omega+i[\Gamma^{\rm i}_{\boldsymbol{k}}(\Omega)+\Gamma^{\rm j}_{\boldsymbol{q}}(\Omega)]/2} \tag{3.67}$$

and the Pauli-blocking factor $N_{\boldsymbol{k}}=1-f^{\rm c}_{\boldsymbol{k}}-f^{\rm v}_{\boldsymbol{k}}$. Within the linear response theory the macroscopic polarization $P(\omega)$ is related to the medium susceptibility $\chi(\omega)$ via

$$P(\omega)=\chi(\omega)E(\omega)=\sum_{\boldsymbol{k}}d^{*}_{\rm cv}p^{\rm cv}_{\boldsymbol{k}}(\omega). \tag{3.68}$$

With the quasi-particle energy and damping rates the susceptibility can be obtained from Eqs (3.66) and (3.68) for given carrier densities.

Let us now look more closely on the vacuum-induced photon GF for squeezed optical radiation. The anomaleous correlation function

$$\mathfrak{C}_{\boldsymbol{k}}=\langle\xi_{\boldsymbol{k}}|\hat{a}_{\boldsymbol{k}}\hat{a}_{\boldsymbol{k}}|\xi_{\boldsymbol{k}}\rangle=-\cosh|\xi_{\boldsymbol{k}}|\sinh|\xi_{\boldsymbol{k}}|e^{i\phi_{\boldsymbol{k}}},$$

that enters into the expression for $D^{\rm vac}_{\rm sv}$, depends on the phase $\phi_{\boldsymbol{k}}$ of the squeezing strength $\xi_{\boldsymbol{k}}$. The dispersion of a medium causes the change of this phase during the beam propagation in medium. Since $\Sigma^{\rm ph}_{\rm sv}$ defined in Eq. (3.65) and $\Theta_{\rm sv}$ in Eq. (3.67) are both contain the phase dependent photon GF, the solution of the semiconductor Bloch equation (3.66) and the resulting macroscopic polarization (3.68) both depend on $\phi_{\boldsymbol{k}}$. Thus, the influence of the polarization effects due to the interaction with quantum light on the dielectric properties of a medium is twofold. The squeezing phase dependence of the macroscopic polarization leads to the shifts of medium absorption resonances into the direction of lower energies. The magnitudes of these shifts vary for different energies due to the change of the phase of the squeezing strength. On the other hand, the photon self-energy contributions lead to the broadening of the absorption profiles. This effect is simmilar to the line broadening due to the interaction of electrons and holes with a phonon bath (Urbach tail effect) [124].

These effects, however, should be verified experimentally. We note that for small squeezing strength parameter $\xi_{\boldsymbol{k}}$ the self-energy contributions $\Sigma^{\rm ph}_{\rm sv}$ are of the same order as another self-energy contributions due to the scattering processes (e.g. electron-phonon, exciton-electron, exciton-exciton scattering). In the next section we calculate squeezing spectra for the case of relative small squeezing strength. We neglect in these calculations the influence of $\Sigma^{\rm ph}_{\rm sv}$ on the dielectric properties of a semiconductor medium.

3.6 Propagation of squeezed light through a semiconductor slab

We now turn to the discussion of the numerical calculations of the squeezing spectrum for light propagating in an absorbing or amplifying semiconductor media of slab geometry. We

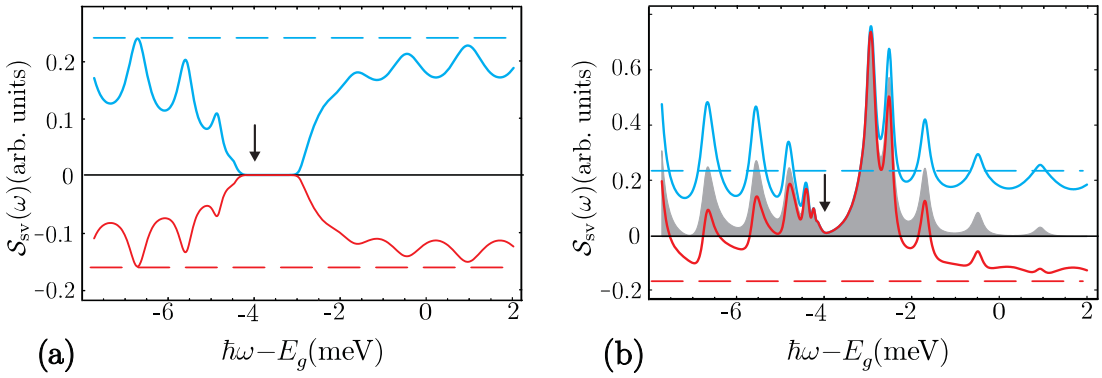

Figure 3.3: Output squeezing spectrum for a GaAs slab ($L = 25\mu$m) near the $1s$-excitonic resonance (indicated by an arrow) of bandwidth = 0.2meV. The squeezing spectrum is shown for the temperatures T=3K (a), T=300K, and for $|\xi| = 0.2$. The blue and red lines indicate the maximum and minimum noise level of the squeezed field, respectively. Horizontal dashed lines represent the maximum and minimum noise level of the squeezed input field.

shall firstly discuss the squeezing spectrum obtained within the input-output formalism. As we have mentioned already, within this framework the cruicial assumption is to neglect spatial inhomogeneities such as spatial dispersion.

Analysing Eq. (3.47), one sees that the squeezing spectrum is modulated by the propagation phase $2i\omega_0 L/c + i\phi_\xi + \arg[\mathcal{T}^2(\omega)]$. This is the well-known consequence of the fact that squeezing is an intrinsically phase-dependent property of a light [125]. The dispersion effects alone ($\chi'' \equiv 0$) do not decrease the squeezing. However, in the vicinity of the absorption resonance the correlated photon pairs contained in the squeezing state become uncorrelated and squeezing disappears. In the amplification region, due to the decaying exponential prefactor in Eq. (3.47b), the squeezing effects in the spectrum (3.46) are also reduced.

In Fig. 3.3 we show the influence of a single excitonic resonance at $E_{1s}=\hbar\omega_0$ on squeezed light propagating through an absorbing semiconductor slab, for different temperatures, where the Lorentz oscillator model has been used to model excitonic absorption. In this case the imaginary part of the susceptibility is given by [117]

$$\chi''(\omega) = \frac{\gamma\Delta}{(\hbar\omega - E_g - E_{1s})^2 + \gamma^2}.$$

The following parameters were used for the calculation: the gap energy E_g=1519meV and the oscillator strength Δ=1.038meV. The $1s$-exciton absorption resonance is chosen as E_{1s}=1515meV with a line broadening of γ=0.2meV. The input (squeezed white noise)

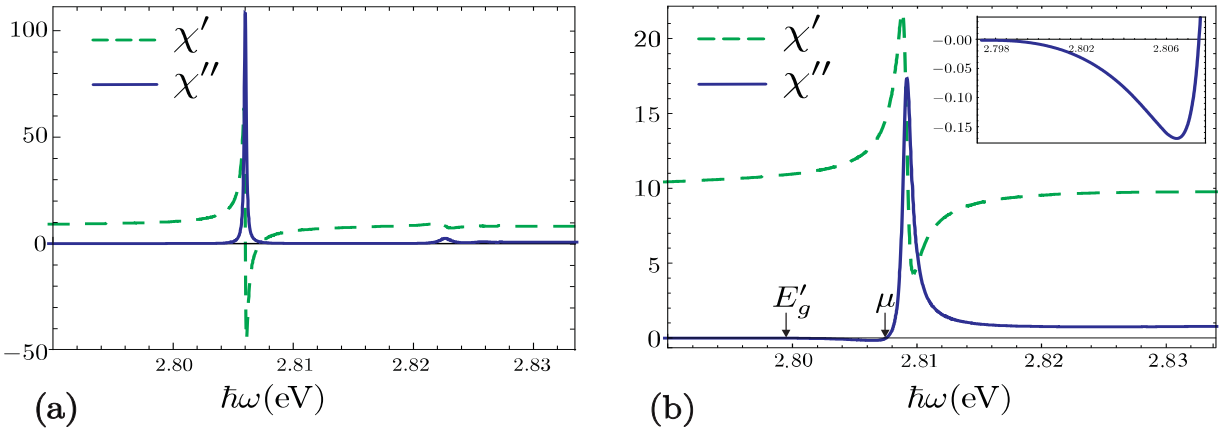

Figure 3.4: The real (χ') and imaginary (χ'') parts of the susceptibility function are shown for a ZnSe slab of thickness L=5μm, at temperature T=77K, excited to carrier densities of n=1×10^{14}cm^{-3} (a) and n=2×10^{17}cm^{-3} (b). The inset in (b) shows the magnified plot of χ'' for the energy range where amplification occurs.

spectrum is depicted with dashed lines. Here we assume that the measurement of spectrum is performed at x=L. Defining

$$\mathcal{S}_{\rm sv}^{\rm max/min}(\omega)\equiv 2\varepsilon_0 c\langle\hat{E}^{(-)}(\omega)\hat{E}^{(+)}(\omega)\rangle \pm 4\varepsilon_0 c\,{\rm Re}\int d\omega'\langle\hat{E}^{(-)}(\omega)\hat{E}^{(-)}(\omega')\rangle \qquad (3.69)$$

as the squeezing spectra with maximum and minimum noise level, we can gain some insight into the influence of absorption on the nonclassicality of the input radiation. The functions $\mathcal{S}_{\rm sv}^{\rm max}$ and $\mathcal{S}_{\rm sv}^{\rm min}$ are represented on Figs 3.3 (a), (b) by the upper (blue) and the lower (red) curves, respectively. For the normally-ordered squeezing spectrum (3.46) the standard quantum limit is defined as $\mathcal{S}_{\rm sv}$=0. Thus, $\mathcal{S}_{\rm sv}^{\rm min}$ lies below this line and manifests the purely nonclassical nature of the spectra. For comparison, the maximum (minimum) flat noise spectrum of the squeezed input field is depicted by the upper (lower) horizontal line.

The results for low temperature are in reasonable qualitative agreement with those of Artoni and Loudon [120]. Note that in this paper the effects of emission on squeezing were not considered. In our approach, for high temperatures the emission spectrum $I_{\rm em}(\omega)$ plays a pronounced role and it leads to a significant decrease of the nonclassical properties of the input field in the vicinity of the absorption resonance.

After considering the simplified model of susceptibility functions, we present here more realistic plots [V]. In Figs 3.4 (a) and (b) we show the real and imaginary parts of the susceptibility functions for a ZnSe slab of 5μm thickness, pumped at T=77K to the carrier densities n=1×10^{14}cm^{-3} and n=2×10^{17}cm^{-3}, respectively. These susceptibilities are calculated by the procedure outlined in Sec. 3.5 and are given by Eq. (3.68). Here we

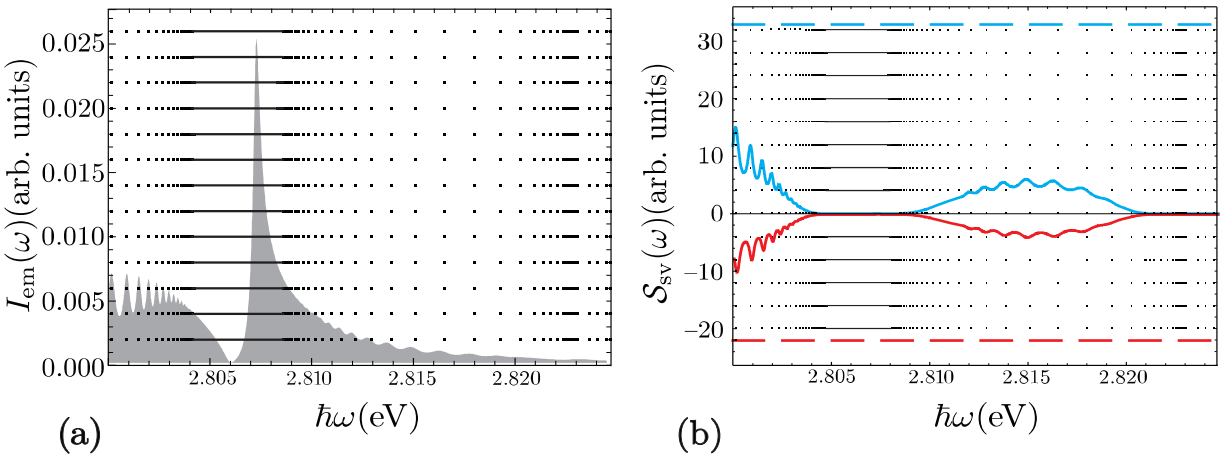

Figure 3.5: Emission spectrum, (a), maximal (blue) and minimal (red) squeezing spectra (b) are shown along with the Fabry-Perot resonances (dots) at frequencies ω_s calculated with the susceptibility depicted in Fig. 3.4(a). The input maximal and minimal flat squeezing spectra are indicated in (b) by horizontal lines. Here, we have chosen $\hbar\omega_0$=2.806eV and $\hbar\Delta\omega$=0.03eV and a squeezing strength $|\xi|$=0.2.

have neglected the polarization effects due to the interaction of the semiconductor with the nonclassical radiation by setting the self-energy contributions $\Sigma^{\rm ph}$ given in Eq. (3.15) equal to zero.

Figures 3.5(a), 3.6(a) represent the spontaneous emission spectra. Figure 3.5(b) shows that the nonclassicality vanishes for transmitted radiation near the excitonic resonance and the absorption edge. For other energy regions it becomes oscillating with a maximum nonclassicality preserved at the Fabri-Perot frequency ω_s. Similarly to Fig. 3.3, for comparison the maximum (minimum) flat noise spectrum of the squeezed input field is also depicted by the upper (lower) horizontal line. In the case of amplification (Fig. 3.6) the nonclassicality is nearly almost destroyed at the gain region due to the incoherent emission. On the other hand, close to the renormalized gap energy E_g' the squeezing spectrum is amplified and gives even more pronounced nonclassicality than that of the input field.

In Figures 3.7(a) and 3.7(b) we present for comparison the spectrum of squeezed vacuum transmitted through a slab without and with inclussion of spatial dispersion effects, respectively. Here we consider a ZnSe slab with L=250nm the dielectric properties of which have been modeled by the Lorentz oscillator model, with two resonance energies at 2806.0meV and 2818.4meV [conf. with the susceptibility function in Fig. 3.4(a)]. For the calculation of spectrum with spatial dispersion the Pekar's *additional boundary conditions* [126] have been used. Here, following original ansatz of Pekar, we assume the vanishing of macroscopic polarization at the semiconductor surface. Calculated in this

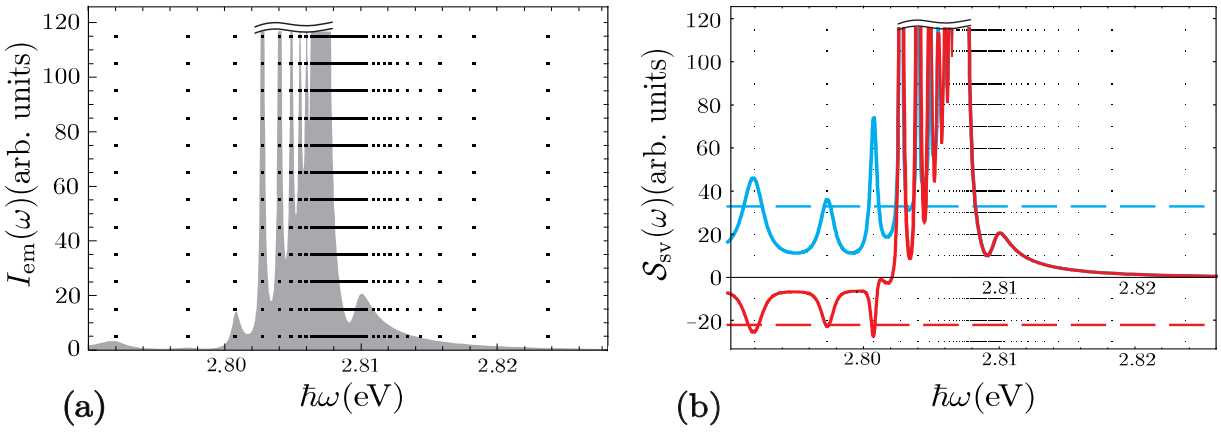

Figure 3.6: The same as in Fig. 3.5 but calculated for the susceptibility function plotted in Fig. 3.4(b). Since for the spectral region, where the amplification occurs, the spontaneous emission is strong, just the lower parts of plots (a) and (b) are depicted for clarity. Here, $\hbar\omega_0$=μ=2.80751eV.

way spectrum [Fig. 3.7(b)] is affected by the additional resonances arising from spatial dispersion. In comparison with the case without spatial dispersion [Fig. 3.7(a)] the spectrum in Fig. 3.7 appears to be strongly modulated. Therefore one can conclude that the microscopic method of Sec. 3.4 becomes more preferable than the macroscopic input-output treatment for thin semiconductor slabs for which the spatial dispersion effects are of great relevance.

3.7 Conclusions

In this chapter we have shown the relationship between the microscopic and macroscopic QED methods of description of light propagation in media. Within the framework of the macroscopic QED, which relies on the properties of the photon Green functions, the quantization of dispersive and absoprbing/amplifying media is achieved through the introduction of stochastic noise currents into the Maxwell equations. These photon GFs as well as noise currents play a decisive role in the derivation of the input-output formalism, which in turn is a convenient tool applied in quantum optics for studying the nonclassical properties of the field.

The macroscopic formalism is compared with the microscopic one based on the nonequilibrium GFs technique. This allows one to establish the link between the correlation functions of noise current operators and the polarization propagators. Moreover, we derived the nontrivial relationship between the correlation functions of noise current operators and the correlation functions of medium currents, which can be measured experimentally.

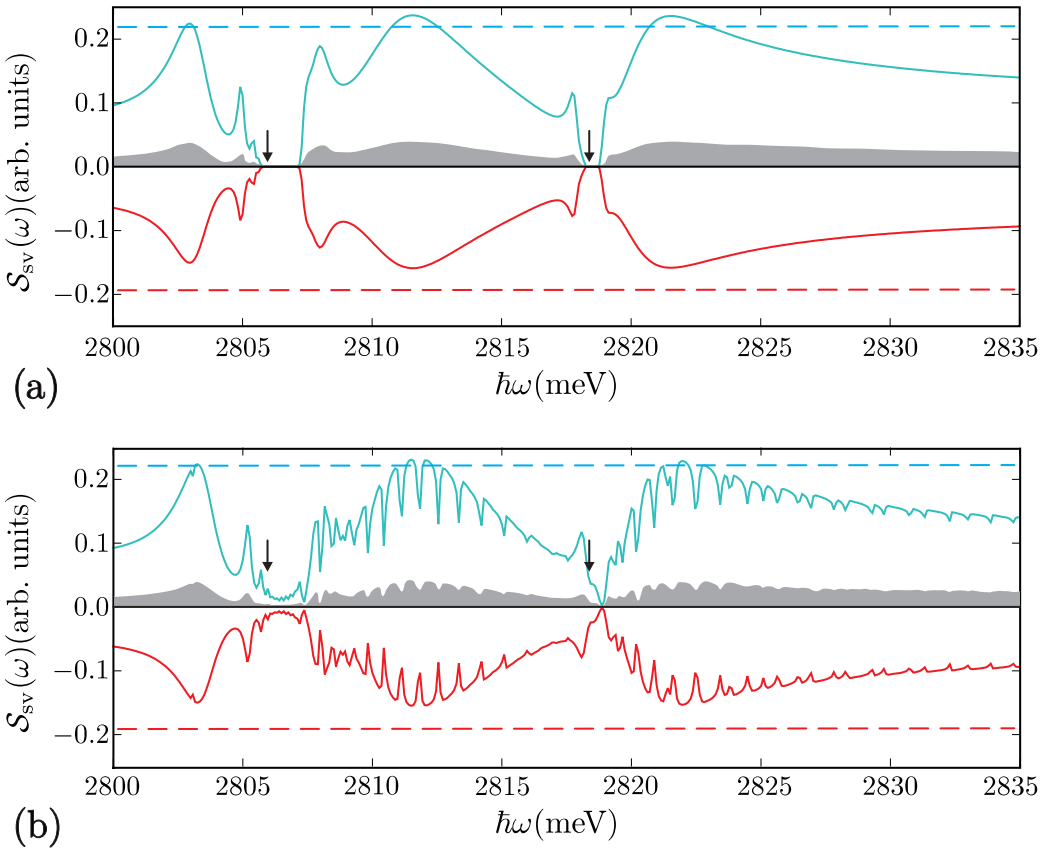

Figure 3.7: Output squeezing spectrum for a ZnSe slab (L=250nm) at T=77K. The excitonic resonances lie at 2806.0meV and 2818.4meV and are indicated by arrows. The squeezing spectrum is shown for $|\xi|$=0.2 for the case when the spatial dispersion has not been taken into account (a), and with accounting for spatial dispersion (b). The emission spectrum is indicated by gray background.

As an example we have studied the propagation of light in a semiconductor slab. In the quasi-equilibrium case, due to the Kubo-Martin-Schwinger condition the correlation function of the noise currents became proportional to a Bose distribution multiplied by an absorption function χ''. This Bose function refers to the distribution function of quasi-particles (polaritons) and is characterized by the chemical potential. The external perturbation varies the chemical potential of the quasi-particles and allows one to switch from the absorption to amplification regimes of the slab operation.

We have also presented the microscopic theory of light propagation in bounded medium. This method serves as an alternative to the input-output formalism of macroscopic QED and is based on the splittiong of field-field fluctuations into contributions induced by the medium or the vacuum. It has been shown that vacuum induced contributions can be related to the free space fluctuations of the externally prepared optical radiation field, whereas medium-induced terms contribute to the medium emission effects. In contrast to the input-output formalism this method allows one to account for the spatial inhomogeneity inherent in bounded media problems.

We also have studied the propagation of squeezed light through a semiconductor slab. We derived here the semiconductor Bloch equation taking into account the polarization effects caused by the interaction of electrons and holes with the squeezed radiation field. Then we have calculated the squeezed spectra of light transmitted through a semiconductor slab with the accounting of absorption, amplification and dispersion by the medium. We have shown that for the absorption case the nonclassical properties of the transmitted radiation vanish in the vicinity of the medium response frequency due to absorption effects and due to the spontaneous emission contribution to the spectrum. We have shown that the phase of the output spectra depends on the media characteristics and nonclassicality remains maximal at frequencies that coincide with Fabri-Perot resonances. In the amplification case the squeezing is reduced and even for low temperatures the nonclassical properties of the output radiation are completely destroyed by incoherent emission in the gain region. We have also shown that squeezing is preserved and even amplified below the energy gap. Finally, we have used the splitting property of the photon Green's function for calculation of the squeezing spectrum for a thin slab with taking into account the spatial dispersion effects.

Summary

The topic of the present thesis is the description of the influence of various dissipation and dispersion mechanisms on the nonclassical properties of optical radiation propagating in stuctured media. In the first chapter we have briefly given an overview of the microscopic theory of light-matter interaction. We have chosen the method of functional integration as an appropriate tool for the description of elementary optical processes in media. This method can be successfully implemented both for equilibrium and nonequilibrium quantum systems and yields the information on the dynamics of these optically excited systems and their statistical properties. The simplest statistical properties of interacting optical and matter fields are given in terms of their two-point Green's functions.

In the second part of chapter 1, we have discussed the quantum statistical properties of the optical radiation using the field-field correlation functions. We also presented some quantum coherence effects peculiar to quantum light and discussed their differences from the classical counterparts. We used the notion of nonclassicality to refer to those statistical (coherence) properties of quantum systems that do not have corresponding analogs in classical optics. Since the coherence is naturally described in terms of measurable correlation functions of normally-ordered field operators, the generating functions as well as the quasi-probability functions for the calculation of these correlation functions have been introduced. We have studied the example of squeezed light generation in optical parametric process. We have shown that the evolution of the interacting system can be given in terms of the corresponding functional integrals, provided the Hamiltonian of the electromagnetic field coupled with media and its density matrix at the initial moment of time are given. Using the example of squeezed light have also discussed such nonclassical phenomena as photon antibunching and sub-Poissonian statistics.

In chapter 2 we have introduced the characterization of nonclassicality by using the Bochner criterion for both quasi-probability functions and their characteristic functions. Since the most convenient method for the experimental testing of the nonclassicality is the measurement of a certain observable, we have formulated the Bochner criterion in terms of its normally ordered symbol (witness function). Negative mean values of this observable indicate nonclassical properties of the corresponding quantum state. Since

usually a nonclassical quantum system is in contact with an environment, its nonclassical properties can be spoiled due to the decoherence, dephasing and other loss processes. In order to characterize the nonclassicality of a system being in contact with the environment, we considered the case of oscillator-like system (e.g., a mode of the electromagnetic field) interacting with the hot environment of other oscillators (other modes of field, absorption system, etc). The evolution of the system of interest in a noisy environment has been described with the help of functional integration techniques (Feynman-Vernon method) and the input-output formalism. In the latter case the interaction of the system with the environment has been modelled by a partially transparent plate that couples the signal and bath modes. We have shown that the Glauber-Sudarshan P-function of such a signal evolves according to a diffusion-like equation, where the mean number of noise quanta plays the role of the 'time variable'. The 'diffusion coefficient' in this equation is expressed in terms of the corresponding efficiency. The criterion for the characterization of nonclassicality has then been studied and it was shown that one can consider the evolution of the witness function for a nonclassical system being in contact with an environment, instead of the evolution of the P-function. Modified in this way, the witness function can be obtained as a solution of a diffusion-like equation with negative diffusion coefficient. Since the solutions of this diffussion-like equation are not well defined for certain values of the diffusion coefficient, the application of the Bochner criterium is limited. We have obtained the expression for the thermal treshold, above which the Bochner criterium does not characterize nonclassiclity of the tested quantum system being in contact with a thermal bath. Possibilities for experimental implementations of this theory based on unbalanced homodyning have been discussed.

In the second part of chapter 2 a phenomenological approach has been developed that allows one to completely describe the effects of unwanted noise, such as the noise associated with absorption and scattering, in high-Q cavities. This noise is modelled by a block of beam splitters and an additional input-output port. The obtained replacement schemes enable us to formulate appropriate quantum Langevin equations and input-output relations. The method of replacement schemes in fact allows one to distinguish, with respect to the unwanted noise, between qualitatively different cavity models. Roughly speaking, one can distinguish between non-degenerate and degenerate replacement schemes. In contrast to non-degenerate schemes, where the parametrization completely describes cavities with unwanted losses, degenerate schemes do not describe all possible cavities but only special classes. It has been also shown that, even though unwanted dissipative channels are included in the model, the situation may resemble that of a cavity without unwanted noise. For such degenerate cavities the information about the relative phase between intracavity and input modes does not exist in the outgoing field. On the other hand, it has

been demonstrated that for non-degenerate cavities unwanted noise renders it possible to combine a cavity input mode and the intracavity mode in a nonmonochromatic output mode. This mode matching effect can be applied for homodyne and cascaded homodyne measurements of the intracavity mode.

Chapter 3 has been treating the nonclassical light propagation in dispersive and absorbing or amplifying semiconductor media with boundaries. For a definite geometry (slab geometry) of a structured medium we derive the corresponding input-output relations of macroscopic QED that allow one to include in the consideration arbitrary quantum states of the input field incident on the slab. On the other hand, based on a microscopic derivation of the emission spectra of a bulk semiconductor, we have arrived at a clear physical interpretation of the noise current operators in macroscopic quantum electrodynamics. This opens the possibility to study medium effects on nonclassical radiation propagating through an absorbing or amplifying semiconductor. We have also presented an approach based on the property of the photon Green's function to split up into parts corresponding to medium- and vacuum-induced contributions to the field-field fluctuations. These contributions enter the physics of emission and absorption in a completely different way. Whereas the medium-related ones are well known from the optical theorem for bulk media, the vacuum-related contributions are more subtle ones and depend on boundary conditions. We have shown that the vacuum-induced fluctuations describe the propagation of arbitrary, even nonclassical light in terms of solutions of the classical wave propagation problem. These results apply independently of specific optical properties or geometrical shapes of the matter for arbitrary nonequilibrium situations. As an example, the transmission of an optical field in a squeezed vacuum through a semiconductor slab is calculated with the help of the input-output formalism and by using the splitting property of the photon Green's function. In contrast to the input-output formalism, the latter approach can be applied to the cases where the effects connected with spatial dispersion cannot be neglected. Here we have also considered the influence of nonclassical radiation, such as squeezed light, on electron-hole kinetics. In particular, we have derived the semiconductor Bloch equation, which contains the self-energy terms induced by the squeezed light. We have also discussed the modification of dielectric properties of the semiconductor medium due to the interaction with nonclassical light.

Appendix A

Functional integration

Bosonic and fermionic coherent states

Since the pioneering papers of R. Glauber [1], the coherent states of bosonic fields, which are the eigenstates of the bosonic annihilation operator, are playing an outstanding role in quantum optics. In contrast to the bosonic fields, the annihilation operators for fermions obey the property $\hat{g}^2 = 0$ that is the manifestation of the Pauli exclusion principle. This property means that the vacuum state is the only physically realizable eigenstate of the fermionic annihilation operators. It is possible, however, to define formally such eigenstates, taking into account the anticommuting nature of the fermionic field operators. This anticommuting behavior as well as the Pauli exclusion principle makes Grassmannian calculus suitable for the description of the fermions. In this appendix we will summarize some properties of the bosonic and fermionic coherent states (see also [1]).

We will denote by $\hat{a}_n$ and $\hat{g}_n$ the annihilation operators for bosons and fermions in Fock space, respectively, with the following commutation relations

$$\begin{aligned} &[\hat{a}_n, \hat{a}_m^\dagger] = \delta_{nm}, \quad [\hat{a}_n, \hat{a}_m] = [\hat{a}_n^\dagger, \hat{a}_m^\dagger] = 0; \\ &\{\hat{g}_n, \hat{g}_m^\dagger\} = \delta_{nm}, \quad \{\hat{g}_n, \hat{g}_m\} = \{\hat{g}_n^\dagger, \hat{g}_m^\dagger\} = 0. \end{aligned} \tag{A.1}$$

The vacuum state is defined in such way that $\hat{a}_n|0\rangle = 0$ for bosons and $\hat{g}_n|0\rangle = 0$ for fermions. We also introduce the complex variables α_n and γ_n for bosons and fermions, respectively, with properties

$$\begin{aligned} &[\alpha_n, \alpha_m^*] = [\alpha_n, \alpha_m] = [\alpha_n^*, \alpha_m^*] = 0; \\ &\{\gamma_n, \gamma_m^*\} = \{\gamma_n, \gamma_m\} = \{\gamma_n^*, \gamma_m^*\} = 0. \end{aligned} \tag{A.2}$$

The anticommutation rules for γ_n are inherent to the Grassmannian variables. We note also that γ_n anticommute with fermionic annihilation operators and commute with the

bosonic ones. As a consecuence of Eq. (A.2) we also have $\gamma_n^2 = \gamma_n^{*2} = 0$. Vanishing of the second powers of Grassmannian variables makes the operation of integration equivalent to differentiation, namely

$$\int d\gamma_n 1 = 0 \quad \text{and} \quad \int d\gamma_n \gamma_m = \delta_{nm}. \tag{A.3}$$

Let us define the displacement operator for bosonic and fermionic fields

$$\begin{aligned} \hat{D}(\alpha) &= \prod_n \exp\left[\hat{a}_n^\dagger \alpha_n - \alpha_n^* \hat{a}_n\right], \\ \hat{D}(\gamma) &= \prod_n \exp\left[\hat{g}_n^\dagger \gamma_n - \gamma_n^* \hat{g}_n\right]. \end{aligned} \tag{A.4}$$

The coherent states one obtains by the displacing the vacuum state with help of these operators, namely

$$\begin{aligned} |\alpha\rangle &= \hat{D}(\alpha)|0\rangle = \exp\Big[-\sum_n (|\alpha_n|^2/2 - \alpha_n \hat{a}_n^\dagger)\Big]|0\rangle, \\ |\gamma\rangle &= \hat{D}(\gamma)|0\rangle = \exp\Big[-\sum_n (|\gamma_n|^2/2 + \gamma_n \hat{g}_n^\dagger)\Big]|0\rangle = \prod_n (1 - \gamma_n \hat{g}_n^\dagger + |\gamma_n|^2/2)|0\rangle, \end{aligned} \tag{A.5}$$

where expressions were obtained by using the Campbell-Baker-Hausdorff formula [84]. Note the sign change in the exponential in the second line of Eq. (A.5) due to the Grassmannian nature of the γ variable. We also set $|\gamma_n|^2 = \gamma_n^* \gamma_n = -\gamma_n \gamma_n^*$ for convenience of notations.

The form in which Eq. (A.5) is written is common in quantum optics. The real and imaginary parts of the complex numbers α and γ can be considered as coordinates of the quantum state in the phase space of the system. Then Eq. (A.5) shows that the coherent states are just the displaced locus of the vacuum states on the distances $|\alpha|$ (bosons) or $|\gamma|$ (fermions). The locations of the locus of the displaced vacuum states are given by the phases of the coherent states.

However, we will rewrite Eq. (A.5) in order to implement the coherent states in many-body calculations. To this end we will use the bosonic and Grassmannian-valued fields instead of complex variables and field operators $\hat{\phi}$ and $\hat{\psi}$ instead of mode operators, i.e.

$$\begin{aligned} \alpha(\boldsymbol{r}) &= \sum_n \alpha_n \chi_n(\boldsymbol{r}), \qquad \hat{\phi}(\boldsymbol{r}) = \sum_n \hat{a}_n \chi_n(\boldsymbol{r}), \\ \gamma(\boldsymbol{r}) &= \sum_n \gamma_n \chi_n(\boldsymbol{r}), \qquad \hat{\psi}(\boldsymbol{r}) = \sum_n \hat{g}_n \chi_n(\boldsymbol{r}), \end{aligned} \tag{A.6}$$

where $\chi_n(\boldsymbol{r}) = \langle \boldsymbol{r}|n\rangle$. Now one can rewrite (A.5) as

$$\begin{aligned} |\alpha\rangle &= \exp\Big[-\int d^3\boldsymbol{r}(|\alpha(\boldsymbol{r})|^2/2 - \alpha(\boldsymbol{r})\hat{\phi}^\dagger(\boldsymbol{r}))\Big]|0\rangle, \\ |\gamma\rangle &= \exp\Big[-\int d^3\boldsymbol{r}(|\gamma(\boldsymbol{r})|^2/2 + \gamma(\boldsymbol{r})\hat{\psi}^\dagger(\boldsymbol{r}))\Big]|0\rangle. \end{aligned} \tag{A.7}$$

It is important to note that these coherent states are not orthonormal. In contrast, from (A.7) we find that

$$\begin{aligned}\langle\alpha|\alpha'\rangle &= \exp\Big[\int d^3\boldsymbol{r}\Big\{\alpha^*(\boldsymbol{r})\alpha'(\boldsymbol{r}) - \frac{1}{2}(|\alpha(\boldsymbol{r})|^2 + |\alpha'(\boldsymbol{r})|^2)\Big\}\Big],\\ \langle\gamma|\gamma'\rangle &= \exp\Big[\int d^3\boldsymbol{r}\Big\{\gamma^*(\boldsymbol{r})\gamma'(\boldsymbol{r}) - \frac{1}{2}(|\gamma(\boldsymbol{r})|^2 + |\gamma'(\boldsymbol{r})|^2)\Big\}\Big].\end{aligned} \tag{A.8}$$

Nevertheless they obey the closure relations

$$\int \mathcal{D}[\alpha]|\alpha\rangle\langle\alpha| = \mathbf{1} \quad \text{and} \quad \int \mathcal{D}[\gamma]|\gamma\rangle\langle\gamma| = \mathbf{1}, \tag{A.9}$$

where we have used common for the functional integral technique notations, i.e.

$$\prod_n d\alpha_n^* d\alpha_n/(2\pi i) = \mathcal{D}[\alpha], \quad and \quad \prod_n d\gamma_n^* d\gamma_n = \mathcal{D}[\gamma].$$

The trace of an operator $\hat{\mathcal{O}}$ over the Fock space can be expressed as

$$\mathrm{Tr}\{\hat{\mathcal{O}}\} = \int \mathcal{D}[\alpha]\langle\alpha|\hat{\mathcal{O}}|\alpha\rangle, \quad \mathrm{Tr}\{\hat{\mathcal{O}}\} = \int \mathcal{D}[\gamma]\langle-\gamma|\hat{\mathcal{O}}|\gamma\rangle. \tag{A.10}$$

The minus sign in the fermionic case arises as an consequence of the anticommutation of the Grassmannian variables. We also point out the following difference between the Gaussian integrals written with help of Euclidean and Grassmannian variables

$$\begin{aligned}\int \mathcal{D}[\alpha]\exp\Big[-\sum_{nm}\alpha_n^*\mathcal{A}_{nm}\alpha_m\Big] &= \frac{1}{\det\mathcal{A}} = e^{-\mathrm{Tr}[\ln\mathcal{A}]},\\ \int \mathcal{D}[\gamma]\exp\Big[-\sum_{nm}\gamma_n^*\mathcal{B}_{nm}\gamma_m\Big] &= \det\mathcal{B} = e^{\mathrm{Tr}[\ln\mathcal{B}]}.\end{aligned} \tag{A.11}$$

In the terms of bosonic and Grassmannian-valued fields notations these expressions read as

$$\begin{aligned}\int \mathcal{D}[\alpha]\exp\Big[-\int d^3\boldsymbol{r}d^3\boldsymbol{r}'\alpha^*(\boldsymbol{r})\mathcal{A}(\boldsymbol{r},\boldsymbol{r}')\alpha(\boldsymbol{r}')\Big] &= e^{-\mathrm{Tr}[\ln\mathcal{A}]},\\ \int \mathcal{D}[\gamma]\exp\Big[-\int d^3\boldsymbol{r}d^3\boldsymbol{r}'\gamma^*(\boldsymbol{r})\mathcal{B}(\boldsymbol{r},\boldsymbol{r}')\gamma(\boldsymbol{r}')\Big] &= e^{\mathrm{Tr}[\ln\mathcal{B}]}.\end{aligned} \tag{A.12}$$

Another useful integrals that are often encountered are

$$\begin{aligned}\det\mathcal{A}\textstyle\int\mathcal{D}[\alpha]\exp\Big[-\int d^3\boldsymbol{r}d^3\boldsymbol{r}'\alpha^*(\boldsymbol{r})\mathcal{A}(\boldsymbol{r},\boldsymbol{r}')\alpha(\boldsymbol{r}')+\int d^3\boldsymbol{r}\{J_\alpha^*(\boldsymbol{r})\alpha(\boldsymbol{r})+\alpha^*(\boldsymbol{r})J_\alpha(\boldsymbol{r})\}\Big]&\\ = \exp\Big[\int d^3\boldsymbol{r}d^3\boldsymbol{r}'J_\alpha^*(\boldsymbol{r})\mathcal{A}^{-1}(\boldsymbol{r},\boldsymbol{r}')J_\alpha(\boldsymbol{r}')\Big], \quad &\text{(A.13a)}\\ \tfrac{1}{\det\mathcal{B}}\textstyle\int\mathcal{D}[\gamma]\exp\Big[-\int d^3\boldsymbol{r}d^3\boldsymbol{r}'\gamma^*(\boldsymbol{r})\mathcal{B}(\boldsymbol{r},\boldsymbol{r}')\gamma(\boldsymbol{r}')+\int d^3\boldsymbol{r}\{J_\gamma^*(\boldsymbol{r})\gamma(\boldsymbol{r})+\gamma^*(\boldsymbol{r})J_\gamma(\boldsymbol{r})\}\Big]&\\ = \exp\Big[\int d^3\boldsymbol{r}d^3\boldsymbol{r}'J_\gamma^*(\boldsymbol{r})\mathcal{B}^{-1}(\boldsymbol{r},\boldsymbol{r}')J_\gamma(\boldsymbol{r}')\Big], \quad &\text{(A.13b)}\end{aligned}$$

where J_α and J_γ are some axillary fields. Eqs (A.13a,b) are easily proved by shifting the α and γ fields in the numerator of the right hand sides according to

$$\alpha(\boldsymbol{r}) \to \alpha(\boldsymbol{r}) + \int d^3\boldsymbol{r}' \mathcal{A}^{-1}(\boldsymbol{r},\boldsymbol{r}') J_\alpha(\boldsymbol{r}'),$$
$$\gamma(\boldsymbol{r}) \to \gamma(\boldsymbol{r}) + \int d^3\boldsymbol{r}' \mathcal{B}^{-1}(\boldsymbol{r},\boldsymbol{r}') J_\gamma(\boldsymbol{r}').$$

This shift transformation is known as a Hubbard-Stratonovich transformation [127].

Coherent-state functional integral

Let us calculate the coherent-state matrix elements of the evolution operator $\langle\alpha|e^{-i\hat{H}t/\hbar}|\alpha'\rangle$ for the system with D degrees of freedom. We note that the equations of this section are equivalent both for fermionic and bosonic coherent state variables. The expression for matrix elements of the evolution operator may be rewritten by splitting the time interval on N pieces of the duration $\epsilon{=}t/(N+1)$ as

$$\begin{aligned}\langle\alpha|e^{-i\hat{H}\epsilon/\hbar}e^{-i\hat{H}\epsilon/\hbar}...e^{-i\hat{H}\epsilon/\hbar}|\alpha'\rangle &= \int \prod_{k=1}^{N} \frac{d^D\alpha_k d^D\alpha_k^*}{(2\pi i)^D} \prod_{k=0}^{N} \langle\alpha_{k+1}|e^{-i\hat{H}\epsilon/\hbar}|\alpha_k\rangle \\ &= \lim_{\epsilon\to 0} \int \mathcal{D}[\alpha] \prod_{k=0}^{N} \Big[\langle\alpha_{k+1}|\alpha_k\rangle - \frac{i}{\hbar}\epsilon\langle\alpha_{k+1}|\hat{H}|\alpha_k\rangle\Big];\end{aligned} \tag{A.14}$$

here we have use the boundary conditions $\alpha_{N+1}{=}\alpha$ and $\alpha_0{=}\alpha'$.

Additionally, we recall the formal path integral expression that arises when the order of the integration and the limit are interchanged. In such a way, the propagator reads

$$\begin{aligned}&\int \mathcal{D}[\alpha] \exp\Big[-\frac{i}{\hbar}\int_0^t dt' \big\{-i\hbar\langle\alpha|\frac{d}{dt'}|\alpha\rangle + \langle\alpha|\hat{H}|\alpha\rangle\big\}\Big] \\ &\qquad = \int \mathcal{D}[\alpha] \exp\Big[-\frac{i}{\hbar}\int_0^t dt' \big\{-i\hbar\alpha^*\dot{\alpha} + \mathcal{H}[\alpha]\big\}\Big].\end{aligned} \tag{A.15}$$

Performing the Wick rotation to the imaginary time $\tau{=}it$ the last expression gives the evolution operator for fields interacting with thermal reservoir

$$\int \mathcal{D}[\alpha] \exp\Big[-\frac{1}{\hbar}\int_0^{\hbar\beta} d\tau' \big\{\hbar\alpha^*\frac{d}{d\tau'}\alpha - \mathcal{H}[\alpha]\big\}\Big]. \tag{A.16}$$

where as usually $\beta = \tau/\hbar = 1/k_{\mathbf{B}}T$ is the inverse temperature of the reservoir.

Appendix B

Perturbative expansions and Feynman diagrams

In this appendix we discuss the derivation of Green's functions for the interacting system from the corresponding generating functional (S-matrix functional). We shall discuss the Masubara imaginary-time Green functions for many-particle system being in thermal equilibrium at the temperature T. Usually, for small interaction one expand the S-matrix functional in the series with respect to the interaction strength parameter. The technique of Feynman graphs allows one to write down these asymptotic series for the S-matrix functional of a QFT in a neighborhood of a free QFT. Moreover, Feynman diagrams are convenient for visualization of elementary processes that accompanying the dynamics of interacting many-particle system.

Let we first introduce the shorthand notation for the interaction $\hat{V}(\tau)$ given by the charges-field interaction Hamiltonian $\hat{H}^{(1)}_{\rm ph}+\hat{H}^{(2)}_{\rm ph}$ in Eq. (1.2) written in the second-quantization form

$$\hat{V}(\tau_1) = -\int d^3\boldsymbol{r}_1 \hat{U}(\boldsymbol{r}_1)\hat{\psi}^\dagger_s(1)\hat{\psi}_s(1) = -\int d^3\boldsymbol{r}_1 \Big[\hat{\boldsymbol{J}}^{\rm par}\cdot\hat{\boldsymbol{A}}(\boldsymbol{r}_1) - \frac{(eZ_s)^2}{2m_s c}\hat{\rho}(\boldsymbol{r}_1)\hat{A}^2(\boldsymbol{r}_1)\Big], \tag{B.1}$$

where we have suppressed the spin indices. The scattering event of a particle on the "potential" $\hat{U}(\boldsymbol{r})$ diagrammatically can be represented as

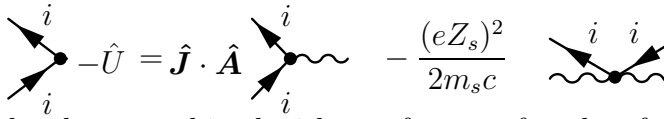

(B.2)

and $-$ sign before U has been combined with two factors of i taken from the incoming and outgoing propagators to produce a real "scattering" amplitude $U(\boldsymbol{r})$. In similar manner we represent diagrammatically the Coulomb interaction term $v(\boldsymbol{r})$ in Eq. (1.1) as

$$v(\boldsymbol{r}_1-\boldsymbol{r}_2) = \frac{1}{2}$$ 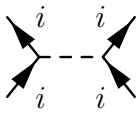 (B.3)

For clarity of method of diagrams construction, however, we will "switch" off the Coulomb interaction for a while.

Now we will use the trick implemented first by J. Schwinger [128] and add additional source terms of electrons and photons to the interacting part of the Hamiltonian $V(1)$. This source terms let us examine how the S-matrix

$$\hat{\mathcal{S}} = \mathcal{T}\exp\Big[-\frac{1}{\hbar}\int\limits_0^{\hbar\beta} d\tau \hat{V}(\tau)\Big], \qquad \beta{=}1/k_{\rm B}T \tag{B.4}$$

responds to incoming currents of particles. In Eq. (B.4) the interaction term $\hat{V}(\tau)$ is taken in the interaction representation and $\mathcal{T}$ denotes the usual time ordering operator. We add directly the source terms to the scattering potential

$$\widetilde{\hat{V}}(\tau_1) = \hat{V}(\tau_1) + \int d^3\boldsymbol{r}_1\big\{J_s^*(1)\hat{\psi}_s(1) + \hat{\psi}_s^\dagger(1)J_s(1) + \hat{\boldsymbol{A}}(1)\cdot\boldsymbol{J}^{\rm ph}(1)\big\}, \tag{B.5}$$

where J_s and $\boldsymbol{J}^{\rm ph}$ are the source terms of electrons and photons, respectively. The term $\hat{\psi}_s^\dagger(1)J_s(1)$ describes the process of creation of charged particle of s-species by a "source" J_s in point $1{=}\{\boldsymbol{r},\tau\}$ and the term $J_s^*(1)\hat{\psi}_s(1)$, in contrary, describes the annihilation of this particle by a "sink" J_s^* in point 1. Since the vector potential $\hat{\boldsymbol{A}}$ enters the interaction term (B.2) without explicit splitting into creation and annihilation operators [cf. Eq. (1.7)] we have introduced just one source current vector $\boldsymbol{J}^{\rm ph}$ for photons.

According to the Wick theorem [129] each product $\langle\hat{V}(1)\hat{V}(2)...\hat{V}(n)\rangle_0$ one can split into pairs of creation and annihilation operators and then replace each such a pair as follows

$$\langle\hat{\psi}_s\overbrace{(2)...\hat{\psi}_s^\dagger}(1)\rangle_0 \to (i)^2\times G_s^{(0)}(2-1). \tag{B.6}$$

This contraction represent the free propagation of electron from the point 1 to 2 and diagrammatically can be denoted by

$$G_s^{(0)}(2-1) = 2 \longleftarrow 1 \tag{B.7}$$

and is called the free electronic Green function. In the same way the contraction of two photonic operators yields the photon Green function

$$\langle\hat{A}_\mu\overbrace{(2)...\hat{A}_\nu}(1)\rangle_0 \to (i)^2\times D_{\mu\nu}^{(0)}(2-1) = -2,\mu \sim\sim 1,\nu \tag{B.8}$$

and is represented by wavy line in Feynman diagrams.

In order to construct the Feynman diagrams for the problem of matter-field interaction, we will use the variational technique. First we note that the Wick contractions of products

of scattering potentials (B.5) in the expansion of the S-matrix

$$\langle\widetilde{\hat{\mathcal{S}}}\rangle_0 = \sum_{n=0}^{\infty}\frac{(-1/\hbar)^n}{n!}\int_0^{\hbar\beta} d\tau_1...d\tau_n \sum_{\text{contractions}} \langle\mathcal{T}\,\widetilde{\hat{V}}(\tau_1)\widetilde{\hat{V}}(\tau_2)\widetilde{\hat{V}}(\tau_3)...\widetilde{\hat{V}}(\tau_n)\rangle_0 \tag{B.9}$$

can be separated into two groups. The contractions between the scattering potentials $V(\tau_n)$ that contribute to the interaction part of the full S-matrix belongs to the first group. As we will see later this part is essential for the construction of the perturbative expansion of the S-matrix in terms of the Feynman diagrams via variational differentiation.

The second group of contractions contains products of sources J_s and $J_\mu^{\rm ph}$. For simplicity we consider only the electronic source currents contributions. Let us substitute (B.5) in (B.9) and perform the contractions using the Wick theorem. For example, the simplest contraction of additional electron source terms reads as

$$\begin{aligned}\frac{(-1)^2}{2!}\int d1d2\langle[J_s^*(2)\hat{\psi}_s(2)+\hat{\psi}_s^\dagger(2)J_s(2)][J_s^*(1)\hat{\psi}_s(1)+\hat{\psi}_s^\dagger(1)J_s(1)]\rangle_0 \\ = \int d1d2\, iJ_s^*(2)G_s^{(0)}(2-1)iJ_s(1) = -J_s^* \longleftarrow J_s\ ,\end{aligned} \tag{B.10}$$

where we have used the definition of the Green function (B.7) for noninteracting system. Contracting in the similar way the higher powers of source potential one can derive the following relation

$$\Big\langle\mathcal{T}\exp\big[-i\int d1(\hat{\psi}_s^\dagger(1)J_s(1)+J_s^*(1)\hat{\psi}_s(1))\big]\Big\rangle_0 = \exp\big[-\int d1d2J_s^*(2)G_s^{(0)}(2-1)J_s(1)\big]. \tag{B.11}$$

Similar expression one can obtain also for the photon source term.

The averaged interaction part of the S-matrix can be rewritten now by replacing field operators in (B.1) by the variational derivatives with respect to the corresponding currents. Namely, one can write

$$\begin{aligned}\mathcal{S}[\alpha_\mu,\alpha_\nu;\gamma^*,\gamma] = \langle\widetilde{\hat{\mathcal{S}}}\rangle_0 = \exp\Bigg[-\frac{1}{\hbar}\int_0^{\hbar\beta}d\tau\Big(\overset{\partial_\gamma}{\underset{\partial_{\gamma^*}}{\wedge}}\sim\partial_{\alpha_\sigma} - \underset{\partial_{\alpha_\lambda}}{\partial_\gamma}\sim\overset{\partial_{\gamma^*}}{\partial_{\alpha_\sigma}}\Big)\Bigg] \\ \times\exp\Big[\gamma^*\longleftarrow\gamma+\tfrac{1}{2}\,\alpha_\mu\sim\alpha_\nu\Big],\end{aligned} \tag{B.12}$$

where we have omitted for simplicity of notations all constant prefactors appearing in the definition of potential $V(\tau)$. Here, we have introduced the following variables

$$\alpha_\mu(1) = J_\mu^{\rm ph}(1), \qquad \gamma(1) = J_s(1), \qquad \gamma^*(1) = -J_s^*(1) \tag{B.13}$$

and the functional derivatives

$$\partial_{\alpha_\mu} = \frac{\delta}{\delta J_\mu^{\rm ph}}, \qquad \partial_\gamma = \frac{\overleftarrow{\delta}}{\delta J_s}, \qquad \partial_{\gamma^*} = -\frac{\overrightarrow{\delta}}{\delta J_s^*}, \tag{B.14}$$

where the last two derivatives act on the left and on the right of expression, respectively, and are natural consequence of the fermionic nature of electrons. Such selectiveness to direction of action of derivatives appears in Grassmannian calculus that is quite natural for the description of fermionic fields (see Appendix A). The prefactor 1/2 that appears in exponent before the photon propagator ensures that we exclude by summation over μ and ν terms that repeats.

The Feynman Diagrams one can obtain now by simply "gluing" the ends of propagators by corresponding functional derivatives of the scattering potential. Expansion of the exponentials in (B.12) leads then to the perturbative series in terms of Feynman diagrams. Explicitly it reads as

$$\mathcal{S}=\sum_{m,n,k}\frac{1}{m!n!k!}\Big[-\frac{1}{\hbar}\int_0^{\hbar\beta}d\tau\Big(\quad-\quad\Big)\Big]^m\Big[\longleftarrow\Big]^n\Big[\frac{1}{2}\sim\sim\Big]^k. \tag{B.15}$$

For example for $m=1$, $n=1$, $k=1$ we obtain the following diagrams

$\alpha_\nu +$, (B.16)

where the first and the second diagrams come from $\boldsymbol{J}\cdot\boldsymbol{A}$ and A^2 interaction parts of Hamiltonian, respectively. As an another examples we present topologically distinct diagrams for terms in (B.15) with $m=1$, $n=1$, $k=2$:

α_ν , α_μ α_ν , α_μ α_ν , (B.17)

and for $m=1$, $n=2$, $k=1$

α_μ γ^* γ , γ^* γ . (B.18)

The processes represented by the second diagrams in Eqs (B.17) and (B.18) play an important role in our consideration. They represent the contributions to the particle and photon propagators arising from the polarization processes due to the A^2-interaction.

The particle Green's function (1.13) one obtains from the perturbation series (B.15) by applying to the partition function the variational derivatives, i.e.

$$G_s(1,2)=-\partial_{\gamma^*(2)}\partial_{\gamma(1)}\ln\mathcal{S}\big|_{\substack{\alpha_\mu=0\\ \gamma=0}}=\frac{\overrightarrow{\delta}}{\delta J_s^*(2)}\ln\mathcal{S}[J_s,\boldsymbol{J}^{\rm ph}]\frac{\overleftarrow{\delta}}{\delta J_s(1)}\Big|_{\substack{J=0\\ \boldsymbol{J}^{\rm ph}=0}}. \tag{B.19}$$

Here we have applied the linked-cluster theorem that states that the logarithm of the S-matrix involves just the sum of the linked cluster diagrams [130] and eliminates disconnected diagrams like those given by the first diagram in Eq. (B.17). The requirement

α_μ=γ=0 (or equivalently $\boldsymbol{J}^{\rm ph}$=J_s=0) eliminates another type of diagrams that have more than two external legs (for example, the first diagram in Eq. (B.18), which disapears since it contains one external photon leg).

Inserting Eq. (B.15) in Eq. (B.19) one finally arrive at the following diagrammatic representation of the particle GF:

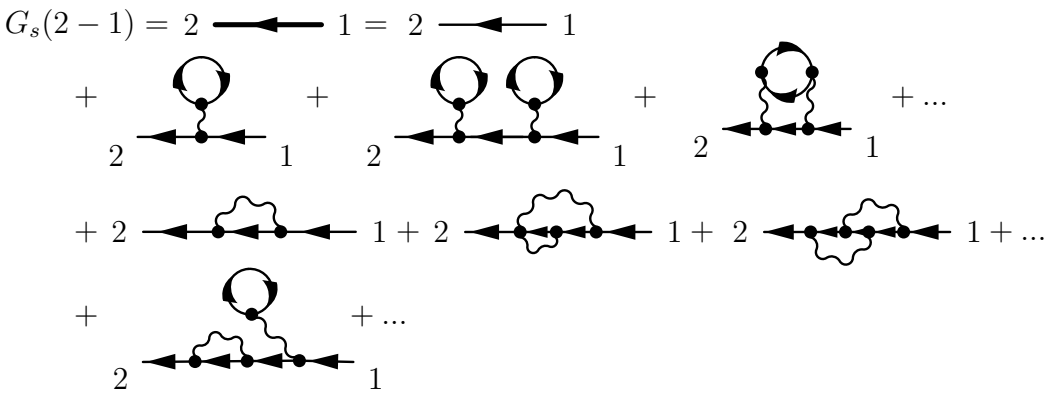

(B.20)

Here, the fat line represents the full particle Green function with the inclusion of all polarization effects that arise due to the interaction with electromagnetic field.

Analogously to (B.19) one can define also the photon Green's function

$$D_{\mu\nu}(1,2) = +\partial_{\alpha_\mu(2)}\partial_{\alpha_\nu(1)} \ln \mathcal{S}\Big|_{\substack{\alpha_\mu=0\\ \gamma=0}} = \frac{\delta^2}{\delta J^{\rm ph}_\mu(2)\delta J^{\rm ph}_\nu(1)} \ln \mathcal{S}[J_s, \boldsymbol{J}^{\rm ph}]\Big|_{\substack{J_s=0\\ \boldsymbol{J}^{\rm ph}=0}}, \tag{B.21}$$

where $J^{\rm ph}_\mu$ is the μ-th component of the photon source term defined in Eq. (B.5). The photon GF (B.21) is represented diagrammatically as

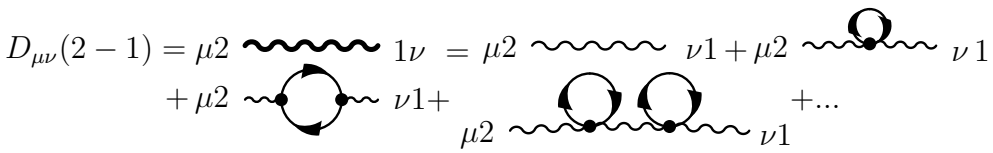

(B.22)

Let us define the self-energies as polarization contributions obtained from Eqs (B.20) and (B.22) by amputating the input and output propagator legs. The proper self-energies are obtained from these amputated graphs by the elimination of diagrams that can be split into two disconnected parts by cutting one propagator line. For example, the diagrams

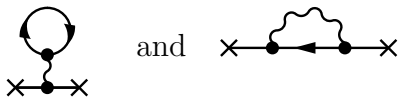

contribute to the proper self-energies, whereas the diagram

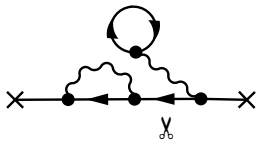

does not contribute since it can be cut as indicated along one propagator line into two separate diagrams. It can be shown that using the definition of proper self-energies Eqs (B.20) and (B.22) can be rewritten compactly in the following diagrammatic form

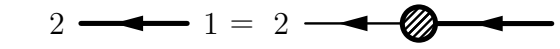

(B.23a)

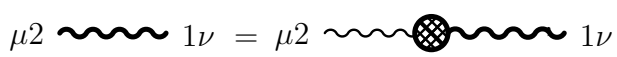

(B.23b)

where $\Sigma_s(1,2)$= 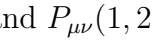 and $P_{\mu\nu}(1,2) = \mu 2$ 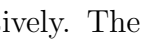 1ν are the proper self-energies of particles and photons, respectively. The Dyson equations given by Eqs (B.23a,b) read in the integral form as

$$G_s(1,2) = G_s^{(0)}(1,2) + \int d3 G_s^{(0)}(2,3)\Sigma_s(3,4)G_s(4,1), \tag{B.24a}$$

$$D_{\mu\nu}(1,2) = D_{\mu\nu}^{(0)}(1,2) + \int d3 D_{\mu\rho}^{(0)}(2,3)P_{\rho\sigma}(3,4)D_{\sigma\nu}(4,1). \tag{B.24b}$$

These Dyson equations can be generalized by including the Coulomb term (B.3) in the interaction Hamiltonian (B.1). This leads to the appearance of additional contributions to the particle and photon self-energies caused by the Coulomb interaction.

Since within the formalism of gauge theories one views the Coulomb interaction between two particles as an exchange of (longitudinal) virtual photon, one can consider the interaction term (B.3) as the Green's function of the longitudinal photon field. We denote this longitudinal photon GF as $D_{00}^{(0)}(\boldsymbol{r},\boldsymbol{r}')$=$v(\boldsymbol{r}_1-\boldsymbol{r}_2)$. In the coherent state representation the contribution to the functional integral (A.16) from the Coulomb interaction term has the same structure as the contribution from the particle free evolution given in the right hand side of Eq. (B.11). Thus, one can interpret $eZ_s\rho_s$ as "source" of static electromagnetic potential $\phi_s(\boldsymbol{r})$=$eZ_s\int d^3\boldsymbol{r}' D_{00}^{(0)}(\boldsymbol{r},\boldsymbol{r}')\rho_s(\boldsymbol{r}')$ in the full analogy to our interpretation of J_s or $\boldsymbol{J}^{\rm ph}$ being the "sources" of charged particles and photons. Consequently, the S-matrix functional with the included Coulomb interaction depends on three "current" variables. In this case particle and transversal photon GFs are obtained in the same way as in Eqs (B.19), (B.21) with the only difference that new variable ρ_s leads to the new terms in self-energies. Additionally one contains the Green function for longitudinal electromagnetic field

$$D_{00}(1,2) = \frac{\delta^2}{\delta\rho^*_{s'}(2)\delta\rho_s(1)} \ln \mathcal{S}[J_s,\rho_s,\boldsymbol{J}^{\rm ph}]\Big|_{\substack{J_s=0\\ \rho_s=0\\ \boldsymbol{J}^{\rm ph}=0}}. \tag{B.25}$$

The full GF of longitudinal photons is known as the effective (screened) Coulomb interaction $v^{\rm eff}(1,2)$. The charged particle polarizes neighboring charges and produce an induced charge density. This induced charge density screens the charges of the interacting particles and thus modifies the Coulomb interaction to the effective one.

Let us now investigate the self-energy effects for the longitudinal and transversal photons in more details. To this end we perform the Hubbard-Stratonovich transformation (A.13) with respect to all "current variables" and for simplicity we Fourier transform S-matrix functional with respect to space and imaginary time variables. We adopt the following notations for wave-vector and Matsubara frequencies: $k{=}\{\boldsymbol{k},\omega_l\}$ for fermions and $\bar{k}{=}\{\boldsymbol{k},\Omega_l\}$ for bosons. Here the Matsubara frequencies are defined as $\omega_l{=}\pi[2l{+}1]/\hbar\beta$, $\Omega_l{=}2\pi l/\hbar\beta$ for $l{=}0,\pm1,\pm2,...$ The resulting S-matrix functional we use in order to obtain the Dyson equations for particles and electromagnetic field

$$\frac{\overrightarrow{\partial}}{\partial\psi^*_{s,k}}\ln\mathcal{S}[0,0,0]\frac{\overleftarrow{\partial}}{\partial\psi_{s,k}}\Big|_{\substack{\psi=0\\ \phi=0\\ \boldsymbol{A}=0}} = G_s^{-1}(k) = G_s^{(0)-1}(k){-}\Sigma_s(k), \tag{B.26}$$

$$\frac{\partial^2}{\partial\phi_{s,-\bar{k}}\partial\phi_{s',\bar{k}}}\ln\mathcal{S}[0,0,0]\Big|_{\substack{\psi=0\\ \phi=0\\ \boldsymbol{A}=0}} = D_{00}^{-1}(\bar{k}) = D_{00}^{(0)-1}(\bar{k}){-}e^2Z_sZ_{s'}\Pi_{\parallel}(\bar{k}), \tag{B.27}$$

$$\frac{\partial^2}{\partial\mathcal{A}_{\mu,-\bar{k}}\partial\mathcal{A}_{\nu,\bar{k}}}\ln\mathcal{S}[0,0,0]\Big|_{\substack{\psi=0\\ \phi=0\\ \boldsymbol{A}=0}} = D_{\mu\nu}^{-1}(\bar{k}) = D_{\mu\nu}^{(0)-1}(\bar{k}){-}P_{\mu\nu}(\bar{k}). \tag{B.28}$$

These equations are equivalent to the Dyson equations derived early and the inversion of these equations gives the full Green's functions.

The self-energies of longitudinal and transverse electromagnetic fields are related with the density-density and current-current correlation functions of the medium, respectively. One has

$$\Pi_{\parallel}(\bar{k}) = \frac{1}{\hbar\beta\mathfrak{v}}\int\limits_0^{\hbar\beta}d\tau\int\limits_0^{\hbar\beta}d\tau' e^{i\Omega_l(\tau-\tau')}\langle\mathcal{T}\hat{\rho}_{s,\boldsymbol{k}}(\tau);\hat{\rho}_{s',-\boldsymbol{k}}(\tau')\rangle^{\rm irr}, \tag{B.29}$$

$$\begin{aligned}P_{\mu\nu}(\bar{k}) =& \frac{1}{\hbar\beta\mathfrak{v}}\int\limits_0^{\hbar\beta}d\tau\int\limits_0^{\hbar\beta}d\tau' e^{i\Omega_l(\tau-\tau')}\langle\mathcal{T}\hat{J}_{\mu,\boldsymbol{k}}(\tau);\hat{J}_{\nu,-\boldsymbol{k}}(\tau')\rangle^{\rm irr}\\ &= P_{\perp}(\bar{k})\left(\delta_{\mu\nu}-\frac{k_\mu k_\nu}{\boldsymbol{k}^2}\right)+P_{\parallel}(\bar{k})\frac{k_\mu k_\nu}{\boldsymbol{k}^2},\end{aligned} \tag{B.30}$$

where $P_{\parallel}=e^2Z_sZ_{s'}(i\Omega_l)^2v_{\boldsymbol{k}}\Pi_{\parallel}$ is the correlation function of the longitudinal current components. The averaging $\langle...\rangle^{\rm irr}$ denotes that we are taking into account just the irreducible part of the correlation functions.

The inversion of the Dyson equations (B.27) and (B.28) leads to the expressions for the full GFs in terms of the correlation functions as follows:

$$D_{00}(\bar{k})\equiv v_{\boldsymbol{k}}^{\rm eff}(\Omega_l) = \frac{1}{D_{00}^{(0)-1}(\bar{k})-e^2Z_sZ_{s'}\Pi_{\parallel}(\bar{k})} = \frac{1}{\varepsilon_0\boldsymbol{k}^2-e^2Z_sZ_{s'}\Pi_{\parallel}(\boldsymbol{k},\Omega_l)}, \tag{B.31}$$

$$D_{\mu\nu}(\bar{k}) = \frac{1}{D_{\mu\nu}^{(0)-1}(\bar{k})-P_{\mu\nu}(\bar{k})} = \frac{\delta_{\mu\nu}^{\perp}(\boldsymbol{k})}{(i\Omega_l/c)^2-\boldsymbol{k}^2-P_{\perp}(\boldsymbol{k},\Omega_l)}, \tag{B.32}$$

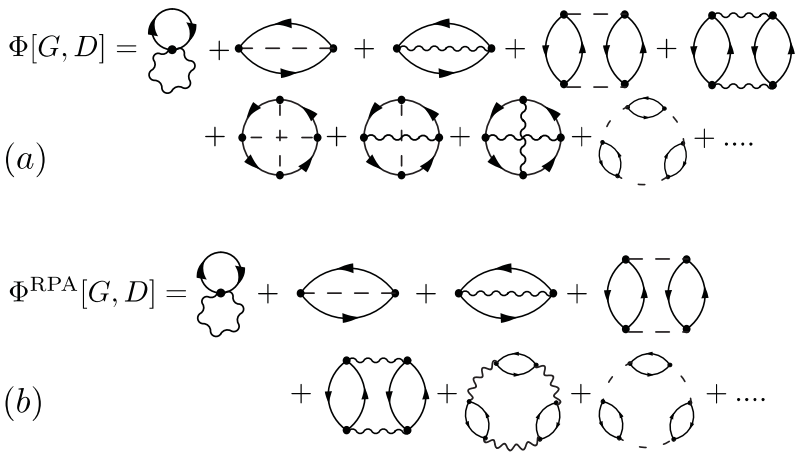

Figure B.1: (a) The Luttinger-Ward generating functional $\Phi[G, D]$ for the system of charged particles interacting with themselves through Coulomb interaction and with electromagnetic field. (b) The simplest approximation for $\Phi[G, D]$ (RPA approximation) where just the ring diagrams are retained.

which after the analytic continuation into the upper frequency half-plane become

$$D_{00}^{\mathrm{ret}}(\boldsymbol{k}, \omega) = \frac{1}{\varepsilon_0 \boldsymbol{k}^2 - e^2 Z_s Z_{s'} \Pi_{\parallel}(\boldsymbol{k}, \omega) + i0^+}, \tag{B.33}$$

$$D_{\mu\nu}^{\mathrm{ret}}(\boldsymbol{k}, \omega) = \frac{\delta_{\mu\nu}^{\perp}(\boldsymbol{k})}{(\frac{\omega + i0^+}{c})^2 - \boldsymbol{k}^2 - P_{\perp}(\boldsymbol{k}, \omega)}. \tag{B.34}$$

As one can see the effects of the interaction with matter are conventionally expressed by self-energy corrections. The effective (screened) Coulomb interaction $v_{\boldsymbol{k}}^{\mathrm{eff}}$ has now the frequency dependence that represent the retardation effect, connected with the characteristic time of particles response on instant Coulomb interaction $v_{\boldsymbol{k}}$. One should note that just the (transverse) photons with the polarization vectors perpendicular to the direction of the propagation of the electromagnetic wave contribute to the self energy of the transverse bosonic field. Thus in the transverse GF (B.32) just the $P_{\perp}$ contribution survives.

The strength of quantum electrodynamics is that it treats the particle-electromagnetic field system as one whole complex. So far from Eqs (B.33) and (B.34) one cannot see this coupled dynamics of photons and charged particles. However, inspection of the photon and particle self-energies shows that these quantities are functionals of both particle and photon propagators. Let us define the Luttinger-Ward generation functional [131]

$$\Phi[G, D] = -\ln(\mathcal{Z}_0 \mathcal{S}[0, 0, 0]). \tag{B.35}$$

It is the sum of all vacuum skeleton diagrams, i.e. these diagrams which do not contain self-energy subdiagrams [see Fig. B.1], or, in another words, it is the correction to the

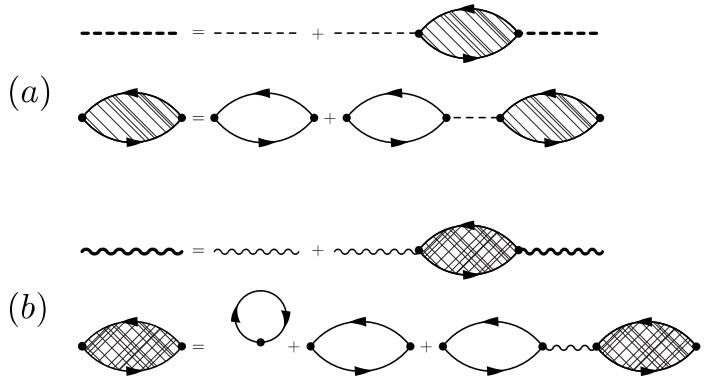

Figure B.2: (a) The Dyson equation for the screened Coulomb interaction between charged particles and the corresponding iteration scheme of charge redistribution in RPA. (b) The Dyson equation for the photon propagator and the iteration scheme for the polarization insertion in RPA. In contrast to the longitudinal interaction the additional loop diagram appears that gives Drude term in the transverse dielectric function.

ground state energy of the system by adding into the system additional charged particle and one photon. Using this functional we can write the self-energies as

$$\Sigma_s(\bar{k}) = -\frac{1}{\hbar\beta\nu}\frac{\delta\Phi[G,D]}{\delta G_s(\bar{k})}, \tag{B.36a}$$

$$\Pi_{\parallel}(\bar{k}) = -\frac{1}{2}\frac{1}{\hbar\beta\nu}\frac{\delta\Phi[G,D]}{\delta D_{00}(\bar{k})} \qquad P_{\perp}(\bar{k})\delta^{\perp}_{\mu\nu}(\bar{k}) = -\frac{1}{2}\frac{1}{\hbar\beta\nu}\frac{\delta\Phi[G,D]}{\delta D_{\mu\nu}(\bar{k})}. \tag{B.36b}$$

In the simplest approximation, the so called *Random Phase Approximation* (RPA) [132], $\Phi[G,D]$ is given by the sum of the ring diagrams shown in Fig. B.1. One should note that in RPA the internal propagator lines are thin, i.e., this approximation not only neglect some definite topological type of the diagrams, but also replaces the full propagators with the free ones. Physically this means that the charged particles are assumed to respond only to the total electric potential which is the sum of the perturbing potential and a screening potential. On the other hand, the contribution to the photon self-energies (B.29) and (B.30) from the total electric potential induced by the charged particles is assumed to average out, so that only the definite potential of frequency $\boldsymbol{k}$ contributes with $\boldsymbol{k}$ being the wavevector of the perturbing potential.

The Dyson equations (B.31) and (B.32) in RPA are represented diagrammatically on Fig. B.2. These diagrams are obtained from the Φ^{RPA} given in Fig. B.1(b) by cutting one (longitudinal or transversal) photon propagator line in each diagram in accordance with Eq. (B.36b). The susceptibilities (filled bubbles) are the infinite sums over the polariza-

tions (open bubbles) diagrams (Lindhard functions)

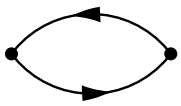

$$= -\frac{1}{\hbar\beta\upsilon}\sum_{\bar{q}} G_s^{(0)}(\bar{k}+\bar{q})G_s^{(0)}(\bar{q}) = -\frac{1}{\upsilon}\sum_{q}\frac{f(\varepsilon^s_{\boldsymbol{k}+\boldsymbol{q}})-f(\varepsilon^s_{\boldsymbol{q}})}{\varepsilon^s_{\boldsymbol{k}+\boldsymbol{q}}-\varepsilon^s_{\boldsymbol{q}}-i\hbar\omega_l} \tag{B.37}$$

multiplied by the corresponding propagators lines, i.e. dashed for the Coulomb interaction and wavy lines for the transverse photon interaction. In Eq (B.37) $f(\varepsilon^s_{\boldsymbol{k}})$ is the Fermi-Dirac distribution function for fermions with energy $\varepsilon^s_{\boldsymbol{k}}$ and chemical potential μ_s. Beyond the RPA approximation we should also include in this diagram the interaction lines inside the loop.

The transverse susceptibility on Fig. B.2(b) in contrast to the longitudinal one contains the additional loop with only one vertex (denoted by dot) that arises from the diamagnetic part of the interaction Hamiltonian. This term can be evaluated and appears to be the so-called Drude term $\sum_s (eZ_s)^2 n_0/m_s$, where n_0 is the density of particles of s-spice. The remaining part of the photon self-energy is the paramagnetic current-current correlation function.

The longitudinal and transverse photon self-energies are related with the corresponding components of the medium dielectric function, $\varepsilon_{\mu\nu}(\bar{k})=\varepsilon^{\perp}(\bar{k})\delta^{\perp}_{\mu\nu}(\boldsymbol{k})+\varepsilon^{\parallel}(\bar{k})k_\mu k_\nu/\boldsymbol{k}^2$, via

$$\varepsilon^{\parallel}(\bar{k}) = \varepsilon_0 - \frac{1}{(i\Omega_l)^2}P_{\parallel}(\bar{k}) = \varepsilon_0\left\{1 - e^2 Z_s Z_{s'} v_{\boldsymbol{k}}\Pi_{\parallel}(\bar{k})\right\}, \tag{B.38}$$

$$\varepsilon^{\perp}(\bar{k}) = \varepsilon_0 - \frac{1}{(i\Omega_l)^2}P_{\perp}(\bar{k}) \tag{B.39}$$

and can be reconstructed by analyzing the absorption spectra in light scattering experiments. In order to do this we first perform the analytical continuation in Matsubara frequency plane and then Fourier transform the Eqs (B.38) and (B.39) to the coordinate plane. As a result we obtain

$$\varepsilon^{\parallel,\perp}(\boldsymbol{r},\boldsymbol{r}',\omega) = \varepsilon_0 - \frac{1}{\omega^2}P^{*}_{\parallel,\perp}(\boldsymbol{r},\boldsymbol{r}',\omega). \tag{B.40}$$

For further references we introduce the complex transversal susceptibility function of the medium via

$$\varepsilon_0\omega^2\chi^{\perp}(\boldsymbol{r},\boldsymbol{r}',\omega) = -P_{\perp}(\boldsymbol{r},\boldsymbol{r}',\omega), \quad \chi^{\perp}_{\mu\nu}(\boldsymbol{r},\boldsymbol{r}',\omega)=\chi(\boldsymbol{r},\boldsymbol{r}',\omega)\delta^{\perp}_{\mu\nu}(\boldsymbol{r}-\boldsymbol{r}') \tag{B.41}$$

such that $\varepsilon^{\perp}=\varepsilon_0(1+\chi^{\perp})$.

The longitudinal dielectric function is also related to the structure factor of a medium. In order to show this we define in the same way as it was done in (B.29) the density-density correlation function $\Pi^{\mathrm{irr}}_{\parallel}$ but without restriction on irreducibility of the corresponding Feynman diagrams. This correlation function is related to its proper part $\Pi_{\parallel}$ as

$\Pi_{\parallel}^{\mathrm{irr}}(\bar{k})$=$\Pi_{\parallel}(\bar{k})/\varepsilon^{\parallel}(\bar{k})$ and to the structure factor $\mathfrak{S}(\boldsymbol{k},\omega)$ [133] as

$$\Pi_{\parallel}^{\mathrm{irr}}(\boldsymbol{k},\Omega_l \to i\omega) = \int_0^{\infty} d\omega[1-e^{-\beta\hbar\omega'}]\mathfrak{S}(\boldsymbol{k},\omega')\frac{2\omega'}{(\omega')^2+\omega^2}. \tag{B.42}$$

The structure factor can be measured from the scattering experiments in media [134]. We note that the dielectric function that enters in measurable quantities such as $\Pi_{\parallel}^{\mathrm{irr}}$ is taken in the long-wavelength limit. This ensures the correct transition from the microscopic dielectric function to the macroscopic one. Moreover in this limit the $1/\boldsymbol{k}^2$ singularity of the Coulomb potential in (B.38) cancels out and the dielectric function is regular in the zero frequency and long-wavelength limit.

The transverse dielectric function $\varepsilon_{\perp} = \varepsilon'_{\perp} + i\varepsilon''_{\perp}$ can be determined from the light scattering in medium. With the knowledge of the dielectric function one can calculate the index of refraction n and absorption coefficient α via

$$n(\boldsymbol{k},\omega) + i\frac{c}{2\omega}\alpha(\boldsymbol{k},\omega) = \sqrt{\varepsilon_{\perp}(\boldsymbol{k},\omega)}. \tag{B.43}$$

In particular, the long wavelength limit of the absorption coefficient

$$\alpha(\omega) = \frac{\omega}{c}\frac{\varepsilon''_{\perp}(\omega)}{n(\omega)} \tag{B.44}$$

can be reconstructed experimentally in virtue of the Lambert-Beer law by measurement of the intensity of light transmitted through the medium. The refraction index one obtains then by the appropriate Hilbert transformation of the absorption function that leads to the well-known Kramers-Kronig relations.

Appendix C

S-Matrix and the input-output relations

The quantum dynamics of the light field propagating through the optical setups can be described as a series of scattering events. In this case the involved optical devices (beam splitters, interferometers, etc.) are described by some potential. The incoming fields scatter on this potential and proceed to the detectors to be measured. Although the usual setups for the quantum optical and scattering experiments differs from teach other, nevertheless, in both kinds of experiments the experimentator controls the input radiation sources and detect the generated outputs. In this appendix we derive the S-matrices for simple optical instrumentals. In scattering theory the S-matrix describes the dependence of the detected outputs on the characteristics of the scattering potential. In quantum optics the knowledge of the S-matrix allows one to construct the so-called input-output relations between the incoming and outgoing fields.

Let us consider two propagating waves (given in terms of operators $\hat{a}_1$ and $\hat{a}_2$) coupled by a partly reflecting, partly transmitting lossless mirror with the reflection amplitude r (see Fig. C.1). We assume that the modes are geometrically matched and have the same polarization. Reflection from the mirror constitutes a scattering event. Incident waves are transformed into reflected ones. The transformation is naturally described by means of the S-matrix. Since we suppose that the interaction is linear, the Hamiltonian must be a quadratic expression in $\hat{a}_i$. If we suppress the natural time dependence $\exp[-i\omega t]$ of the operators, we may assume the Hamiltonian of the form

$$\hat{H} = \hbar(\lambda_{12}\hat{a}_1^\dagger\hat{a}_2 + \lambda_{21}\hat{a}_2^\dagger\hat{a}_1), \tag{C.1}$$

where λ_{12}=λ_{21}^*, since the Hamiltonian is Hermitian and thus λ_{12}=$\lambda e^{i\theta}$ with λ real. The Hamiltonian of this type is used usualy for modelling open quantum systems interacting

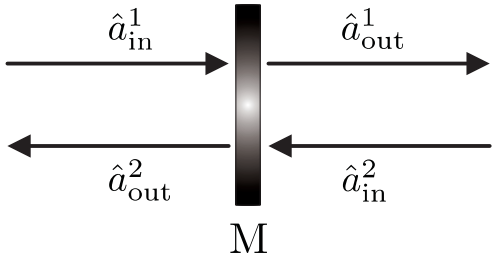

Figure C.1: A partially transmitting mirror M. $\hat{a}^1_{\rm in}$ and $\hat{a}^1_{\rm out}$ are input and output operators of the field-mode impinging the mirror from the left. $\hat{a}^2_{\rm in}$ and $\hat{a}^2_{\rm out}$ are operators of the field-mode passing in the oposite direction.

with some dissipative chanel [28]. Thus, the semitransparent mirror can serve as a toy model to describe dissipation effects.

The real-time S-matrix functional for the Hamiltonian (C.1) reads as [cf. Eq. (B.28)]:

$$\mathcal{S} = \frac{1}{\mathcal{Z}_0}\int \mathcal{D}[\alpha_1]\mathcal{D}[\alpha_2] e^{-\frac{i}{\hbar}\mathscr{S}[\alpha_1,\alpha_2,t]}. \tag{C.2}$$

The integration is performed with the account of the periodic boundary condition $\alpha(0)=\alpha(t)$. The canonical action functional in Eq. (C.2) reads as

$$\mathscr{S}[\alpha_1,\alpha_2,t] = \int_0^t dt' \Big(-i\hbar\alpha_1^*\frac{d}{dt'}\alpha_1 - i\hbar\alpha_2^*\frac{d}{dt'}\alpha_2 + \mathcal{H}[\alpha_1,\alpha_2]\Big), \tag{C.3}$$

where $\mathcal{H}$ is the functional form of the Hamiltonian (C.1). We evaluate the integrals in Eq. (C.2) using the method of the steepest descend. Variation of the action (C.3) leads to the system of equations

$$\begin{aligned} \frac{1}{\hbar}\frac{\delta}{\delta\alpha_1^*}\mathscr{S}[\alpha_1,\alpha_2,t] &= -i\frac{d}{dt}\alpha_1 + \lambda_{12}\alpha_2 = 0, \\ \frac{1}{\hbar}\frac{\delta}{\delta\alpha_2^*}\mathscr{S}[\alpha_1,\alpha_2,t] &= -i\frac{d}{dt}\alpha_2 + \lambda_{21}\alpha_1 = 0. \end{aligned} \tag{C.4}$$

The solution of Eq. (C.4) one obtains by taking into account the periodicity conditions an it reads as

$$\exp[-i\underline{\Lambda}t] = \begin{pmatrix} \cos(\lambda t) & -ie^{i\phi}\sin(\lambda t) \\ -ie^{-i\phi}\sin(\lambda t) & \cos(\lambda t) \end{pmatrix}. \tag{C.5}$$

The S-matrix functional reads now as[1]

$$\mathcal{S} = \exp[\{\boldsymbol{a}^T\}^*\cdot\exp[-i\underline{\Lambda}t]\cdot\boldsymbol{a}], \tag{C.6}$$

[1]Here, the function $1/\mathcal{Z}_0=\sqrt{\sin(\lambda t)/\lambda}$ simplifies with the prefactor $1/\sqrt{\det[\delta^2\mathscr{S}]}=\sqrt{\lambda/\sin(\lambda t)}$, which arises by evalaution of the integral in Eq. (C.2).

where $\boldsymbol{a}=(\alpha_1, \alpha_2)$ and superscript T denotes the transposition.

The elements of the scattering matrix is obtained from the generation functional (C.6) as follows:

$$\underline{S}_{ij} = \frac{\partial^2 \mathcal{S}}{\partial \alpha_i^* \partial \alpha_j}\Big|_{\substack{\alpha_i^*=0 \\ \alpha_j=0}} = \big[\exp(-i\underline{\Lambda}t)\big]_{ij}, \quad i,j{=}1,2, \tag{C.7}$$

i.e., S-matrix coincides with the matrix $\exp[-i\underline{\Lambda}t]$. One should note, that Eq. (C.7), in contrast to the similar expression (B.28), contains also the contributions from the disconnected diagrams and thus describes all kinds of scattering of two modes in the mirror. The scattered radiation fields, which we refer as the output fields, are assumed to be the free fields in the remote future. The S-matrix relates the output fields with the input ones that are assumed to be free before the scattering event. This implies the following *input-output relation* between the field operators of the radiation field before and after the scattering event:

$$\begin{pmatrix} \hat{a}^1_{\text{out}} \\ \hat{a}^2_{\text{out}} \end{pmatrix} = \underline{S} \cdot \begin{pmatrix} \hat{a}^1_{\text{in}} \\ \hat{a}^2_{\text{in}} \end{pmatrix}. \tag{C.8}$$

Since for the free input and output fields the incoming and the emerging beams are both independent bosonic modes, their annihilation operators must satisfy

$$\begin{aligned} [\hat{a}^i_{\text{out}}, \hat{a}^{j\dagger}_{\text{out}}] &= [\hat{a}^i_{\text{in}}, \hat{a}^{j\dagger}_{\text{in}}] = \delta_{ij} \\ [\hat{a}^i_{\text{out}}, \hat{a}^{j}_{\text{out}}] &= [\hat{a}^i_{\text{in}}, \hat{a}^{j}_{\text{in}}] = 0. \end{aligned} \tag{C.9}$$

Consequently, the S-matrix must obey the unitarity condition $\underline{S}^{-1}{=}\underline{S}^{\dagger}$. This condition reflects the fact that a lossless plate conserves energy and that the total intensity proportional to $\sum_{i=1,2} \hat{a}^{i\dagger}_{\text{in}} \hat{a}^i_{\text{in}}$ is thus an invariant quantity.

Identifying the amplitude reflection coefficient with $\sin \lambda t$ one obtains from Eq. (C.5)

$$\underline{S} = \begin{pmatrix} \sqrt{1-\text{r}^2} & -ie^{i\phi}\text{r} \\ -ie^{-i\phi}\text{r} & \sqrt{1-\text{r}^2} \end{pmatrix}. \tag{C.10}$$

If one considers the mirror within the framework of the classical Maxwellian optics, one obtains the scattering matrix (C.10) with $\phi{=}0$. This is a consequence of the requirement for the mirror to be reciprocal since it is described by the reciprocal Maxwell's equations. The quantum analysis does not necessarily implies reciprocity and thus it ends up with an arbitrary phase angle.

The model of the semitransparent mirror serves in quantum optics as a theoretical paradigm for large variety for other linear optical devices. Interferometers, beam splitters, polarizers, and waveguide couplers are all described effectively by this simple model. Strictly speaking, however, the listed above optical instruments should not be necessary the two-port devices. Let us look more closely at a lossless four-port device, a beam splitter, Fig. C.2. This figure shows that the excitation from each port propagate to some

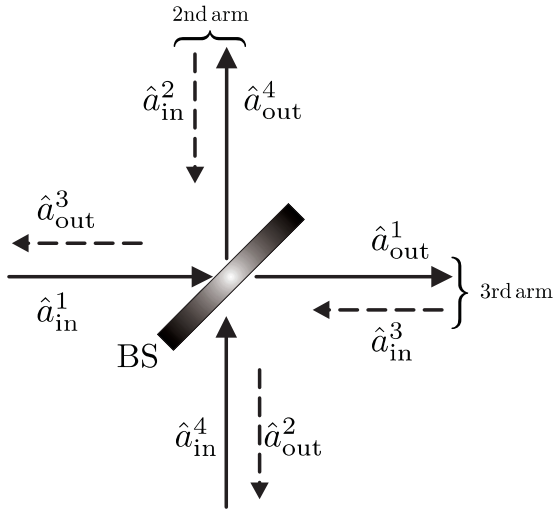

Figure C.2: Schematic representation of a lossless beam splitter *BS*.

other port after the scattering on the glass plate. The interaction Hamiltonian for this case has the same form as in Eq. (C.1)

$$\hat{H} = \hbar[\hat{\boldsymbol{a}}^T]^\dagger \underline{\Lambda} \hat{\boldsymbol{a}}, \tag{C.11}$$

where $\underline{\Lambda}$ is now an 4×4 matrix. The scattering matrix for beam splitter is obtained to be

$$\underline{S} = \exp(-i\underline{\Lambda}t)$$

and the corresponding input-output relations read as

$$\begin{pmatrix} \hat{a}^1_{\rm out} \\ \hat{a}^2_{\rm out} \\ \hat{a}^3_{\rm out} \\ \hat{a}^4_{\rm out} \end{pmatrix} = \begin{pmatrix} \sqrt{1-\mathrm{r}^2} & 0 & 0 & -i\mathrm{r}e^{-\mathrm{i}\phi} \\ 0 & \sqrt{1-\mathrm{r}^2} & -i\mathrm{r}e^{\mathrm{i}\phi} & 0 \\ 0 & -i\mathrm{r}e^{-\mathrm{i}\phi} & \sqrt{1-\mathrm{r}^2} & 0 \\ -i\mathrm{r}e^{\mathrm{i}\phi} & 0 & 0 & \sqrt{1-\mathrm{r}^2} \end{pmatrix} \begin{pmatrix} \hat{a}^1_{\rm in} \\ \hat{a}^2_{\rm in} \\ \hat{a}^3_{\rm in} \\ \hat{a}^4_{\rm in} \end{pmatrix}. \tag{C.12}$$

The S-matrix for the beam-splitter (in contrast to the case of the mirror) is symmetric and hence obey the conditions of reciprocity. Due to this reciprocity symmetry we can freely adjust the phase ϕ. The common choice is $\phi{=}\pi/2$, so that the scattering matrix is real.

In optical experiments usually just the two output arms of the beam splitter are of interest. If we choose the second and third output arms as indicated in Fig. C.2, we get from Eq. (C.12) the following input-output relations for the relevant output operators

$$\begin{pmatrix} \hat{a}^1_{\rm out} \\ \hat{a}^4_{\rm out} \end{pmatrix} = \begin{pmatrix} \sqrt{1-\mathrm{r}^2} & \mathrm{r} \\ -\mathrm{r} & \sqrt{1-\mathrm{r}^2} \end{pmatrix} \begin{pmatrix} \hat{a}^1_{\rm in} \\ \hat{a}^4_{\rm in} \end{pmatrix}. \tag{C.13}$$

The S-matrix in this expression is similar to those for the semitransparent mirror (C.10), though in the latter we have an additional phase parameter.

We conclude this appendix by the implementation of the input-output relations (C.13) for the description of light detection by the *heterodyne detection scheme* [71, 135]. This method allows measurements of the field amplitudes (the quadrature components) instead of the photon number (by the direct photodetection). Additionally, the field amplitudes contain phase information, and so they are dependent on phase. In the four-port variant of this scheme (Fig. C.3), a signal field is combined through a beam splitter with a reference field and the superimposed fields impinge on the photodetectors. Then, however, the noise of the reference field gives parasitic contribution to the photocurrent signal of the signal field. In order to overcome this difficulty in heterodyne detection, a highly stable reference field is used, also called *local oscillator*. The field of the local oscillator (LO) is usually prepared in a coherent state of large amplitude $\alpha_{\rm LO}$. In this case fluctuations of the LO power are coherent at two detectors and cancel in the subtraction circuit.

Homodyne detection is the heterodyne detection that occurs when the LO and signal frequencies are equal. Then, the photocurrent is a measure of the electric field that is in phase with the LO. Here, we use the input-output formalism for the description of the fields transmitted and reflected from the beam splitter. We assume for simplicity that the measured photocurrents $\hat{i}_1$ and $\hat{i}_4$ are proportional to the photon numbers $\hat{n}_{1,\rm out}$ and $\hat{n}_{4,\rm out}$ of the beams striking each detector. They are given by

$$\hat{n}_{1,\rm out} = \hat{a}^{1\dagger}_{\rm out}\hat{a}^{1}_{\rm out}, \quad \hat{n}_{4,\rm out} = \hat{a}^{4\dagger}_{\rm out}\hat{a}^{4}_{\rm out} \tag{C.14}$$

in terms of the output operators (C.13), with $\hat{a}^1_{\rm in}{\equiv}\hat{a}$ and $\hat{a}^4_{\rm in}{\equiv}\alpha_{\rm LO}$ are the input mode operators of the signal and LO fields, respectively. The difference $\Delta\hat{n}{=}\hat{n}_{4,\rm out}{-}\hat{n}_{1,\rm out}$ is the quantity of interest because it contains the interference term of LO and the signal. From (C.13) and (C.14) one obtains

$$\Delta\hat{n} = (1-2{\rm r}^2)(\hat{n}-|\alpha_{\rm LO}|^2) + 2{\rm r}\sqrt{1-{\rm r}^2}|\alpha_{\rm LO}|\,\hat{x}(\phi), \tag{C.15}$$

where

$$\hat{x}(\phi) = \hat{a}e^{i\phi} + \hat{a}^\dagger e^{-i\phi}, \quad \phi = -\arg[\alpha_{\rm LO}] \tag{C.16}$$

is the phase-rotated quadrature operator of the signal mode and $\hat{n}{=}\hat{a}^\dagger\hat{a}$ is the photon number operator of the signal field.

It can be shown [136,137] that in perfect balanced (${\rm r}{=}1/\sqrt{2}$) homodyning the quadrature component statistics of the signal mode are indeed measured, provided that the local oscillator is sufficiently strong, i.e., $|\alpha_{\rm LO}|^2{\gg}\langle\hat{n}\rangle$, such that

$$\Delta n = \langle\Delta\hat{n}\rangle = |\alpha_{\rm LO}|\langle\hat{x}(\phi)\rangle. \tag{C.17}$$

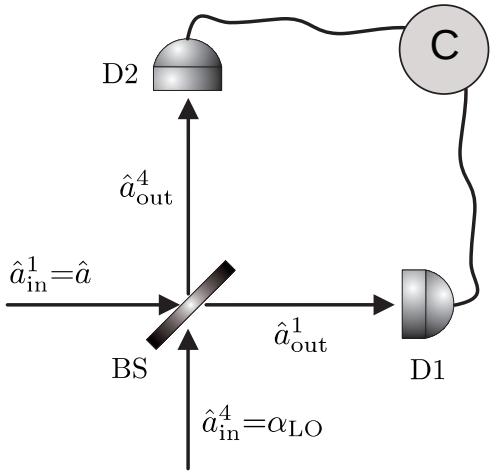

Figure C.3: The optical implementation of balanced heterodyne detection. The signal field, represented by the field mode operator $\hat{a}$, is mixed by the beam-splitter BS with the coherent signal of local oscillator LO. The output field in both arms of the beam-splitter is then measured by detectors D1 and D2 and the corresponding photocurrents are subtracted.

Varying the phase of LO one can obtain the set of averaged quadrature operators for the signal field. Then with the help of quantum tomography [71] one can reconstruct the Wigner quasi-probability distribution for the field of interest.

Appendix D

Poynting's theorem for bounded media

The optical output of some source of optical radiation follows from the Poynting vector operator

$$\hat{\mathfrak{s}}(\boldsymbol{r},t)=\frac{1}{2\mu_0}\left\{\hat{\boldsymbol{E}}(\boldsymbol{r},t)\times\hat{\boldsymbol{B}}(\boldsymbol{r},t)-\hat{\boldsymbol{B}}(\boldsymbol{r},t)\times\hat{\boldsymbol{E}}(\boldsymbol{r},t)\right\}. \tag{D.1}$$

Here, we have symmetrized the operator products in order the expectation value of the Poynting vector to be real. From the other side, instead of Eq. (D.1) we can use the standard quantum field-theoretical definition of the energy-momentum tensor. Namely, taking into account the fact that the electromagnetic vacuum should remain invariant under the Poincaré transformations, it is necessary to define the total momentum of the electromagnetic field as normally ordered operator. If we now make the natural requirement that the Poynting vector should be the spatial density of the total momentum of the electromagnetic field, we arrive at the following definition (for the one mode field)

$$\begin{aligned}:\hat{\mathfrak{s}}(\boldsymbol{r},t):=&\frac{1}{\mu_0}:\hat{\boldsymbol{E}}(\boldsymbol{r},t)\times\hat{\boldsymbol{B}}(\boldsymbol{r},t):\\ &=\frac{c^2}{2\upsilon}\sum_{\boldsymbol{k}}\hbar\boldsymbol{k}\left(2\hat{a}^{\dagger}_{\boldsymbol{k}}\hat{a}_{\boldsymbol{k}}+\hat{a}_{\boldsymbol{k}}\hat{a}_{\boldsymbol{k}}e^{i2(\boldsymbol{k}\cdot\boldsymbol{r}-\omega_{\boldsymbol{k}}t)}+\hat{a}^{\dagger}_{\boldsymbol{k}}\hat{a}^{\dagger}_{\boldsymbol{k}}e^{-i2(\boldsymbol{k}\cdot\boldsymbol{r}-\omega_{\boldsymbol{k}}t)}\right).\end{aligned} \tag{D.2}$$

It should be noticed that this definition cuts off any possible vacuum contributions so that no divergences appear. The standard optical detectors eliminate fast oscillating terms appearing in (D.2) and measure the mean of the Poynting vector operator with magnitude

$$I(t)=\frac{1}{|\boldsymbol{k}|}\left\langle:\boldsymbol{k}\cdot\hat{\mathfrak{s}}(\boldsymbol{r},t):\right\rangle|_{\mathrm{T}}=2\varepsilon_0 c\left\langle\hat{E}^{(-)}(\boldsymbol{r},t)\hat{E}^{(+)}(\boldsymbol{r},t)\right\rangle\Big|_{\mathrm{T}}=\frac{c}{\upsilon}\sum_{\boldsymbol{k}}\hbar\omega_{\boldsymbol{k}}\langle\hat{a}^{\dagger}_{\boldsymbol{k}}\hat{a}_{\boldsymbol{k}}\rangle, \tag{D.3}$$

where the sign $...|_{\mathrm{T}}$ indicates that we have averaged the expression over the mode period $\mathrm{T}=\frac{2\pi}{c|\boldsymbol{k}|}$.

If the light under study propagates in structured material systems it is reasonable to keep in mind the requirement of total energy conservation of the system. As a starting point one can use the Poynting theorem here

$$\frac{\partial}{\partial t}\langle\hat{\omega}_{\rm E}+\hat{\omega}_{\rm H}\rangle+\nabla\cdot\langle\hat{\mathfrak{s}}\rangle=-\langle\hat{\boldsymbol{J}}\cdot\hat{\boldsymbol{E}}\rangle \tag{D.4}$$

where $\hat{\omega}_{\rm E}=\frac{\varepsilon_0}{2}\hat{\boldsymbol{E}}^{\perp 2}$ and $\hat{\omega}_{\rm H}=\frac{1}{2\mu_0}\hat{\boldsymbol{H}}^2$ are the electric and magnetic energy density operators of the plane wave and $W=\langle\hat{\boldsymbol{J}}\cdot\hat{\boldsymbol{E}}\rangle$ characterizes the loss affected the electromagnetic field due to the interaction with media.

Using definitions of $\hat{\omega}_{\rm E}$, $\hat{\omega}_{\rm H}$ for the electric and magnetic contributions to the change in field energy, we obtain after some algebra

$$\frac{\partial}{\partial t_1}\langle\hat{\omega}_{\rm E}(1)\rangle=\frac{i\hbar}{2c^2}\frac{\partial}{\partial t_1}\frac{\partial^2}{\partial t_2^2}\Big\{D^{>}_{\mu\mu}(1,2)+D^{<}_{\mu\mu}(1,2)\Big\}\Big|_{2\to 1}, \tag{D.5}$$

$$\begin{aligned}\frac{\partial}{\partial t_1}\langle\hat{\omega}_{\rm H}(1)\rangle=&\frac{i\hbar}{2c^2}\frac{\partial}{\partial t_1}\Big\{\nabla_\mu(1)\nabla_\mu(2)\big[D^{>}_{\mu\mu}(1,2)+D^{<}_{\mu\mu}(1,2)\big]\\&-\nabla_\mu(1)\nabla_\mu(2)\big[D^{>}_{\nu\mu}(1,2)+D^{<}_{\nu\mu}(1,2)\big]\Big\}\Big|_{2\to 1}.\end{aligned} \tag{D.6}$$

The dissipation term in turn expresses in terms of the photon GFs and polarization functions as (see for details Appendix B of Ref. [122])

$$W(1)=i\hbar\frac{\partial}{\partial t_2}\int d^3\boldsymbol{r}_3\int_{-\infty}^{t_1}dt_3\Big\{P^{>}_{\mu\nu}(1,3)D^{<}_{\nu\mu}(3,2)-P^{<}_{\mu\nu}(1,3)D^{>}_{\nu\mu}(3,2)\Big\}\Big|_{2\to 1}. \tag{D.7}$$

Finally, the GF formulation for the Poynting's vector component is

$$\langle\hat{\mathfrak{s}}_\mu(1)\rangle=\frac{i\hbar}{2}\frac{\partial}{\partial t_1}\Big\{\nabla_\nu(2)\big[D^{>}_{\nu\mu}(1,2)+D^{<}_{\nu\mu}(1,2)\big]-\nabla_\mu(2)\big[D^{>}_{\nu\nu}(1,2)+D^{<}_{\nu\nu}(1,2)\big]\Big\}\Big|_{2\to 1}. \tag{D.8}$$

For stationary conditions the energy density does not vary in time so that from Eq. (D.5) one can obtain for the energy flow hrough the boundary of a medium of volume $\mathscr{V}$ the following relation:

$$\int_{\delta\mathscr{V}}d\boldsymbol{f}\cdot\langle\hat{\mathfrak{s}}\rangle=\int_{\mathscr{V}}d^3\boldsymbol{r}\nabla\cdot\langle\hat{\mathfrak{s}}\rangle=-\int_{\mathscr{V}}d^3\boldsymbol{r}\langle\hat{\boldsymbol{J}}\cdot\hat{\boldsymbol{E}}\rangle=-\int_{\mathscr{V}}d^3\boldsymbol{r}_1W(1). \tag{D.9}$$

Applying this formula to the semiconductor slab described in Sec. 3.3 and noting that due to the transversal translational invariance of the system, energy can flow in the x direction, we write for the Poynting energy flux through the slab surface of area F $[\langle\hat{\mathfrak{s}}\rangle=(\mathcal{S},0,0)]$

$$\Delta\mathcal{S}=\frac{1}{F}\int_{\delta\mathscr{V}}d\boldsymbol{f}\cdot\langle\hat{\mathfrak{s}}\rangle=\mathcal{S}(L/2)-\mathcal{S}(-L/2)=-\int_{-L/2}^{L/2}dxW(x). \tag{D.10}$$

For a TE-polarized light with the polarization chosen along z axis such that

$$\boldsymbol{e}_{\rm TE}=\boldsymbol{e}_z\perp\boldsymbol{k},\boldsymbol{k}_\parallel,\quad \boldsymbol{k}_\parallel\parallel\boldsymbol{e}_y,\quad \boldsymbol{k}_\perp\parallel\boldsymbol{e}_x,\quad \boldsymbol{k}=\boldsymbol{k}_\parallel+\boldsymbol{k}_\perp \tag{D.11}$$

the mode function (3.53) takes the form

$$\mathbf{A}_{p,\boldsymbol{k}}(\boldsymbol{r},t) = \boldsymbol{e}_{\mathrm{TM}} \exp\bigl[i\boldsymbol{k}_{\parallel}\cdot\boldsymbol{r}_{\parallel} - ickt\bigr]\mathcal{A}_{\boldsymbol{k}}(x). \tag{D.12}$$

The only nonzero contribution to $\mathcal{S}$ comes from the zz components of the photon GF, since the chosen light polarization in Eq. (D.11) yields $D_{\mu\nu} = \delta_{\mu z}\delta_{\nu z}D$. Therefore, we finally obtain from Eq. (D.8)

$$\langle\hat{\mathfrak{s}}_x(1)\rangle = \mathcal{S}(1) = \frac{\hbar}{2i}\frac{\partial}{\partial t}\frac{\partial}{\partial x_2}\Bigl\{D^{>}_{zz}(1,2) + D^{<}_{zz}(1,2)\Bigr\}\Big|_{2\to 1}. \tag{D.13}$$

We split $\mathcal{S}$ into the spontaneous and stimulated contributions in accordance with the splitting conventions (3.48a) (3.54) for the photon GFs. From Eqs (D.13) and (3.55b), we obtain for the contribution to the spontaneous emission due to quantum vacuum fluctuations

$$\mathcal{S}_{\mathrm{sp}}(1) = -\frac{\hbar c^2}{2\upsilon}\sum_{\boldsymbol{k}} \operatorname{Im}\mathcal{A}_{\boldsymbol{k}}(x)\frac{\partial}{\partial x}\mathcal{A}^{*}_{\boldsymbol{k}}(x), \tag{D.14}$$

while for the medium-induced spontaneous emission for spatially homogeneous medium we get from Eqs (3.48b) and (D.13)

$$\mathcal{S}_{\mathrm{em}}(1) = -\frac{\hbar c^2}{2\upsilon}\sum_{\boldsymbol{k}} b(\boldsymbol{k}_{\perp}) \operatorname{Im}\mathcal{A}_{\boldsymbol{k}}(x)\frac{\partial}{\partial x}\mathcal{A}^{*}_{\boldsymbol{k}}(x). \tag{D.15}$$

Here $b(\boldsymbol{k}_{\perp})$ is the quasi-particle distribution function at thermal equilibrium. We note also that $\mathcal{S}_{\mathrm{em}}$ vanishes at zero temperature for the non-excited media in the equilibrium. For the spontaneous contribution similar calculations yield

$$\begin{aligned}\mathcal{S}_{\mathrm{stim}}(1) = -\frac{\hbar c^2}{2\upsilon}\sum_{\boldsymbol{k},\boldsymbol{k}'}\frac{1}{\sqrt{kk'}}\Bigl\{ & -ik\exp\bigl[i(\boldsymbol{k}_{\parallel}-\boldsymbol{k}'_{\parallel})\cdot\boldsymbol{r}_{\parallel} - ic(k-k')t\bigr]\mathcal{C}^{<}_{\boldsymbol{k}\boldsymbol{k}'}\mathcal{A}_{\boldsymbol{k}}(x)\frac{\partial}{\partial x}\mathcal{A}^{*}_{\boldsymbol{k}'}(x) \\ & + ik\exp\bigl[-i(\boldsymbol{k}_{\parallel}-\boldsymbol{k}'_{\parallel})\cdot\boldsymbol{r}_{\parallel} + ic(k-k')t\bigr]\mathcal{C}^{<}_{\boldsymbol{k}'\boldsymbol{k}}\mathcal{A}^{*}_{\boldsymbol{k}}(x)\frac{\partial}{\partial x}\mathcal{A}_{\boldsymbol{k}'}(x) \\ & + 2\operatorname{Im}k\exp\bigl[i(\boldsymbol{k}_{\parallel}+\boldsymbol{k}'_{\parallel})\cdot\boldsymbol{r}_{\parallel} - ic(k+k')t\bigr]\mathfrak{C}_{\boldsymbol{k}'\boldsymbol{k}}\mathcal{A}_{\boldsymbol{k}}(x)\frac{\partial}{\partial x}\mathcal{A}_{\boldsymbol{k}'}(x)\end{aligned} \tag{D.16}$$

where coefficients $\mathcal{C}^{<}$ and $\mathfrak{C}$ are defined in Eq. (3.51). It is worth to mention that if one perform the photodetection of optical radiation transmitted and/or emitted from the semiconductor slab one measures normally-ordered quantities. Therefore, by means of Eq. (D.2) the detected spectral characteristics do not contain terms arising from quantum vacuum contributions (D.14).

Appendix E

Evaluation of some photon Green's functions

The Free Photon Green functions for some quantum states of the electromagnetic field

In this section we give the expressions of free photon GFs calculated using expression (1.13b) for several quantum states. Ordering the time argument in GFs along the Keldysh contour given by Fig. 1.1 we arrive at the following expressions for the $\gtrless$-components of the free photon GFs:

$$D^{(0)>}_{\mu\nu}(\boldsymbol{r},\boldsymbol{r}',t,t')=D^{(0)<}_{\nu\mu}(\boldsymbol{r}',\boldsymbol{r},t',t)=\frac{1}{i\hbar\mu_0}\left[\langle\hat{A}_\mu(\boldsymbol{r},t)\hat{A}_\nu(\boldsymbol{r}',t')\rangle-\langle\hat{A}_\mu(\boldsymbol{r},t)\rangle\langle\hat{A}_\nu(\boldsymbol{r}',t')\rangle\right]. \tag{E.1}$$

We also introduce the photon GF $D^{(0)\gtrless}(\boldsymbol{r},\boldsymbol{r}',t,t')$ such that

$$D^{(0)\gtrless}_{\mu\nu}(\boldsymbol{r},\boldsymbol{r}',t,t') = \sum_{p,p'=1,2} D^{(0)\gtrless}(\boldsymbol{r},\boldsymbol{r}',t,t')e_{\mu,p}e_{\nu,p'}$$

where $\boldsymbol{e}_p$ is the unit polarization vector of a electromagnetic wave (1.7).

- **Fock state.** The photon GFs calculated for field in the n-th Fock state with the density matrix $\hat{\rho}_n=|n\rangle\langle n|$ read as

$$D^{(0)>}_n(\boldsymbol{r},\boldsymbol{r}',t,t')=-i\int\frac{d^3\boldsymbol{k}}{(2\pi)^3}\frac{c}{2k}\left[n^>_k e^{i\boldsymbol{k}\cdot(\boldsymbol{r}-\boldsymbol{r}')-ick(t-t')}+n^<_k e^{-i\boldsymbol{k}\cdot(\boldsymbol{r}-\boldsymbol{r}')+ick(t-t')}\right], \tag{E.2}$$

  where we have used the free photon dispersion relation $k=|\boldsymbol{k}|=\omega/c$ and denote the populations of photons in Fock state n_k as $n^<_k=n^>_k-1$.

- **Thermal state.** Starting from the Gibbs canonical distribution function [cf. with Eq. (2.8)]

$$\hat{\rho}_{\rm th} = \frac{1}{1+\bar{N}_{\rm th}}\left(\frac{\bar{N}_{\rm th}}{1+\bar{N}_{\rm th}}\right)^{\hat{n}} = (1-e^{-\beta\hbar\omega})\sum_n |n\rangle\langle n|e^{-n\beta\hbar\omega} \tag{E.3}$$

one obtains the following photon GFs:

$$\begin{aligned} D_{\rm th}^{(0)>}(\boldsymbol{r},\boldsymbol{r}',t,t') = -i\int \frac{d^3\boldsymbol{k}}{(2\pi)^3}\frac{c}{2k}\Big[\big\{1+\bar{N}_{\rm th}(k)\big\}e^{i\boldsymbol{k}\cdot(\boldsymbol{r}-\boldsymbol{r}')-ick(t-t')} \\ +\bar{N}_{\rm th}(k)e^{i\boldsymbol{k}\cdot(\boldsymbol{r}-\boldsymbol{r}')-ick(t-t')}\Big] \end{aligned} \tag{E.4}$$

where $\bar{N}_{\rm th}(k)=(e^{\beta\hbar ck}-1)^{-1}$ is the number of thermal photons.

- **Squeezed vacuum state.** We consider the multimode squeezed light produced in nonlinear crystal in the second-harmonic generation process. The squeezed photons are emitted then from the crystal in pairs with correlated momenta $\boldsymbol{k}_0-\boldsymbol{q}$ and $\boldsymbol{k}_0+\boldsymbol{k}$. The quantum state generated in this manner, $|\xi_k\rangle$, is obtained from vacuum state by application on it the squeezing operator

$$\hat{S} = \exp\Big[\frac{1}{\mathfrak{v}}\sum_{\boldsymbol{k}} \xi_k^*\hat{a}_{\boldsymbol{k}_0+\boldsymbol{k}}\hat{a}_{\boldsymbol{k}_0-\boldsymbol{k}} - \text{H.c.}\Big] \tag{E.5}$$

where $\xi_k=|\xi_k|e^{i\phi_k}$ is the squeezing strength. The squeezing operator transforms the electromagnetic mode operators as follows:

$$\begin{aligned} \hat{S}^\dagger\hat{a}_{\boldsymbol{k}}\hat{S} &= \mu_{|k_0-k|}\hat{a}_{\boldsymbol{k}} - \nu_{|k_0-k|}\hat{a}^\dagger_{2\boldsymbol{k}_0-\boldsymbol{k}}, \\ \hat{S}^\dagger\hat{a}^\dagger_{\boldsymbol{k}}\hat{S} &= \mu_{|k_0-k|}\hat{a}^\dagger_{\boldsymbol{k}} - \nu^*_{|k_0-k|}\hat{a}_{2\boldsymbol{k}_0-\boldsymbol{k}} \end{aligned} \tag{E.6}$$

with $\mu_k=\cosh|\xi_k|$ and $\nu_k=\sinh|\xi_k|e^{i\phi_k}$. Using Eqs (1.7), (E.1) and (E.6) the photon GF can be evaluated as

$$\begin{aligned} D_{\rm sq}^{(0)>}(\boldsymbol{r},\boldsymbol{r}',t,t') = -i\frac{1}{\mathfrak{v}}\sum_{\boldsymbol{k}}\frac{c}{\sqrt{(\omega_0/c)^2-k^2}}\cos[\boldsymbol{k}\cdot(\boldsymbol{r}-\boldsymbol{r}')-ck(t-t')] \\ \times\Big\{\mathfrak{C}_k e^{i\boldsymbol{k}_0\cdot(\boldsymbol{r}+\boldsymbol{r}')-i\omega_0(t+t')} + \mathfrak{C}_k^* e^{-i\boldsymbol{k}_0\cdot(\boldsymbol{r}+\boldsymbol{r}')+i\omega_0(t+t')} \\ + \mathcal{C}_k^> e^{i\boldsymbol{k}_0\cdot(\boldsymbol{r}-\boldsymbol{r}')-i\omega_0(t-t')} + \mathcal{C}_k^< e^{-i\boldsymbol{k}_0\cdot(\boldsymbol{r}-\boldsymbol{r}')+i\omega_0(t-t')}\Big\} \end{aligned} \tag{E.7}$$

where $\mathcal{C}_k^<=\mathcal{C}_k^>-1=|\nu_k|^2$ and $\mathfrak{C}_k=-\mu_k\nu_k$. The summation in Eq. (E.7) can be replaced by integration in the usual manner ($\frac{1}{\mathfrak{v}}\sum_{\boldsymbol{k}}\to\int\frac{d^3\boldsymbol{k}}{(2\pi)^3}$).

The simple example of multimode squeezed state is the squeezed vacuum state

$$|\psi\rangle_{\rm sv} = \hat{S}|\psi\rangle_{\rm v}, \tag{E.8}$$

where the squeeze operator,

$$\hat{S} = \exp\Big\{ \int_0^{\Delta\omega} d\omega \, [\xi^* \hat{a}(\omega_0+\omega)\hat{a}(\omega_0-\omega) - \text{H.c.}] \Big\} \tag{E.9}$$

acts on the multimode vacuum state $|\psi\rangle_{\text{v}}$. We assume that the electromagnetic wave propagates in the positive x direction and has a single polarization parallel to z axis. The squeezing parameter ξ is assumed to be frequency independent so that the input squeezing spectrum is flat and varies in region $[\omega_0-\Delta\omega/2, \omega_0+\Delta\omega/2]$. One usually supposes that $\Delta\omega \ll \omega_0$, i.e., the squeezing spectral width being much smaller than the mid frequency [57], which is usually realized experimentally. The transformations (E.6) for each mode can be written as

$$\begin{aligned} \hat{S}^\dagger \hat{a}(\omega)\hat{S} &= \mu \hat{a}(\omega) - \nu \, \hat{a}^\dagger(2\omega_0 - \omega), \\ \hat{S}^\dagger \hat{a}^\dagger(\omega)\hat{S} &= \mu \hat{a}^\dagger(\omega) - \nu^* \, \hat{a}(2\omega_0 - \omega). \end{aligned} \tag{E.10}$$

Finally with the help of Eq. (E.10) the free photon GF (E.1) can be easilly evaluated and reads as

$$D_{\text{sq}}^{(0)>}(x,x',t,t') = -i\frac{2c^2}{\omega_0}\Big\{ \big(|\mu|^2+|\nu|^2\big)\cos[\omega_0(\tau-\tau')] - |\mu||\nu|\cos[\omega_0(\tau+\tau')-\phi] \Big\}, \tag{E.11}$$

where the notation $\tau = t - x/c$ has been used.

Evaluation of photon Green's functions for a semiconductor slab

For the TE-polarized light with polarization direction $\boldsymbol{e}_{\text{TM}}$ [see Eq. (D.11)] we write $D_{\mu\nu}^{\text{ret}} = \delta_{\mu z}\delta_{\nu z} D^{\text{ret}}$. Then one can solve Eq. (3.25) by choosing

$$D^{\text{ret}}(x,x',\omega) = -\frac{1}{W(\omega)}\Big[\theta(x-x')\mathcal{A}(x,\omega)\mathcal{A}(-x',\omega) + \theta(x'-x)\mathcal{A}(x',\omega)\mathcal{A}(-x,\omega)\Big], \tag{E.12}$$

where

$$\mathcal{A}(x,\omega) = \begin{cases} e^{i\omega x/c} + \mathcal{R}(\omega)\, e^{-i\omega x/c} & x < -L/2 \\ \mathcal{V}_+(\omega) e^{-i\omega n x/c} + \mathcal{V}_-(\omega) e^{i\omega n x/c} & |x| < L/2 \\ \mathcal{T}(\omega)\, e^{i\omega x/c} & x > L/2 \end{cases} \tag{E.13}$$

is the forward propagating plane wave defined in Eq. (D.12) and $W(\omega)$ is the Wronskian $W(\omega) = \mathcal{A}'(x,\omega)\mathcal{A}(-x,\omega) - \mathcal{A}(x,\omega)\mathcal{A}'(-x,\omega)$. The function $\mathcal{A}(x,\omega)$ for $|x| < L/2$ defines

the propagating forward quasi-particles with the wave vector $\boldsymbol{k}$. From Eq. (E.13) the dispersion relation $|\boldsymbol{k}|=\pm\omega n(\omega)/c$ for these quasi-particles can be obtained. It defines the transverse propagation modes and is called polariton dispersion relation [138].

The coefficients in (E.13) are determined from the Maxwell boundary conditions as

$$\mathcal{T}(\omega) = \frac{4n(\omega)}{\{n^2(\omega)-1\}}\rho(\omega)e^{-i\omega L/c}; \tag{E.14a}$$

$$\mathcal{R}(\omega) = 2i\rho(\omega)e^{-i\omega L/c}\sin\big[\omega n(\omega)L/c\big]; \tag{E.14b}$$

$$\mathcal{V}_{\pm}(\omega) = \frac{2}{\{n(\omega)\pm 1\}}\rho(\omega)e^{i\omega(n(\omega)\mp 1)L/2c}, \tag{E.14c}$$

$$\rho(\omega) = \frac{\mathscr{r}(\omega)}{1-\mathscr{r}^2(\omega)} = \sum_{l=0}^{\infty}\big\{\mathscr{r}(\omega)\big\}^{2l+1}. \tag{E.15}$$

The waves, reflected inside the slab with the internal reflectivity coefficient $\mathscr{r}(\omega)$, interfere constructively for $\omega_s=2\pi s/Ln'(\omega)$ with integer s (Fabry-Perot resonances) and, hence, $|\rho(\omega)|^2$ exhibits an oscillating behavior with maxima at ω_s.

The GFs for different spatial domains are determined from Eq. (E.12) and may be split into four cases:

A) For $|x'|<L/2$ and $x>L/2$ (upper sign) or $x<-L/2$ (lower sign):

$$D^{\rm ret}(x,x',\omega) = -\frac{ic}{2\omega}\left[\mathcal{V}_{+}(\omega)\exp\left(\pm\frac{i\omega[x+nx']}{c}\right)+\mathcal{V}_{-}(\omega)\exp\left(\pm\frac{i\omega[x-nx']}{c}\right)\right]; \tag{E.16}$$

B) For $x,x'>L/2$ (upper sign) or $x,x'<-L/2$ (lower sign):

$$D^{\rm ret}(x,x',\omega) = -\frac{ic}{2\,\omega}\left[\exp\left(\frac{i\omega|x-x'|}{c}\right)+\mathcal{R}(\omega)\exp\left(\pm\frac{i\omega[x+x']}{c}\right)\right]; \tag{E.17}$$

C) For $x'<-L/2$, $x>L/2$ (upper sign) and $x'>L/2$, $x<-L/2$ (lower sign):

$$D^{\rm ret}(x,x',\omega) = -\frac{ic}{2\,\omega}\mathcal{T}(\omega)\exp\left(\pm\frac{i\omega[x-x']}{c}\right); \tag{E.18}$$

D) Green's function inside the slab:

$$\begin{aligned} D^{\rm ret}(x,x',\omega) = &-\frac{ic}{2\omega n}\Big[e^{i\omega n|x-x'|/c}+\frac{\mathscr{r}(\omega)[1+n]^2}{4\rho(\omega)}\Big\{\mathcal{V}_{-}^2(\omega)e^{i\omega n(x-x')/c} \\ &+\mathcal{V}_{+}^2(\omega)e^{-i\omega n(x-x')/c}+2\mathcal{V}_{-}(\omega)\mathcal{V}_{+}(\omega)\cos[\omega n(x+x')/c]\Big\}e^{-i\omega(n-1)L/c}\Big]. \end{aligned} \tag{E.19}$$

The first terms on the right hand side of Eqs. (E.17), (E.19) result from the free photon GFs.

Publication list

[I] A. A. Semenov, D. Yu. Vasylyev, and B. I. Lev, *Nonclassicality of noisy quantum states*, J. Phys. B **39**, 905-916 (2006).

[II] A. A. Semenov, D. Yu. Vasylyev, W. Vogel, M. Khanbekyan, and D.-G. Welsch, *Leaky cavities with unwanted noise*, Phys. Rev. A **74**, 033803(12) (2006).

[III] A. A. Semenov, D. Yu. Vasylyev, W. Vogel, M. Khanbekyan, and D.-G. Welsch, *Characterization of unwanted noise in realistic cavities*, Opt. and Spectroscop. **103**, 226-232 (2007).

[IV] D. Yu. Vasylyev, W. Vogel, K. Henneberger, T. Schmielau, and D.-G. Welsch, *Propagation of nonclassical optical radiation through a semiconductor slab*, Phys. Rev. A **78**, 033837(8) (2008).

[V] D. Yu. Vasylyev, W. Vogel, G. Manzke, K. Henneberger, and D.-G. Welsch, *Nonclassicality of radiation fields propagating in complex material systems*, Phys. Status Solidi (b) **246**, 293-297 (2009).

[VI] F. Richter, D. Yu. Vasylyev, and K. Henneberger, *Green function approach to scattering of nonclassical light by bounded media*, arXiv:0903.5238 (2009).

Bibliography

[1] R. Glauber, *Quantum Theory of Optical Coherence* (Weinheim: Wiley-VCH Verlag, 2007).

[2] A. Einstein, Phys. Zeitschrift **18**, 121 (1917).

[3] C. Cohen-Tannoudji, J. Dupont-Roc, and G. Grynberg, *Atom-Photon Interactions. Basic Processes and Applications* (Berlin, Wiley VCH., 1998).

[4] A. Prykarpatsky, U. Taneri, and N.N. Bogolubov (Jr), *Quantum Field Theory with Application to Quantum Nonlinear Optics* (Singapore: World Scientific, 2002).

[5] H. Haug and S. Schmitt-Rink, Prog. Quant. Electr. **9**, 3 (1984); M. Kira and S.W. Koch, Prog. Quant. Electr. **30**, Issue 5, 155 (2006).

[6] D. Klyshko, Usp.–Phys. **41**, 885 (1998).

[7] R.E. Slusher, L.W. Hollberg, B. Yurke, J.C. Mertz, and J. F. Valley, Phys. Rev. Lett. **55**, 2409 (1987).

[8] A. Ourjoumtsev, R. Tualle-Brouri, J. Laurat, and P. Grangier, Science **312**, 83 (2006); A. Ourjoumtsev, H. Jeong, R. Tualle-Brouri, and P. Grangier, Nature **448**, 784 (2007).

[9] G. Nogues, A. Rauschenbeutel, S. Osnaghi, M. Brune, J.M. Raimond, and S. Haroche, Nature **400**, 239 (1999); B. Lounis and M. Orrit, Rep. Prog. Phys. **68**, 1129 (2005).

[10] D.M. Meejhof, C. Monroe, B.E. King, W.M. Itano, and D.J. Wineland, Phys. Rev. Lett. **76**, 1796 (1996); B.T. Varcoe, S. Brattke, M. Weidinger, and H. Walther, Nature **403**, 743 (2002); M. Hofheinz, E.M. Weig, M. Ansmann, R.C. Bialczak, E. Lucero, M. Neely, A.D. O'Connell, H. Wang, J.M. Martinis, and A.N. Cleland, Nature **454**, 310 (2008).

[11] V.V. Dodonov, J. Opt. B: Quantum Semiclass. Opt. **4**, R1 (2002).

[12] M.H. Anderson, J.R. Ensher, M.R. Matthews, C.E. Wieman, and E.A. Cormell, Science **269**, 198 (1995); K. Davis, M.O. Mewes, M.R. Andrews, N.J. van Druten, D.S. Durfee, D.M. Kurn, and W. Ketterle, Phys. Rev. Lett. **75**, 3969 (1995); C.C. Bradley, C.A. Sackett, J.J. Tollett, and R.G. Hulet, Phys. Rev. Lett. **75**, 1687 (1995).

[13] Y. Shin, M. Saba, T.A. Pasquini, W. Ketterle, D.E. Pritchard, and A.E. Leanhardt, Phys. Rev. Lett. **92**, 050405 (2001); ibid., Nature Physics **1**, 57 (2005); T. Schumm, S. Hofferberth, L.M. Andersson, S. Wildermuth, S. Groth, I. Bar-Joseph, J. Schmiedmayer, and P. Krger, Nature Physics **1**, 57 (2005).

[14] M. Kitagawa and M. Ueda, Phys. Rev. A **47**, 5138 (1993); J. Estve, C. Gross, A. Weller, S. Giovanazzi, and M.K. Oberthaler, Nature **455**, 1216 (2008).

[15] A. Sørensen, L.-M. Duan, J. I. Cirac and P. Zoller, Nature **409**, 63 (2001); K. Helmerson1 and Li You, Phys. Rev. Lett. **87**, 170402 (2001).

[16] D. Bouwmeester, A. Ekkert, and A. Zeilinger, (eds.) *The Physics of Quantum Information* (Berlin: Springer, 2000).

[17] C.H. Bennett, G. Brassard, C. Crèpeau, R. Jozsa, A. Peres, and W.K. Wootters, Phys. Rev. Lett. **70**, 1895 (1993); D. Bouwmeester, Jian-Wei Pan, K. Mattle, M. Eibl, H. Weinfurter, and A. Zeilinger, Nature **390**, 575 (1997).

[18] C.H. Bennett and D.J. Wiesner, Phys. Rev. Lett. **69**, 2881 (1992).

[19] A.K. Ekkert, Phys. Rev. Lett. **67**, 661 (1991).

[20] A. Einstein, B. Podolsky, and N. Rosen, Phys. Rev. **47**, 777 (1935).

[21] J. Bell, Physics **1**, 195 (1964); J. Bell, *Speakable and Unspeakable in Quantum Mechanics* (Cambridge: Cambridge University Press, 1997).

[22] A. Aspect, G. Roger, S. Reynaud, J. Dalibard, and C. Cohen-Tanoudji, Phys. Rev. Lett. **45**, 617 (1980); A. Aspect, P. Grangier and G. Roger, Phys. Rev. Lett. **47**, 460 (1981); A. Aspect, J. Dalibard, and G. Roger, Phys. Rev. Lett. **49**, 1804 (1982).

[23] A. Zeilinger, Rev. Mod. Phys. **71**, S288 (1998).

[24] A. Peres, Phys. Rev. Lett. **77**, 1413 (1996).

[25] M. Horodecki, P. Horodecki, and R. Horodecki, Phys. Lett. A **223**, 1 (1996); R. Horodecki, Phys. Lett. A **232**, 333 (1997).

[26] R. Simon, Phys. Rev. Lett. **84**, 2726 (2000).

[27] E. Shchukin and W. Vogel, Phys. Rev. Lett. **95**, 230502 (2005).

[28] U. Weiss, *Quantum Dissipative Systems* (Singapore: World Scientific, 2008).

[29] H.-P. Breuer and F. Petruccione, *The Theory of Open Quantum Systems* (Oxford: Clarendon Press, 2006).

[30] H.J. Kimble, Phil. Trans. R. Soc. Lond. A **355**, 2327 (1997).

[31] *Cavity Quantum Electrodynamics, Advances in Atomic, Molecular and Optical Physics. Suplement 2*, ed. by P. Berman (New York: Academic Press, 1994).

[32] C. Gardiner and P. Zoller, *Quantum Noise* (Berlin: Springer, 2000).

[33] M.J. Collett and C.W. Gardiner, Phys. Rev. A **30**, 1386 (1984); C.W. Gardiner and M.J. Collett, Phys. Rev. A **31**, 3761 (1985).

[34] L. Knöll, S. Scheel, E. Schmidt, D.-G. Welsch and A. Chizhov, Phys. Rev. A **59**, 4716 (1999).

[35] M. Khanbekyan, L. Knöll, A. Semenov, W. Vogel and D.-G. Welsch, Phys. Rev. A **69**, 043807 (2004).

[36] C.J. Hood, H.J. Kimble, and J. Ye, Phys. Rev. A **64**, 033804 (2001).

[37] C.K. Law and J.H. Eberly, Phys. Rev. Lett. **76**, 1055 (1995).

[38] W. Lange and H. J. Kimble, Phys. Rev. A **61**, 063817 (2000).

[39] M.D. Frogley, J.F. Dynes, M. Beck, J. Faist, and C.C. Phillips, Nature Materials **5**, 175 (2006).

[40] E. Moreau, I. Robert, L. Manin, V. Thierry-Mieg, J. M. Gèrard, and I. Abram, Phys. Rev. Lett. **87**, 183601 (2001).

[41] D.V. Regelman, U. Mizrahi, D. Gershoni, E. Ehrenfreund, W.V. Schoenfeld, and P.M. Petroff, Phys. Rev. Lett. **87**, 257401 (2001).

[42] M. Bayer, T.L. Reinecke, F. Weidner, A. Larionov, A. McDonals, and A. Forchel, Phys. Rev. Lett. **86**, 3168 (2001).

[43] Y. Masumoto, I.V. Ignatieva, K. Nishibayashia, T. Okunoa, S. Yu. Verbina, and I.A. Yugova, Journal of Luminescence **108**, 177 (2004); D. Lagarde, A. Balocchi, P. Renucci, H. Carrére, T. Amand, X. Marie, Z. X. Mei, and X. L. Du, Phys. Rev. D **79**, 045204 (2009).

[44] A.J. Shields, Nature Photonics **1**, 215 (2007).

[45] S. Machida, Y. Yamamoto, and Y. Itaya, Phys. Rev. Lett. **58**, 1000 (1987).

[46] J. Kim, S. Somani, and Y. Yamomoto, *Nonclassical Light from Semiconductor Lasers and LEDs* (Berlin: Springer, 2001).

[47] P. Michler, A. Kiraz, C. Becher, W. Schoenfeld, P. Petroff, L. Zang, E. Hu, and A. Imamoglu, Science **290**, 2282 (2000).

[48] Ch. Santori, D. Fatta, M. Pelton, G. S. Solomon, and Y. Yamamoto, Phys. Rev. B **66**, 045308 (2002).

[49] S. Strauf, P. Michler, M. Klude, D. Hommel, G. Bacher, and A. Forchel, Phys. Rev. Lett. **89**, 177403 (2002).

[50] W. Hoyer, M. Kira, S.W. Koch, H. Stolz, S. Mosor, J. Sweet, C. Ell, G. Khitrova, and H.M. Gibbs, Phys. Rev. Lett. **93**, 067401 (2004).

[51] L. Lanco, S. Ducci, J.-P. Likforman, X. Marcadet, J.A van Houwelingen, H. Zbinden, G. Leo, and V. Berger, Phys. Rev. Lett. **97**, 173901 (2006).

[52] R.M. Stevenson, R.J. Young, P. Atkinson, K. Cooper, D.A. Ritchie, and A.J. Shields, Nature **439**, 179 (2006).

[53] P.J. Young, R.M. Stevenson, P. Atkinson, K. Cooper, D.A. Ritchie, and A.J. Shields, New J. Phys. **8**, 29 (2006).

[54] N. Akopian, N.H. Lindner, E. Poem, Y. Berlatzky, J. Avron, and D. Gershoni, Phys. Rev. Lett. **96**, 130501 (2006).

[55] H. Haug and Antti-Pekka Jauho, *Quantum Kinetics in Transport and Optics of Semiconductors* (Berlin: Springer, 1998).

[56] D.S. Citrin, ed., *OSA Trends in Optics and Photonics Series. Vol 18, Radiative Processes and Dephasing in Semiconductors* (Washington DC: OSA, 1998).

[57] W. Vogel and D.–G. Welsch, *Quantum Optics* (Weinheim: Wiley-VCH Verlag, 2006).

[58] P.W. Miloni, *The Quantum Vacuum* (New York: Academic Press, 1994).

[59] L.V. Keldysh, Sov. Phys. JETP, **20**, 1018 (1964); original in russian: Zh. Eksper. Teor. Fiziki **47**, 1515 (1964).

[60] L. Kadanoff and G. Baym, *Quantum Statistical Mechanics: Green's Function Methods in Equilibrium and Nonequilibrium Problems* (Perseus Books, 1994).

[61] V. Korenman, Ann. Phys. **39**, 72 (1966).

[62] R.A. Craig, Ann. Phys. **40**, 416 (1966).

[63] J. Schwinger, Proc. Nat. Sci. Am. **37**, 452 (1951).

[64] L. Fadeev in *Les Houches, Session XXVIII. Methods in Field Theory*, ed. by R. Balian and J. Zinn-Justin, (Singapore: World Scientific Publishing, 1981); also in *Quantum Fields and Strings: a Course for Mathematicians*, ed. by P. Deligne et al., (Rhode Island: AMS, 1999).

[65] V.N. Popov, *Functional Integrals and Collective Excitations* (Cambrige: Cambridge University Press, 1988).

[66] V.N. Popov and J. Niederle, *Functional integrals in Quantum Field Theory and Statistical Physics* (New York: Kluwer, 2001).

[67] R. Feynman and A. Hibbs, *Quantum mechanics and path integrals* (New York,Mc Graw-Hill, 1965).

[68] D.C. Langreth, in *Linear and Nonlinear Electron Transport in Solids*, NATO ASI Series B, vol. 17, J.T. Devreese and E. van Doren, eds. (Plenum, New York, 1984).

[69] M. Bonitz, *Quantum Kinetic Theory* (Stuttgart: Teubner Verlag, 1998).

[70] D.T. Smithey, M. Beck, M.G. Raymer, and A. Faridani, Phys. Rev. Lett. **70**, 1244 (1993).

[71] D.-G. Welsch, W. Vogel, and T. Opartný, *Homodyne Detection and quantum State Reconstruction*, Progress in Optics Vol. 39, ed. by E. Wolf (Elsevier. Amsterdam, 1999).

[72] E. Schukin and W. Vogel, Phys. Rev. A **72**, 043808 (2005); ibid., Phys. Rev. Lett. **96**, 200403 (2006).

[73] R. Hanburry-Brown and R. Q. Twiss, Nature **177**, 27 (1956).

[74] L. Mandel and E. Wolf, *Optical Coherence and Quantum Optics* (Cambridge: Cambridge University Press, 1995).

[75] L. Mandel, Prog. Phys. Soc. **74**, 233 (1959).

[76] D. Walls and G. Milburn, *Quantum optics* (Berlin: Springer, 1994).

[77] X. T. Zou and L. Mandel, Phys. Rev. A **41**, 475 (1990).

[78] E.P. Wigner, Phys. Rev. **40**, 749 (1932).

[79] E. Sudarshan, Phys. Rev. Lett. **10**, 277 (1963).

[80] K. Husimi, Proc. Phys. Math. Soc. Jpn. **22**, 264 (1940).

[81] Y. Kano, J. Math. Phys. **6**, 1913 (1965).

[82] A. Kolmogorov, *Foundations of the Theory of Probability* (New York: Chelsea Publishing Company, 1956).

[83] K.E. Cahil and R.J. Glauber, Phys. Rev. **177**, 1857 (1969); ibid., Phys. Rev. **177**, 1882 (1969).

[84] S. M. Barnett and P.M. Radmore, *Methods in Theoretical Quantum Optics* (Oxford: Oxford University Press, 1997).

[85] P.D. Drummond and Z. Ficek (eds.), *Quantum Squeezing* (Berlin: Springer, 2004).

[86] V.N. Popov and V.S. Yarunin, *Collective Effects in Quantum Statistics of Radiation and Matter* (Dordrecht: Kluwer 1988).

[87] I.A. Syurakshina and V.S. Yarunin, Theor. i Matem. Fizika **92**, 158 (1992).

[88] M.S. Kim, F.A. de Oliveira, and P.L. Knight, Phys. Rev. A **40**, 2494 (1989).

[89] D.F. Walls, Nature **306**, 141 (1983).

[90] J. Perina, *Quantum Statistics of Linear and Nonlinear Optical Phenomena* (Dordrecht: Reidel 1984).

[91] W. Vogel, Phys. Rev. Lett. **84**, 1849 (2000).

[92] Th. Richter and W. Vogel, Phys. Rev. Lett. **89**, 283601 (2002).

[93] S. Bochner, Math. Ann. **108**, 378 (1933).

[94] A. Lvovsky and J. Shapiro, Phys. Rev. A **65**, 033830 (2002).

[95] J. Korbicz, J. Cirac, J. Wehr, and M. Lewenstein, Phys. Rev. Lett. **94**, 153601 (2005).

[96] E. Schukin, Th. Richter, and W. Vogel, Phys. Rev. A **71**, 011802(R) (2005).

[97] R.P. Feynman and F.L. Vernon, Ann. Phys. (N.Y.) **24**, 118 (1963).

[98] R. Kubo, J. Phys. Soc. Jpn. **12**, 570 (1966); P.C. Martin and J. Schwinger, Phys. Rev. **115**, 1432 (1959).

[99] D. Loss and K. Mullen, Phys. Rev. B **43**, 13252 (1991).

[100] D. Giulini, E. Joos, C. Kiefer, J. Kupsch, I.–O. Stamatescu, and H.D. Zeh, *Decoherence and the Appearance of a Classical World in Quantum Theory* (Berlin: Springer, 2003).

[101] S. Wallentowitz and W. Vogel, Phys. Rev. A **53**, 4528 (1996); K. Banaszek and K. Wódkiewicz, Phys. Rev. Lett. **76**, 4344 (1996).

[102] A.A. Semenov, A.V. Turchin, and H.V. Gomonay, Phys. Rev. A **78**, 055803 (2008).

[103] S. M. Dutra and G. Nienhuis, Phys. Rev. A **62**, 063805 (2000).

[104] C. Viviescas and G. Hackenbroich, Phys. Rev. A **67**, 013805 (2003); ibid. J. Opt. B **6**, 211 (2004).

[105] M. Khanbekyan, L. Knöll, D.–G. Welsch, A.A. Semenov, and W. Vogel, Phys. Rev. A **72**, 053813 (2005).

[106] H.J. Carmichael, *Statistical Methods in Quantum Optics 2. Non-Classical Fields* (Berlin: Springer, 2008).

[107] Z. Kis, T. Kiss, J. Janszky, P. Adam, S. Wallentowitz, and W. Vogel, Phys. Rev. A **59**, R39 (1999).

[108] M. Munroe, D. Boggavarapu, M.E. Anderson, and M.G. Raymer, Phys. Rev. A **52**, R924 (1995).

[109] K. Henneberger and H. Haug, Phys. Rev. B **38**, 9759 (1988).

[110] L. Knöll, W. Vogel, and D.–G. Welsch, Phys. Rev. A **36**, 3803 (1987).

[111] B. Huttner and S. M. Barnett, Phys. Rev. A **46**, 4306 (1992).

[112] T. Gruner and D.–G. Welsch, Phys. Rev. A **53**, 1818 (1996).

[113] K. Henneberger and S.W. Koch, Phys. Rev. Lett. **76**, 1820 (1996).

[114] K. Henneberger and S.W. Koch in *Quantum Theory of the Optical and Electronic Properties of Semiconductors*, ed. by S. W. Koch (Singapore: World Scientific, 1996).

[115] K. Henneberger and T. Schmielau in *Progress in nonequilibrium Green's functions*, ed. by M. Bonitz and D. Semkat (Singapore: World Scientific, 2003).

[116] W. Schäfer and M. Wegener, *Semiconductor Optics and Transport Phenomena* (Berlin: Springer, 2002).

[117] H. Haug and S.W. Koch, *Quantum Theory of the Optical and Electronic Properties of Semiconductors* (Singapore: World Scientific, 2005).

[118] K. Henneberger, Phys. Status Solidi (b) **246**, 283 (2009).

[119] M. Janowicz, D. Reddig, and M. Holthaus, Phys. Rev. A **68**, 043823 (2003).

[120] M. Artoni and R. Loudon, Phys. Rev. A **55**, 1347 (1996); ibid., Phys. Rev. A **59**, 2279 (1999).

[121] K. Henneberger, arXiv:0810.5058v1 (2008).

[122] F. Richter, M. Florian, and K. Henneberger, Phys. Rev. B **78**, 205114 (2008).

[123] P. Lipavsky, V. Spicka, and Velicky, Phys. Rev. B **34**, 6933 (1986); P. Lipavsky, F.S. Kahn, A. Kalvova, and J.W. Wilkins, Phys. Rev. B **43**, 6650 (1991); H. Haug, Phys. Status Solidi (b) **173**, 139 (1992).

[124] F. Urbach, Phys. Rev. **92**, 1324 (1953); H. Haug, L. Banyai, J. Liebler, and T. Wicht, Phys. Status Solidi (b) **159**, 309 (1990); M. Hartmann and W. Schäfer, Phys. Status Solidi (b) **173**, 165 (1992).

[125] J. Jeffers and S.M. Barnett, J. Mod. Opt. **41**, 1121 (1993).

[126] S.J. Pekar, Sov. Phys. Solid State 4, 953 (1962).

[127] R.L. Stratonovich, Doklady Akad. Nauk SSSR, **115**, 1097 (1957); [translation: Soviet Phys. Doklady **2**, 416 (1958)]; J. Hubbard, Phys. Rev. Lett. **3**, 77 (1959).

[128] J. Schwinger, *Particles, Sources and Fields* (Massachusetts: Addison-Wesley, 1970).

[129] G.C. Wick, Phys. Rev. *80*, 268 (1950).

[130] J. Iliopoulos, C. Itzykson, and A. Martin, Rev. Mod. Phys. **47**, 165 (1975).

[131] J.M. Luttinger and J. C. Ward, Phys. Rev. **118**, 1417 (1960); C. De Dominicis and P.C. Martin, J. Math. Phys. **5**, 14 and 31 (1964).

[132] D. Bohm and D. Pines, Phys. Rev. **92**, 609 (1953).

[133] D. Pines and P. Nozieres, *The Theory of Quantum Liquids* (Redwood: Addison-Wesley, 1989).

[134] W. Jones and N.H. March, *Theoretical Solid State Physics. Vols. 1-2* (Dover Publications, 1986); S. Lovesey, *Theory of Neutron Scattering from Condensed Matter* (Oxford: Clarendon Press, 1984).

[135] H.P. Yuen and J.H. Shapiro, IEEE Trans. Inf. Theory **24**, 657 (1978); J.H. Shapiro and H.P. Yuen, IEEE Trans. Inf. Theory **25**, 179 (1979); H.P. Yuen and J.H. Shapiro, IEEE Trans. Inf. Theory **26**, 78 (1980).

[136] H.J. Carmichael, J. Opt. Soc. Am. B **4**, 1588 (1987).

[137] W. Vogel and J. Grabow, Phys. Rev. A **47**, 4227 (1993).

[138] J.J. Hopfield, Phys. Rev. **112**, 1555 (1958).

General conclusions

The objective of the present thesis is the theoretical investigation of propagation of nonclassical light in structured media with the accounting of various loss mechanisms. First, the characterization of nonclassicality of quantum light being in contact with a thermal bath was given with the accounting of thermal noise effects.

The second topic studied in this thesis was the description of nonclassical light propagation through the lossy optical cavities. In order to characterize all possible loss mechanisms in the considered system the method of replacement schemes was proposed and the corresponding input-output relations and the Langevin equations were derived.

The third major topic concerns the propagation of light in a semiconductor media with boundaries. At first, the optical spectra of the outcoupled light were calculated using the input-output relations for the field operators. Moreover, using the method of nonequilibrium Green functions it was shown that the propagation of arbitrary, even nonclassical light can be formulated in terms of solutions of the classical wave propagation problem. Furthermore, the influence of absorption (amplification), dispersion, spatial inhomogeneity and spontaneous emission from the medium on the nonclassical properties of squeezed light were studied. Besides, the influence of the nonclassical light on the dielectric properties of a semiconductor was also discussed.

Zusammenfassung

Das Ziel der vorliegenden Promotionsthesen ist die theoretische Beschreibung von nichtklassischem Licht in strukturierten Medien unter bezugnahme von Verlustmechanismen. Zunachst wurde eine Characterisierung von nichtklassischem Licht im Kontakt mit einem thermischen Bad durchgeführt.

Das zweite Thema war die Beschreibung der Ausbreitung von nichtklassischem Licht im optischen Resonatoren mit Verlusten. Mit dem Ziel der vollständigen Charakterisierung aller mögliche Verlustmechanismen wurde die Methode der "Replacement-Schemes" vorgeschlagen sowie die entsprechenden "Input-Output" - Relationen und die Langevin Gleichungen hergeleitet.

Das dritte Hauptthema befasst sich mit der Ausbreitung von Licht im begrenzten Halbleitermedien. Zunächst wurde das optische Spektrum des Lichtes am Ausgang mit Hilfe der "Input-Output" - Relation für die Feldoperatoren berechnet. Darüber hinaus wurde mittels der nichtgleichgewichts-Green'schen Funktion gezeigt dass die Ausbreitung von nichtklassischem Licht als Lösung des Problems der klassischen Wellenausbreitung formuliert werden kann. Weiterhin wurden die Einflüsse von Absorption (Verstärkung), Dispersion, räumlichen Inhomogenitäten und spontaner Emission des Mediums auf die nichtklassischen Eigenschaften vom gequetschtem Licht studiert. Der Einfluss von nichtklassischem Licht auf die dielektrischen Eigenschaften des Halbleiters wurden ebenfalls diskutiert.

Lebenslauf

Name	Vasylyev, Dmytro
Geburtstag	4. February 1981
Geburtsort	Winnitsa, Ukraine
Staatsangehörigkeit	Ukraine
Schulausbildung	1989 bis 1996 Gesamtschule, Winnitsa. 1996 bis 1999 Gymnasium, Winnitsa.
Studium	1999 bis 2004 Physikstudium an der Universität 'Kiew-Mohyla Akademie', Kiew Anfertigung und Verteidigung einer Diplomarbeit zum Thema "Nichtklassizität von Quanten-Systemen hinsichtlich experimentell bestimmbarer Größen", Betreuer Prof. Dr. B. Lev.
Promotion	Seit Mai 2005 wiss. Mitarbeiter/Doktorand bei Prof. Dr. W. Vogel in der Arbeitsgruppe Quantenoptik, Fachbereich Physik, Universität Rostock. Forschungsschwerpunkt: *Quantenoptik von Vielteilchensystemen.*

Erklärung

Hiermit erkläre ich, daß ich die vorliegende Arbeit selbständig und ohne fremde Hilfe angefertigt, andere als die von mir angegebenen Quellen und Hilfsmittel nicht benutzt und die den benutzten Werken wörtlich oder inhaltlich entnommenen Stellen als solche kenntlich gemacht habe.

Rostock, den 2 April 2009

Dmytro Vasylyev